Institute of Thermoelectricity, Academy of Sciences and Ministry of Education and Science of Ukraine

Journal of THERMOELECTRICITY

International Research

Founded in December, 1993

published 6 times a year

No. 2 *2018*

Editorial Board

International Editorial Board

Founders – National Academy of Sciences, Ukraine
Institute of Thermoelectricity of National Academy of Sciences and Ministry of Education and Science of Ukraine

Certificate of state registration № КВ 15496-4068 ПР

Approved for printing by the Academic Council of Institute of Thermoelectricity of the National Academy of Sciences and Ministry of Education and Science, Ukraine

Address of editorial office:
Ukraine, 58002, Chernivtsi, General Post Office, P.O. Box 86.
Phone: +(380-372) 90 31 65.
Fax: +(380-3722) 4 19 17.
E-mail: jt@inst.cv.ua
http://www.jt.inst.cv.ua

Signed for publication 25.05.18. Format 70×108/16. Offset paper №1. Offset printing.
Printer's sheet 11.5. Publisher's signature 9.2. Circulation 400 copies. Order 5.

Printed from the layout original made by "Journal of Thermoelectricity" editorial board
in the printing house of "Bukrek" publishers,
10, Radischev Str., Chernivtsi, 58000, Ukraine

CONTENTS

P.V. Gorskiy

P.V. Gorskiy[1,2], *Doctor Phys.-math. science*

[1]Institute of Thermoelectricity of the NAS and MES of Ukraine,
1, Nauky str, Chernivtsi, 58029, Ukraine;
[2]Yu.Fedkovych Chernivtsi National University,
2, Kotsiubynskyi str., Chernivtsi, 58000, Ukraine
e-mail: anatych@gmail.com

ESTIMATION OF THE ELECTRICAL AND THERMAL CONTACT RESISTANCES AND THERMOEMF OF TRANSIENT CONTACT LAYER "THERMOELECTRIC MATERIAL-METAL" BASED ON THE THEORY OF COMPOSITES

The electrical and thermal contact resistances, the thermoEMF, the power factor and the thermoelectric figure of merit of transient contact layer "thermoelectric material-metal" caused by diffusion of metal particles in semiconductor without formation of new phases were theoretically investigated. The research was performed on the basis of the theory of composites by the example of "bismuth telluride-nickel" pair. It was established that the thermoelectric characteristics of transient contact layer depend both on its thickness and on creation mode, the main feature of which is the intensity of metal diffusion in the semiconductor. In so doing, both the thickness and creation mode govern essentially the electrical and thermal contact resistances, the power factor and the quality of transient layer, while the thermoEMF does not depend on the layer thickness and little depends on creation mode. In the thickness range of transient layer from 20 to 150 μm in the considered creation modes the electrical contact resistance varies in the range from $1.16\cdot10^{-5}$ to $4.41\cdot10^{-7}$ Ω·sm², the thermal contact resistance varies in the range from 0.674 to 0.032 (K·sm²)/W, the thermoEMF – in the range from 199.5 to 198.5 μV/K, the power factor – in the range from 5·10-5 to $1.8\cdot10^{-4}$ W/(m·K²), the thermoelectric figure of merit – in the range from 2.35 10^{-3} to 2.9 10^{-3} K⁻¹. Bibl. 10, Fig. 5.

Key words: electrical contact resistance, thermal contact resistance, thermoEMF, transient layer, composite, diffusion, diffusion intensity.

Introduction

It is known that "thermoelectric material (TEM) – metal" contacts in the process of manufacturing thermoelectric energy converters can be created mainly in two ways: direct soldering of the contact metal to the semiconductor and with creation of an anti-diffusion layer of metal previously electroplated on the surface of TEM. In the former case, the solder, which is combined with TEM, forms new phases, the resistivity, the thermal conductivity, the thermoEMF and layer thickness of which basically determine the thermoelectric parameters and characteristics of transient layer [1]. In the latter case, the metal of the anti-diffusion layer, diffusing into TEM, depending on the technology and creation modes, can either create new phases with TEM or not form them [2 – 5]. Usually, when an anti-diffusion layer is created by galvanic deposition followed by soldering of the contact metal, the metal of the anti-diffusion layer partially diffuses into TEM, and solder can penetrate into it only as a result of cracking in TEM. In so doing, the metal of an anti-diffusion layer does not form new phases with TEM [5]. Therefore, the theory

of composites is suitable for estimating the thermoelectric parameters of the transient layer in this case [6]. Such estimation is the purpose of this paper.

Calculation of the electrical contact resistance and thermoEMF of transient contact layer "TEM-metal" caused by metal diffusion in TEM and discussion of the results

This calculation will begin with the construction of a model of the distribution of metal particles in TEM. To do this, we write the equation of one-dimensional stationary diffusion in the presence of a source:

$$D\frac{d^2n}{dx^2} = -Q, \tag{1}$$

where D – coefficient of diffusion of metal in TEM, n – concentration of metal particles at a depth x, Q – the intensity of a source which is a metal layer. At room temperature it is right to assume that Q is zero or is a low positive value. However, in the process of soldering, both D and Q as a result of temperature increase, grow considerably. If layer thickness is d_0, Eq. (1) should be solved under the boundary conditions $n(0) = n_0, n(d_0) = 0$. In going to dimensionless variable $y = x/d_0$, the solution of Eq. (1) under the specified boundary conditions will be as follows:

$$n(y) = n_0\left[1-(1-A)y - Ay^2\right], \tag{2}$$

where dimensionless parameter $A = Qd_0^2/2Dn_0$ characterizes the mode and conditions of creating a contact.

Let us now pass to calculations of the electrical and thermal contact resistances, the thermoEMF, the power factor and the thermoelectric figure of merit of transient contact layer. To do this, first, using relation (2), we determine the volume fractions of the phases (components), that is, metal v_m and the semiconductor v_s in transient contact layer:

$$v_m = \int_0^1 \frac{(A_m/\rho_m)\left[1-(1-A)y - Ay^2\right]}{(A_m/\rho_m)\left[1-(1-A)y - Ay^2\right] + (A_S/\rho_S)\left[(1-A)y + Ay^2\right]}dy. \tag{3}$$

$$v_S = 1 - v_m$$

In these relations, A_m, A_s, ρ_m, ρ_s – are atomic (molecular) masses and the densities of metal and TEM, respectively.

Further calculations will be performed using the theory of composites in the following order. The electrical conductivity σ and the thermal conductivity κ of transient layer will be found by the formulae:

$$\sigma = 0.25\left\{\sigma_S(2-3v_m) + \sigma_m(3v_m-1) + \sqrt{\left[\sigma_S(2-3v_m) + \sigma_m(3v_m-1)\right]^2 + 8\sigma_m\sigma_S}\right\}, \tag{4}$$

$$\kappa = 0.25\left\{\kappa_S(2-3v_m) + \kappa_m(3v_m-1) + \sqrt{\left[\kappa_S(2-3v_m) + \kappa_m(3v_m-1)\right]^2 + 8\kappa_m\kappa_S}\right\}. \tag{5}$$

The electrical r_c and thermal r_{ct} contact resistances will be found by the formulae:

$$r_c = d_0/\sigma, \tag{6}$$

$$r_{ct} = d_0/\kappa. \tag{7}$$

The thermoEMF of transient layer will be determined by the formula:

$$\alpha = \frac{\alpha_m \kappa_s v_m + \alpha_s \kappa_m (1 - v_m)}{\kappa_s v_m + \kappa_m (1 - v_m)} . \quad (8)$$

After that we determine the power factor $P = \alpha^2 \sigma$ and the thermoelectric figure of merit $z = \alpha^2 \sigma / \kappa$. The results of calculations of the above characteristics of transient contact layer at a temperature of 300K depending on A are given in Figs. 1 – 5.

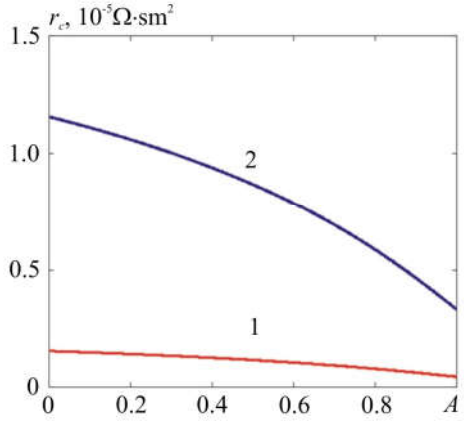

Fig. 1. Dependence of the electrical contact resistance at 300 K on parameter A at transient layer thickness: 1)20μm; 2)150 μm.

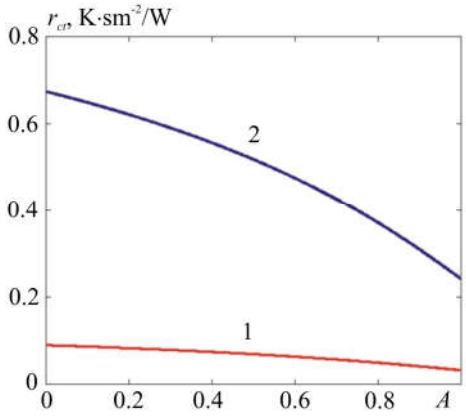

Fig. 2. Dependence of the thermal contact resistance at 300 K on parameter A at transient layer thickness: 1)20μm; 2)150 μm.

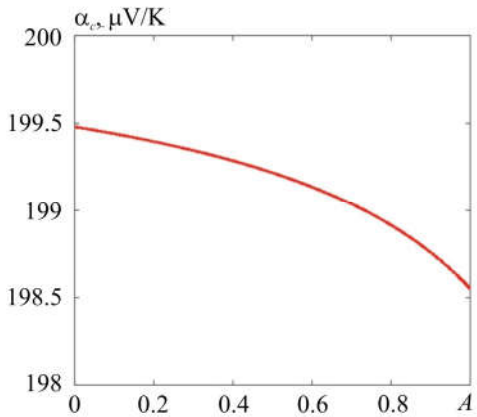

Fig. 3. Dependence of the thermoEMF of transient layer at 300 K on parameter A

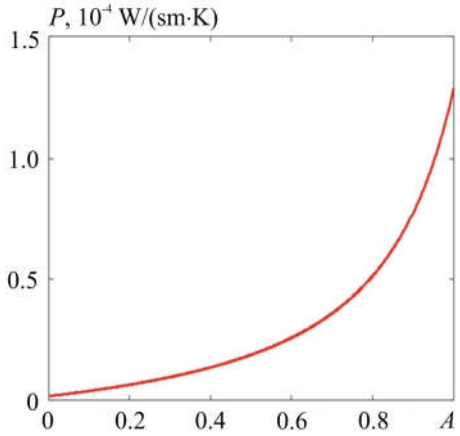

Fig. 4. Dependence of the power factor of transient layer at 300 K on parameter A

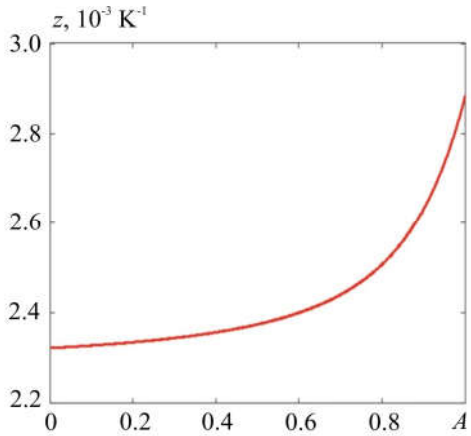

Fig. 5.Dependence of the thermoelectric figure of merit of transient layer at 300 K on parameter A

As long as the contact pair "bismuth telluride – nickel" was considered as an example, in the process of calculations the following material parameters were used: $\sigma_s = 800$ S/sm, $\sigma_m = 1.667 \cdot 10^5$ S/sm, $\kappa_s = 1.4 \cdot 10^{-2}$ W/(sm·K), $\kappa_m = 9.2$ W/(sm·K), $A_s = 801$, $A_m = 58$, $\rho_s = 7700$ kg/m^3, $\rho_m = 8900$ kg/m^3.

From Fig. 1 it is seen that at transient layer thickness equal to 150 μm the electrical contact resistance with increasing parameter A from 0 to 1 decreases from $1.16 \cdot 10^{-5}$ to $3.31 \cdot 10^{-6}$ Ω·sm^2, and at transient layer thickness 20 μm – from $1.55 \cdot 10^{-6}$ to $4.41 \cdot 10^{-7}$ Ω·sm^2. Such a decrease in the electrical contact resistance is due to the fact that with increasing the rate of arrival of metal particles in the semiconductor, the conductivity of the composite should increase. It is also clear from Fig. 2 that at transient layer thickness equal to 150 μm the thermal contact resistance with increasing parameter A from 0 to 1 decreases from 0.674 to 0.24 (K·sm^2)/W, and at transient layer thickness 20 μm – from 0.090 to 0.032 (K·sm^2)/W. Such a decrease in the thermal contact resistance is due to the fact that with increasing the rate of arrival of metal particles in the semiconductor, the thermal conductivity of the composite should increase also. From Fig. 3 it is seen that the thermoEMF of transient contact layer with increasing parameter A from 0 to 1 decreases from 199.5 to 198.5μV/K. This is due to the fact that with increasing the rate of arrival of metal particles in the semiconductor, the thermoEMF of the composite should decrease. From Fig. 4 it is seen that the power factor of transient contact layer with increasing parameter A from 0 to 1 increases from $5 \cdot 10^{-5}$ to $1.8 \cdot 10^{-4}$ W/(m·K^2), and from Fig. 5 it is seen that the thermoelectric figure of merit of transient contact layer with increasing parameter A from 0 to 1 increases from $2.35 \cdot 10^{-3}$ to $2.9 \cdot 10^{-3}$K^{-1}. The growth of the power factor is due to the increase in the electrical conductivity, and the growth of the thermoelectric figure of merit - due to the fact that in this range of

parameter A, the electrical conductivity increases faster than the thermal conductivity. From the nature of the dependences obtained and the fact that with a high concentration of metal particles, the thermoEMF should decrease significantly, it follows that, at least formally, there is such a dimensionless parameter A whereby the power factor and thermoelectric figure of merit of the transition layer reach a maximum. From this point of view, such transient layers could be considered optimized, but the question of the attainability of this value of the parameter A in the actual technological process requires a separate study. However, the content of this parameter may be detailed. For this purpose we will assume that the thickness d_0 of a transient contact layer is determined by diffusion, and, hence, in conformity with the results of solving the nonstationary equation of diffusion for the semi-restricted environment [7] $d_0 = 6\sqrt{D\tau}$, where τ – time during which the most intense diffusion of metal in the semiconductor takes place. Hence, $A = 18Q\tau/n_0$. Consequently, if time τ is fixed, then parameter A is the greater, the higher the rate Q of the arrival of metal particles in the semiconductor in the process of stationary diffusion, and it should be quite large, since n_0 is a fairly large value. For nickel it is equal to $9.14\cdot10^{22}$sm^{-3} [8]. Then it turns out that at a fixed time the thickness of transient layer depends on the diffusion coefficient, which is understandable, since this coefficient depends, in particular, on the presence of defects and disturbances in the material, which contribute to diffusion, and, consequently, to an increase in the thickness of transient layer.

Referring to the comparison of the results with the experimental data, we note that, on the one hand, the value of the electrical contact resistance at 300 K for thermoelectric modules with a height of about 0.25 mm, as stated in [9], obtained in an improved technological process, is $1.12\cdot10^{-6}$ Ω·sm^2. And this is only 2.5 times the lower limit of the contact resistance indicated in this paper. On the other hand, for the thickness of transient layer 20 μm in the worst case, that is, at 0, the calculated value of the electrical contact resistance is $1.55 \cdot 10 – 6$ Ω·sm^2. And this is only a factor of 1.38 higher than the value of the electrical contact resistance at 300K, obtained in the improved technological process of creating contacts.

On the other hand, in Refs [3] and [5], such values of the electrical contact resistances for thermoelectric legs with an anti-diffusion nickel layer are given, which quite significantly exceed the upper limit of the electrical contact resistance specified in this paper, that is, $1.16\cdot10^{-5}$ Ω·sm^2. Thus, we see that there are quite significant technological reserves for reducing the values of the electrical and thermal contact resistances.

Conclusion

1. By solving the one-dimensional diffusion equation, a stationary distribution of the concentration of nickel particles in bismuth telluride over the depth of the transient layer was found.
2. Using the theory of composites, the electrical and thermal contact resistances, the thermoEMF, the power factor and the figure of merit of transient layer were calculated depending on the intensity of arrival of nickel particles with stationary diffusion.
3. It was established that with increasing the intensity of arrival of nickel particles, the electrical and thermal contact resistances and the thermoEMF of transient contact layer decrease, and the power factor and the thermoelectric figure of merit increase.
4. In the considered intensity range of nickel particles arrival with stationary diffusion at transient layer thicknesses 20 – 150 μm the electrical contact resistance can vary in the range from $1.16\cdot10^{-5}$ to $4.41\cdot10^{-7}$ Ω·sm^2, the thermal contact resistance – in the range from 0.674 to 0.032 (K·cm^2)/W, the thermoEMF – in the range from 199.5 to 198.5 μV/K, the power factor – in the range from $5\cdot10^{-5}$ to $1.8\cdot10^{-4}$ W/(m·K^2), and the thermoelectric figure of merit – in the range from $2.35\cdot10^{-3}$ to $2.9\cdot10^{-3}$ K^{-1}. The intervals of change in the electrical and thermal contact resistances can

vary and expand on the one hand due to the presence of potential barriers between TEM and metal, which are overcome by tunneling or emission, on the other, due to the presence of a thin oxide film on the TEM surface, but these factors in this paper are not considered.

References

1. Alieva T.D., Barkhalov B.Sh., Abdinov D.Sh. (1995). Struktura i elektricheskie svoistva granits razdela kristallov $Bi_{0.5}Sb_{1.5}Te_3$ i $Bi_2Te_{2.7}Se_3$ s nekotorymi splavami [Structure and electrical properties of interfaces of $Bi_{0.5}Sb_{1.5}Te_3$ and $Bi_2Te_{2.7}Se_3$ crystals with some alloys]. *Neorganicheskie materialy – Inorganic Materials*, 31(2), 194-198 [in Russian].
2. Chuang C.-H., Lin Y.-C., Lin C.-W. (2016). Intermetallic reactions during the solid-liquid interdiffusion bonding of $Bi_2Te_{2.55}Se_{0.45}$ thermoelectric materials with Cu electrodes using a Sn interlayer. *Metals*, 6(92), 1-10. (doi: 103390/met.6040092).
3. Sabo E.P. (2011). Technology of chalkogen thermoelements. Physical foundations. Section 3. Technology of connection of thermoelement legs. Continuation. 3.5. Electrochemical metallization. *J.Thermoelectricity*, 1, 26-35.
4. Kuznetsov G.D., Polystanskiy Y.G., Evseev V.A. (1995). The metallization of the thermoelement branches by ionic sputtering of the nickel and cobalt. *Proc. of XIV International Conference on Thermoelectrics* (Russia, St.Petersburg, June 27-30, 1995) (pp.166-167).
5. Bublik V.T., Voronin A.I., Ponomarev V.F., Tabachkova N.Yu. (2012). Izmeneniie struktury prikontaktnoi oblasti termoelektricheskikh materialov na osnove telluride vismuta pri povyshennykh temperaturakh [Change in the structure of near-contact area of thermoelectric materials based on bismuth telluride at elevated temperatures] *Izvestiia vysshykh uchebnykh zavedenii*. Materialy elektronnoi tekhniki - *News of Higher Educational Institutions. Electronic Technique Materials,* 2, 17-20 [in Russian].
6. Snarskiy A.O., Zhenirovskiy M.I., Bezsudnov I.V. (2006). On the law of Wiedemann-Franz in thermoelectric composites. *J.Thermoelectricity*, 3, 59-65.
7. Tikhonov A.N., Samarskii A.A. (1972). *Uravneniia matematicheskoi fiziki [Equations of Mathematical Physics]*. Moscow: Nauka [in Russian].
8. Kittel Charles. *Vvedeniie v fiziku tverdogo tela [Introduction to Solid State Physics]*. Moscow: Nauka, 1978 [Russian transl].
9. Gupta R.P., McCarty R., Sharp J. (2013). Practical contact resistance measurement method for bulk Bi_2Te_3-based thermoelectric devices. *J. of Electron. Mat*., 1-5 (doi: 10.10007/s11664-013-2806-6).
10. Drabkin I.A., Osvenskiy V.B., Sorokin A.I. et al. (2017). Kontaktnyie soprotivleniia v sostavnykh termoelektricheskikh vetviakh [Contact resistances in composite thermoelectric legs]. *Fizika i Tekhnika Poluprovodnikov – Semiconductors,* 51 (8), 1038-1040.

Submitted 12.04.2018

Горський П.В.[1,2] *докт. фіз.-мат. наук*

[1]Інститут термоелектрики НАН і МОН України,
вул. Науки, 1,Чернівці, 58029, Україна
[2]Чернівецький національний університет
імені Юрія Федьковича, вул. Коцюбинського 2,
Чернівці, 58012, Україна,
e-mail: anatych@gmail.com

ОЦІНКА ЕЛЕКТРИЧНОГО ТА ТЕПЛОВОГО КОНТАКТНИХ ОПОРІВ ТА ТЕРМОЕРС ПЕРЕХІДНОГО КОНТАКТНОГО ШАРУ«ТЕРМОЕЛЕКТРИЧНИЙ МАТЕРІАЛ-МЕТАЛ» НА ОСНОВІ ТЕОРІЇ КОМПОЗИТІВ

Теоретично досліджено електричний та тепловий контактні опори, термоЕРС, фактор потужності та термоелектричну добротність перехідного контактного шару «термоелектричний матеріал-метал», зумовленого дифузією частинок металу у напівпровідник без утворення нових фаз. Дослідження виконано на основі теорії композитів на прикладі пари «телурид вісмуту – нікель». Встановлено, що термоелектричні характеристики перехідного контактного шару залежать як від його товщини, так і від режиму створення, за основну характеристику якого взято інтенсивність дифузії металу у напівпровідник. При цьому як від товщини так і від режиму створення істотно залежать електричний і тепловий контактні опори,фактор потужності та добротність перехідного шару, в той час, як термоЕРС не залежить від товщини шару і мало залежить від режиму створення. В інтервалі товщин перехідного шару від 20 до 150 мкм за розглянутих режимів створення електричний контактний опір змінюється в інтервалі від 1.16·10-5 до 4.41·10-7 Ом·см^2, тепловий контактний опір змінюється в інтервалі від 0.674 до 0.032(К·см2)/Вт, термоЕРС – в інтервалі від 199.5 до 198.5мкВ/К, фактор потужності – в інтервалі від 5·10-5 до 1.8·10-4 Вт/(м·К^2), термоелектрична добротність – в інтервалі від 2.35 10-3 до 2.9 10-3 К$^{-1}$. Бібл. 10, рис. 5.

Ключові слова: електричний контактний опір, тепловий контактний опір, термоЕРС, перехідний шар, композит, дифузія, інтенсивність дифузії.

Горский П.В.[1,2], *докт. физ.-мат. наук*

[1]Институт термоэлектричества, ул. Науки, 1, Черновцы, 58029, Украина
[2]Черновицкий национальный университет им. Юрия Федьковича,
ул. Коцюбинского, 2, Черновцы,
58000, Украина
e-mail: anatych@gmail.com

ОЦЕНКА ЭЛЕКТРИЧЕСКОГО И ТЕПЛОВОГО КОНТАКТНЫХ СОПРОТИВЛЕНИЙ И ТЕРМОЭДС ПЕРЕХОДНОГО КОНТАКТНОГО СЛОЯ «ТЕРМОЭЛЕКТРИЧЕСКИЙ МАТЕРИАЛ-МЕТАЛЛ» НА ОСНОВЕ ТЕОРИИ КОМПОЗИТОВ

Теоретически исследованы электрический и тепловой контактные сопротивления, термоЭДС, фактор мощности и термоэлектрическая добротность переходного контактного слоя «термоэлектрический материал-металл», обусловленного диффузией частиц металла в полупроводник без образования новых фаз. Исследование выполнено на основе теории композитов на примере пары «телурид висмута – никель». Установлено, что термоэлектрические характеристики переходного контактного слоя зависят как от его толщины, так и от режима создания, в качестве основной характеристики которого взята интенсивность диффузии металла в полупроводник. При этом как от толщины, так и от режима создания существенно зависят электрический и тепловой контактные сопротивления, фактор мощности и добротность переходного слоя, в то время, как термоЭДС не зависит от

толщины слоя и мало зависит от режима создания. В интервале толщин переходного слоя от 20 до 150 мкм при рассмотренных режимах создания электрическое контактное сопротивление изменяется в интервале от $1.16 \cdot 10^{-5}$ до $4.41 \cdot 10^{-7}$ Ом·см^2, тепловое контактное сопротивление изменяется в интервале от 0.674 до 0.032 (К·см2) /Вт, термоЕРС – в интервале от 199.5 к 198.5 мкВ/К, фактор мощности – в интервале от $5 \cdot 10^{-5}$ до $1.8 \cdot 10^{-4}$ Вт/(м·К^2), термоэлектрическая добротность – в интервале от $2.35 \cdot 10^{-3}$ до $2.9 \cdot 10^{-3}$ К$^{-1}$. Библ. 10, рис. 5.
Ключевые слова: электрическое контактное сопротивление, тепловое контактное сопротивление, термоЕРС, переходный слой, композит, диффузия, интенсивность диффузии.

References

1. Alieva T.D., Barkhalov B.Sh., Abdinov D.Sh. (1995). Struktura i elektricheskie svoistva granits razdela kristallov $Bi_{0.5}Sb_{1.5}Te_3$ i $Bi_2Te_{2.7}Se_3$ s nekotorymi splavami [Structure and electrical properties of interfaces of $Bi_{0.5}Sb_{1.5}Te_3$ and $Bi_2Te_{2.7}Se_3$ crystals with some alloys]. *Neorganicheskie materialy – Inorganic Materials*, 31(2), 194-198 [in Russian].
2. Chuang C.-H., Lin Y.-C., Lin C.-W. (2016). Intermetallic reactions during the solid-liquid interdiffusion bonding of $Bi_2Te_{2.55}Se_{0.45}$ thermoelectric materials with Cu electrodes using a Sn interlayer. *Metals*, 6(92), 1-10. (doi: 103390/met.6040092).
3. Sabo E.P. (2011). Technology of chalkogen thermoelements. Physical foundations. Section 3. Technology of connection of thermoelement legs. Continuation. 3.5. Electrochemical metallization. *J.Thermoelectricity*, 1, 26-35.
4. Kuznetsov G.D., Polystanskiy Y.G., Evseev V.A. (1995). The metallization of the thermoelement branches by ionic sputtering of the nickel and cobalt. *Proc. of XIV International Conference on Thermoelectrics* (Russia, St.Petersburg, June 27-30, 1995) (pp.166-167).
5. Bublik V.T., Voronin A.I., Ponomarev V.F., Tabachkova N.Yu. (2012). Izmeneniie struktury prikontaktnoi oblasti termoelektricheskikh materialov na osnove telluride vismuta pri povyshennykh temperaturakh [Change in the structure of near-contact area of thermoelectric materials based on bismuth telluride at elevated temperatures] *Izvestiia vysshykh uchebnykh zavedenii*. Materialy elektronnoi tekhniki - *News of Higher Educational Institutions. Electronic Technique Materials,* 2, 17-20 [in Russian].
6. Snarskiy A.O., Zhenirovskiy M.I., Bezsudnov I.V. (2006). On the law of Wiedemann-Franz in thermoelectric composites. *J.Thermoelectricity*, 3, 59-65.
7. Tikhonov A.N., Samarskii A.A. (1972). *Uravneniia matematicheskoi fiziki [Equations of Mathematical Physics]*. Moscow: Nauka [in Russian].
8. Kittel Charles. *Vvedeniie v fiziku tverdogo tela [Introduction to Solid State Physics]*. Moscow: Nauka, 1978 [Russian transl].
9. Gupta R.P., McCarty R., Sharp J. (2013). Practical contact resistance measurement method for bulk Bi_2Te_3-based thermoelectric devices. *J. of Electron. Mat*., 1-5 (doi: 10.10007/s11664-013-2806-6).
10. Drabkin I.A., Osvenskiy V.B., Sorokin A.I. et al. (2017). Kontaktnyie soprotivleniia v sostavnykh termoelektricheskikh vetviakh [Contact resistances in composite thermoelectric legs]. *Fizika i Tekhnika Poluprovodnikov – Semiconductors,* 51 (8), 1038-1040.

Submitted 12.04.2018

L. I. Anatychuk

L.I. Anatychuk[1,2] *Acad. National Academy of Sciences of Ukraine*,
R.R. Kobylianskyi[1,2] *Candidate Phys.-math. Sciences*

[1]Institute of Thermoelectricity of the NAS and MES of Ukraine, 1, Nauky str, Chernivtsi, 58029,Ukraine;
[2]Yu.Fedkovych Chernivtsi National University, 2, Kotsiubynskyi str., Chernivtsi, 58000, Ukraine,
e-mail: anatych@gmail.com

R.R.Kobylianskyi

COMPUTER SIMULATION OF THE UNSTEADY TEMPERATURE EFFECT ON HUMAN SKIN

This paper presents the results of computer simulation of cyclic temperature effect on human skin in the unsteady mode. A three-dimensional computer model of biological tissue with regard to blood circulation and metabolism has been built. As an example, the case is considered when the skin surface accommodates a work tool whose temperature varies by the law in the temperature range [30÷+30]°C. Temperature distributions in different human skin layers in heating and cooling modes have been determined. The results obtained make it possible to predict the depth of biological tissue freezing with a given temperature effect. Bibl. 20, Fig. 4.
Key words: temperature effect, human skin, unsteady mode, computer simulation.

Introduction

Cryotherapy is widely used in cosmetology for skin rejuvenation. It is known that during cosmetic procedures with cold, generation of collagen and elastin is stimulated, due to which the processes of regeneration in the skin are intensified, it is tightened and toned, and also the corneous cells of the upper layer of the skin (peeling) are peeled off. However, it should be noted that the reaction of the body depends largely on the time and temperature of the cryoeffect [1 – 3].

In dermatological practice, during cryomassage, metabolic and reparative processes are improved and the regression of inflammatory processes is accelerated in cases of chronic dermatoses; there is an increased heat formation and improvement of the trophic function of the tissue of both the skin and internal organs, the work of the heart and blood vessels is stimulated, venous outflow improves, enhanced heat transfer contributes to loss of body weight. Due to the positive effect on the skin, the method of cryomassage is used in the complex treatment of such skin diseases as focal alopecia, pink and vulgar acne, Vidal's disease, itchy skin, chronic eczema, red flat lichen, flat warts, ring-shaped granuloma, etc. [4 – 7].

The literature shows positive applications of thermoelectric cooling in dermatology and cosmetology, in particular for the treatment of superficial hemangiomas in children and other superficial neoplasms [8]. In this paper, Dr. H. Bause describes the treatment of hemangiomas in children with thermoelectric cooling. Under examination were 673 children for 4 months. The treatment occurred at a temperature of -32° C, the optimal time for carrying out therapeutic procedures was 20 seconds (at an exposure time of 40 seconds cell necrosis was observed). In 58 % of patients, treatment was successful the very first time, 25 % had to undergo a second course of cryotherapy, 11 % – 3 times and about 6 % more than 3 times. So, a positive therapeutic effect was observed in the majority of patients during cryotherapy using thermoelectric cooling. This, in turn, shows that for the treatment of certain skin diseases, especially

when performing cryomassage, it is not necessary to use ultralow temperatures (liquid nitrogen -196° C), but rather moderate cooling.

The basis of cryomassage is the rapid decrease in temperature (cooling) of biological tissue under the influence of the cold factor within the range of cryo resistance (5 – 10° C) without significant violation in the body thermoregulation. When the biological tissue is cooled below the threshold of cryo resistance, crystallization of the tissue fluid brings about its destruction (cryodestruction). This is a very complicated process, since it is important to fully control the therapeutic effect in order not to "step over" the threshold of cryo resistance and not to damage healthy tissues. In most cases, it is very difficult to control this process [9, 10]; therefore, it is necessary to learn how to predict the depth of freezing of skin layers at a given temperature effect at different points in time.

Thus, *the purpose of this work* is to develop a method of computer simulation of temperature distribution in human skin in the unsteady mode.

Computer model of cyclic temperature effect on human skin in the unsteady mode

In this work, we used a physical model of biological tissue given in [11 – 15], the surface of which accommodates a medical work tool, whose temperature varies with time according to a predetermined law. In the above works, it was shown that the biological tissue of the human body is a structure of three skin layers (epidermis, dermis, subcutaneous fat) and internal tissue. These skin layers have different physical properties, namely, thermal conductivity κ, density ρ, specific heat capacity *Cp* and blood perfusion ω_b, the values of which are given in [12].

For such a model of biological tissue, the processes of heat exchange are described by a system of unsteady-state heat equations in the form [16]:

$$\rho_i Cp_i \frac{\partial T_i}{\partial t} = \nabla \cdot (\kappa_i \nabla T_i) + (\rho_b Cp_b)\omega_b (T_b - T_i) + q_m, \quad i = 1,...,4, \tag{1}$$

where ρ_i, Cp_i, κ_i are density, specific heat, thermal conductivity of the i^{th} layer of human skin; ρ_b is human blood density; Cp_b is human blood specific heat; ω_b is human blood perfusion; T_b is arterial blood temperature (T_b = 37° C); T_i is temperature of the i^{th} layer of biological tissue; q_m is metabolic heat.

The equation of heat exchange in the biological tissue (1) is solved with the following boundary conditions (2) on the surfaces of the selected volume of biological tissue for an arbitrary moment of time:

$$T_4(x,y,z,t)\Big|_{\substack{z=b\\0\le x\le a\\0\le y\le a}} = T_b, \qquad T_1(x,y,z,t)\Big|_{\substack{z=0\\0\le x\le c\\0\le y\le c}} = T_f(t), \quad q_1(x,y,z,t)\Big|_{\substack{z=0\\c\le x\le a\\c\le y\le a}} = \alpha\cdot(T_0 - T_1(x,y,0,t)),$$

$$q_i(x,y,z,t)\Big|_{\substack{0\le z\le b\\x=0\\0\le y\le a}} = 0, \qquad q_i(x,y,z,t)\Big|_{\substack{0\le z\le b\\x=a\\0\le y\le a}} = 0, \qquad q_i(x,y,z,t)\Big|_{\substack{0\le z\le b\\0\le x\le a\\y=0}} = 0, \qquad q_i(x,y,z,t)\Big|_{\substack{0\le z\le b\\0\le x\le a\\y=a}} = 0, \tag{2}$$

where i = 1,...,4, $q_i(x,y,z,t)$ is the density of heat flux of the i$^{\text{rh}}$ layer of human skin, $T_i(x,y,z,t)$ is the temperature inside the biological tissue, T_0 is ambient temperature (T_0 = 22°C), α is coefficient of convective heat exchange between the skin surface and the environment, a = 10 mm, y = 10 mm, z = 43 mm, c = 2 mm.

The boundary conditions between the layers of human skin are reduced to the equality of temperatures and heat fluxes. At the initial time t = 0 s, it is considered that the temperature in the entire volume of biological tissue is T = 37° C, that is, the initial conditions for solving equation (1) are as follows:

$$T_i(x,y,z,0) = T_b, \qquad i = 1,...,4. \tag{3}$$

As a result of solving the initial boundary value problem (1) – (3), the distribution of temperature T_i (x, y, z, t) and heat flows at an arbitrary time point in all four layers of biological tissue are determined.

As an example, in this paper we consider the case when the temperature of the work tool $T_f(t)$ varies in the range of operating temperatures [-30 ÷ + 30]° C by the following law:

$$T_f(t) = A\cos\omega t, \tag{4}$$

where $A = 303$ K is amplitude, $\omega = 2\pi/p$ is frequency, $p = 60$ s is period, $t = 240$ s is duration of temperature effect.

Computer simulation results

A three-dimensional computer model of biological tissue was created in a cylindrical system of coordinates, on the surface of which there is a cooling element. To construct a computer model, the Comsol Multiphysics application software package [17] was used, which makes it possible to simulate heat physical processes in biological tissue, taking into account blood circulation and metabolism.

The calculation of the distribution of temperature and heat flux densities in biological tissue was carried out by the finite element method, the essence of which is that the object under study is split into a large number of finite elements and in each of them the function value is sought that satisfies the given second-order differential equation with the corresponding boundary conditions. The accuracy of the solution of the problem posed depends on the level of splitting and is provided by using a large number of finite elements [17].

As an example, Fig. 1 – 4 shows the distribution of temperature and isothermal surfaces in the human skin, the surface of which accommodates a work tool whose temperature varies according to the cosine law in the operating temperature range [-30 ÷ + 30]° C at the initial and final moments of heating-cooling cycle.

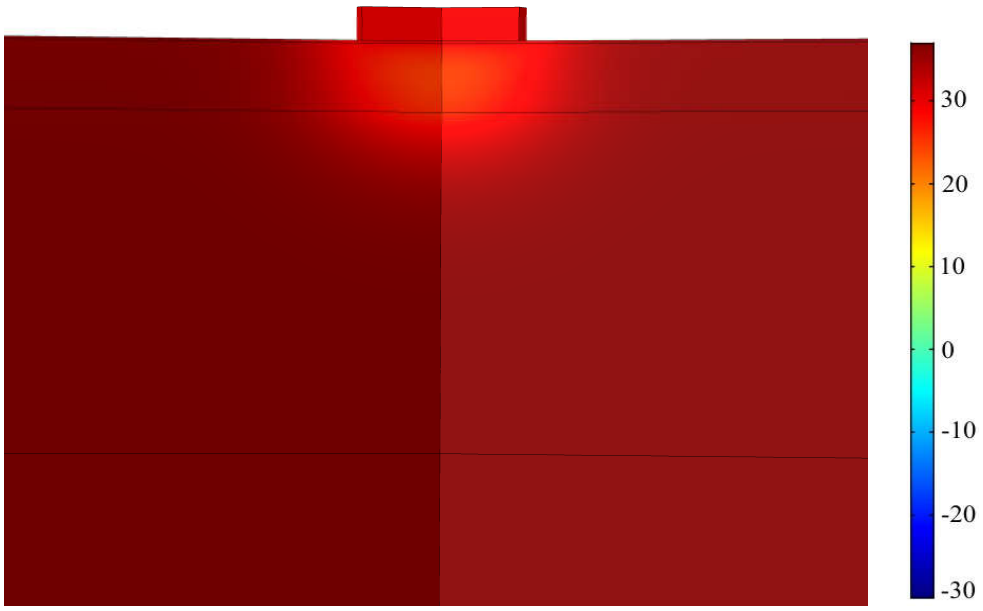

a)

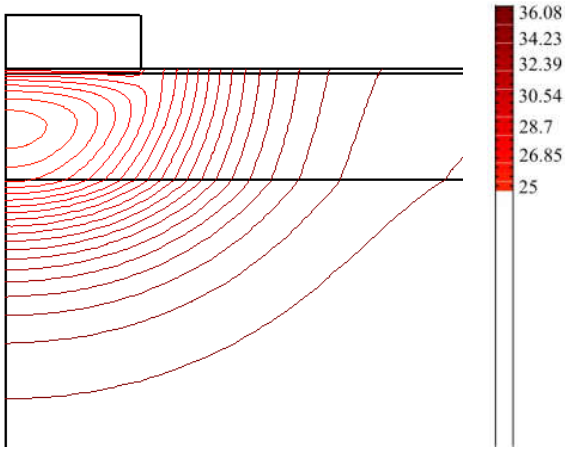

b)

Fig.1. Distribution of temperature (a) and isothermal surafces (b) in the volume of the skin the surface of which accommodates a work tool at a temperature of T=+30°C at time moment t=30s

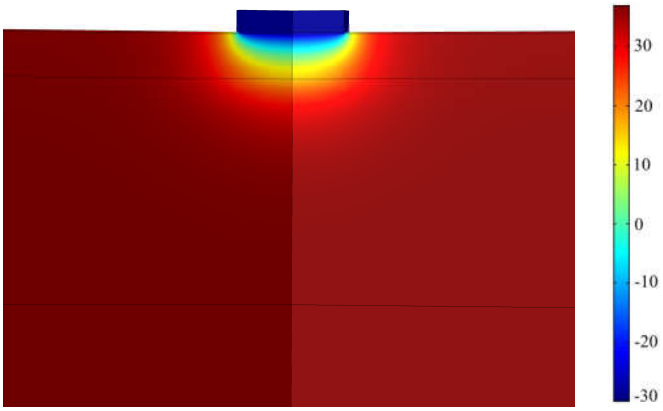

a)

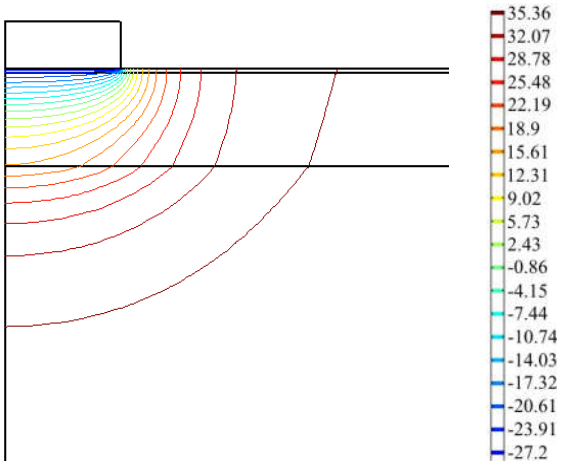

b)

Fig.2. Distribution of temperature (a) and isothermal surfaces (b) in the volume of the skin the surface of which accommodates a work tool at a temperature of T=-30°C at time moment t=60s

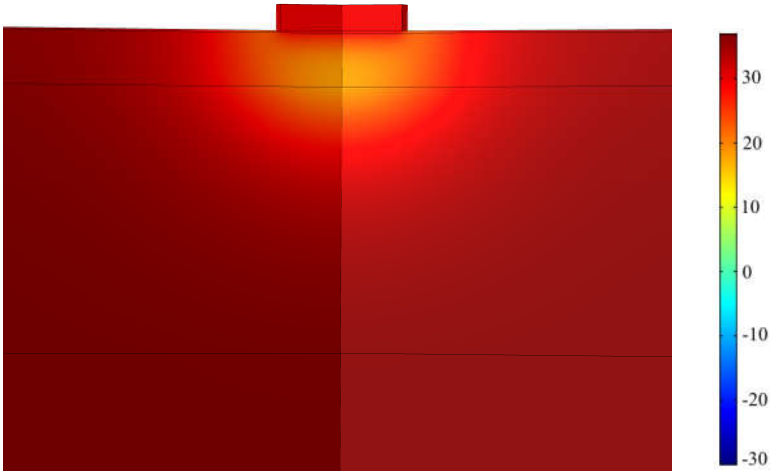

a)

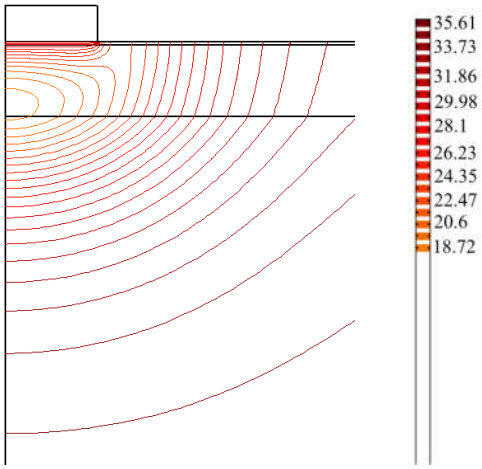

b)

Fig.3. Dostribution of temperature (a) and isothermal surfaces (b) in the volume of the skin the surface of which accommodates a work tool at a temperature of T=+30°C at time moment t=210s

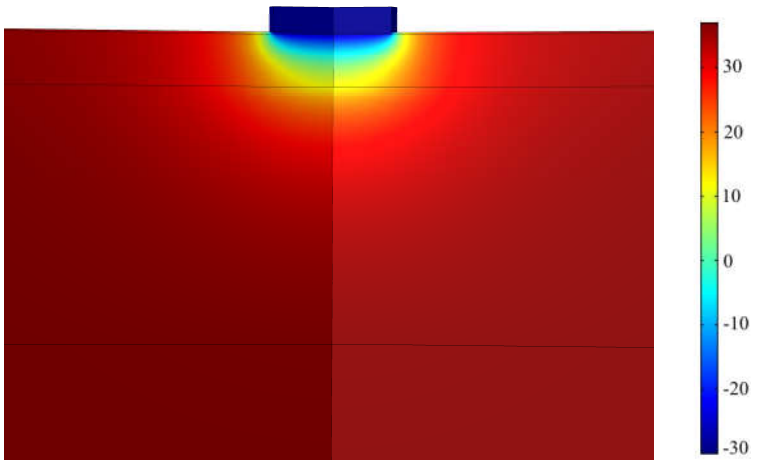

a)

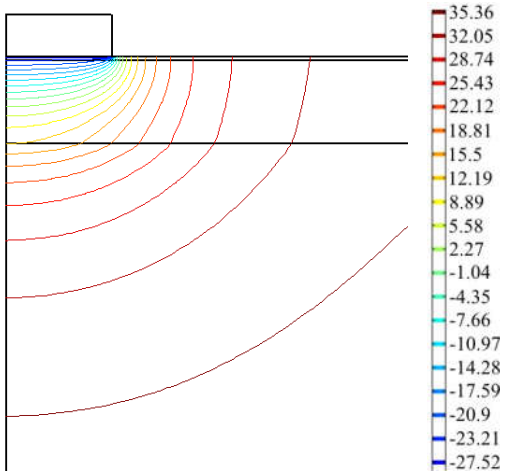

b

Fig.4. Distribution of temperature (a) and isothermal surfaces (b) in the volume of the skin the surface of which accommodates a work tool at a temperature of T=-30°C at time moment t=240s

From Fig.1, 2 it can be seen that at t = 30 s the epidermis warms up to a temperature of 28.7° C, and at t = 60 s the temperature in the epidermis decreases to -28.8° C. Since the top layer of skin (epidermis) has the smallest thickness and perfusion of blood in it, the temperature inside this layer is close to the temperature of the work tool. At the epidermis-dermis boundary, the temperature is 23.9° C, at the dermis-subcutaneous fat boundary the temperature is 15.6° C. Subsequently, with repeated cyclic temperature exposure, it is observed that at t = 210 s after cooling, the temperature inside the skin, for example, at the dermis-subcutaneous fat boundary, reaches 18° C, which contributes to the rapid expansion of blood vessels, blood flow to the surface layers of the skin and improves metabolism (Fig. 3, 4). At t = 240 s, better cooling of the skin occurs: at the epidermis-dermis boundary the temperature is -24.2° C, at the dermis-subcutaneous fat boundary the temperature is 8.8° C. It has been found that with increasing temperature exposure, a deeper cooling of skin layers is achieved. That is, with prolonged temperature exposure (T = -30° C), destruction of near-surface skin neoplasms can be achieved [8].

It should be noted that the cyclic temperature effect on human skin considered in this work is highly effective in treating certain skin diseases and eliminating cosmetic skin defects [18 – 20]. Under the influence of low temperatures, first, there is a short-term sharp narrowing of the skin vessels, which is then quickly replaced by their expansion due to the activation of adrenergic fibers. This, in turn, contributes to an increase in the rate of metabolic processes inside the tissues and cell regeneration occurs, and blood flow increases, supplying oxygen and nutrients to the cells. Active metabolism inside the tissues leads to the renewal of the organism at the cellular level, saturation of cellular structures with nutrients, oxygen, stimulates metabolic processes at the cellular level. Contrast cyclic temperature changes stimulate the vascular tone of the dermis, increase pulmonary ventilation and oxygen utilization, increase tissue respiration.

The results obtained make it possible to predict the depth of freezing of layers of human skin at a given cyclic temperature effect to achieve the maximum effect during cryomassage or cryodestruction. The developed method of computer simulation in the unsteady mode allows us to determine the temperature distribution in different layers of human skin with a predetermined arbitrary function of changing the temperature of the work tool with time $T_f(t)$. It should also be noted that the above results will be the basis for the development of the design of a modernized thermoelectric device for treating skin diseases.

Conclusion

1. The method of computer simulation of temperature distribution in human skin is developed, which enables to predict the results of local temperature effect on the skin and determine the temperature distribution in different skin layers with a predetermined arbitrary temporal function of change in work tool temperature $T_f(t)$.
2. By way of example, computer simulation was used to determine temperature distributions in different skin layers in cooling and heating modes with a change in work tool temperature by the law $T_f(t) = A\cos\omega t$ in the temperature range [-30÷+30]°C. The results obtained give an opportunity to predict the depth of freezing of biological tissue at a given cyclic temperature effect.

References

1. *Dermatologiia, venerologiia. Uchebnik [Dermatology, venerology. Textbook]*. Stepanenko V.I. (Ed.). Kyiv: 2012 [in Russian].
2. Akhtiamov S.N., Butov Yu.S. (2003). *Prakticheskaia dermatokosmetologiia. Uchebnoie posobiie. [Practical dermacosmetology. Manual]*. Moscow: Meditsina [in Russian].
3. Burenina I.A. (2014). Sovremennyie metodiki krioterapii v klinicheskoi praktike [Modern cryotherapy methods in clinical practice]. *Vestnik sovremennoi klinicheskoi meditsiny – Bulletin of Modern Clinical Medicine*, 7, 1, 57 – 61 [in Russian]
4. Deonizio J., Werner B., Fabiane A. Mulinari-Brenner. (2014). *Histological comparison of two cryopeeling methods for photodamaged skin.* Hindawi Publishing Corporation, 2014, 1–5.
5. Mourot L., Mourot L., Cluzeau C., Regnard J. (2007). Hyperbaric gaseous cryotherapy: effects on skin temperature and systemic vasoconstriction. *Archives of physical medicine and rehabilitation, November* 2007, 1339 – 1343.
6. Zemskov V.S., Gasanov L.I. (1988). *Nizkiie temperatury v meditsine [Low temperatures in medicine]*. Kyiv: Naukova dumka [in Russian].
7. Hryshchenko V.I., Sandomyrskyi B.P., Kolontai Yu.Yu. (1987). *Prakticheskaia kriomeditsina [Practical cryomedicine]*. Kyiv: Zdorovie [in Russian].
8. H. Bause. (2004). Kryotherapie lokalisierter klassischer, Neues Verfahren mit Peltier-Elementen (–32°C) Erfahrungsbericht Hamangiome. Monatsschr Kinderheilkd – 2004. 152:16–22.
9. Ponomarenko G.N. (2002). *Fizioterapiia v kosmetologii [Physiotherapy in cosmetology]*. St.Petersburg: Voienno-Meditsinskaia Akademia [in Russian].
10. Zadorozhnyi B.A. (1985). *Krioterapiia v dermatologii (Biblioteka practicheskogo vracha). [Cryotherapy in dermatology (Library of practicing physician)]*. Kyiv: Zdorovie [in Russian].
11. Anatychuk L.I., Vikhor L.M., Kotsur M.P., Kobylianskyi R.R., Kadeniuk T.Ya. (2016). Optimal control of time dependence of cooling temperature in thermoelectric devices. *J.Thermoelectricity,* 5, 5-11.
12. Anatychuk L.I., Kobylianskyi R.R., Kadeniuk T.Ya. (2017). Computer simulation of local thermal effect on human skin. *J. Thermoelectricity*, 1, 66 – 75.
13. Anatychuk L.I., Vikhor L.M., Kobylianskyi R.R., Kadeniuk T.Ya. (2017). Computer simulation and optimization of the dynamic operating modes of thermoelectric device for treatment of skin diseases. *J.Thermoelectricity*, 2, 44-57.
14. Anatychuk L.I., Vikhor L.M., Kobylianskyi R.R., Kadeniuk T.Ya., Zvarych O.V. (2017). Computer simulation and optimization of the dynamic operating modes of thermoelectric reflexotherapy device. *J.Thermoelectricity*, 3, 68-78.

15. L. Anatychuk, L. Vikhor, M. Kotsur, R. Kobylianskyi, T. Kadeniuk. (2018). Optimal control of time dependence of temperature in thermoelectric devices for medical purposes. *International Journal of Thermophysics.* 39:108. https://doi.org/10.1007/s10765-018-2430-z.
16. Pennes H.H. (1948). Analysis of tissue and arterial blood temperatures in the resting forearm *J. Appl. Physiol*. 1 (2), 93 – 122.
17. COMSOL Multiphysics User's Guide // COMSOLAB. 2010. 804 p.
18. Anatychuk L.I., Denisenko O.I., Kobylianskyi R.R., Kadeniuk T.Ya. (2015). On the use of thermoelectric cooling in dermatology and cosmetology. *J.Thermoelectrcity*, 3, 57-71.
19. Kobylianskyi R.R., Kadeniuk T.Ya. (2016 Pro perspektyvy vykorystannia termoelektryky dlia likuvannia zakhvoriuvan shkiry kholodom [On the prospects of using thermoelectricity for treatment of skin diseases with cold]. *Naukovy visnyk Chernivetskogo universitetu: zbirnyk naukovykh ptrats. Fizyka. Elektronika - Scientific Bulletin of Chernivtsi University: Collection of Scientific Papers. Physics. Electronics,* 5, 1, 67 – 72 [in Ukrainian].
20. Anatychuk L.I., Denisenko O.I., Kobylianskyi R.R., Kadeniuk T.Ya., Perepichka M.P. (2017). Modern methods of cryotherapy in dermatological practice. *Klinichna ta etsperymentalna patologiia- Clinical and Experimental Pathology,* XVI, 1 (59), 150-156 [in Ukrainian].

Submitted 16.05.2018

Анатичук Л.І. *ак. НАН України*,[1.2]
Кобилянський Р.Р. *канд. фіз.-мат. наук*[1,2]

[1]Інститут термоелектрики, вул. Науки, 1;Чернівці, 58029, Україна;
[2]Чернівецький національний університет імені Юрія Федьковича,
вул. Коцюбинського 2, Чернівці, 58012, Україна;

КОМП'ЮТЕРНЕ МОДЕЛЮВАННЯ НЕСТАЦІОНАРНОГО ТЕМПЕРАТУРНОГО ВПЛИВУ НА ШКІРУ ЛЮДИНИ

У роботі наведено результати комп'ютерного моделювання циклічного температурного впливу на шкіру людини у нестаціонарному режимі. Побудовано тривимірну комп'ютерну модель біологічної тканини з врахуванням кровообігу та метаболізму. Як приклад, розглянуто випадок, коли на поверхні шкіри знаходиться робочий інструмент, температура якого змінюється за законом $T(t) = A\cos\omega t$ *у діапазоні температур [-30÷+30]°C. Визначено розподіли температури у різних шарах шкіри людини в режимах охолодження та нагріву. Отримані результати дають можливість прогнозувати глибину промерзання біологічної тканини при заданому температурному впливі. Бібл. 20, Рис. 4.*
Ключові слова: температурний вплив, шкіра людини, нестаціонарний режим, комп'ютерне моделювання.

Анатычук Л.И.[1,2] *ак. НАН Украины*,
Кобылянский Р.Р.[1,2] *канд.физ.-мат. наук*

[1]Институт термоэлектричества, ул. Науки, 1;Черновцы, 58029, Украина;
[2]Черновицкий национальный университет имени Юрия Федьковича,
ул. Коцюбинского 2, Черновцы, 58012, Украина;

КОМПЬЮТЕРНОЕ МОДЕЛИРОВАНИЕ НЕСТАЦИОНАРНОГО ТЕМПЕРАТУРНОГО ВЛИЯНИЯ НА КОЖУ ЧЕЛОВЕКА

В работе приведены результаты компьютерного моделирования циклического температурного влияния на кожу человека в нестационарном режиме. Построена трехмерная компьютерная модель биологической ткани с учетом кровообращения и метаболизма. В качестве примера, рассмотрен случай, когда на поверхности кожи находится рабочий инструмент, температура которого изменяется по закону $T(t) = A\cos\omega t$ *в диапазоне температур [-30÷+30]°C. Определены распределения температуры в разных слоях кожи человека в режимах охлаждения и нагрева. Полученные результаты дают возможность прогнозировать глубину промерзания биологической ткани при заданном температурном влиянии. Библ.20, Рис.4.*

Ключевые слова: температурное влияние, кожа человека, нестационарный режим, компьютерное моделирование.

References

1. *Dermatologiia, venerologiia. Uchebnik [Dermatology, venerology. Textbook]*. Stepanenko V.I. (Ed.). Kyiv: 2012 [in Russian].
2. Akhtiamov S.N., Butov Yu.S. (2003). *Prakticheskaia dermatokosmetologiia. Uchebnoie posobiie. [Practical dermacosmetology. Manual]*. Moscow: Meditsina [in Russian].
3. Burenina I.A. (2014). Sovremennyie metodiki krioterapii v klinicheskoi praktike [Modern cryotherapy methods in clinical practice]. *Vestnik sovremennoi klinicheskoi meditsiny – Bulletin of Modern Clinical Medicine*, 7, 1, 57 – 61 [in Russian]
4. Deonizio J., Werner B., Fabiane A. Mulinari-Brenner. (2014). *Histological comparison of two cryopeeling methods for photodamaged skin.* Hindawi Publishing Corporation, 2014, 1–5.
5. Mourot L., Mourot L., Cluzeau C., Regnard J. (2007). Hyperbaric gaseous cryotherapy: effects on skin temperature and systemic vasoconstriction. *Archives of physical medicine and rehabilitation, November* 2007, 1339 – 1343.
6. Zemskov V.S., Gasanov L.I. (1988). *Nizkiie temperatury v meditsine [Low temperatures in medicine]*. Kyiv: Naukova dumka [in Russian].
7. Hryshchenko V.I., Sandomyrskyi B.P., Kolontai Yu.Yu. (1987). *Prakticheskaia kriomeditsina [Practical cryomedicine]*. Kyiv: Zdorovie [in Russian].
8. H. Bause. (2004). Kryotherapie lokalisierter klassischer, Neues Verfahren mit Peltier-Elementen (–32°C) Erfahrungsbericht Hamangiome. Monatsschr Kinderheilkd – 2004. 152:16–22.
9. Ponomarenko G.N. (2002). *Fizioterapiia v kosmetologii [Physiotherapy in cosmetology]*. St.Petersburg: Voienno-Meditsinskaia Akademia [in Russian].
10. Zadorozhnyi B.A. (1985). *Krioterapiia v dermatologii (Biblioteka practicheskogo vracha). [Cryotherapy in dermatology (Library of practicing physician)]*. Kyiv: Zdorovie [in Russian].
11. Anatychuk L.I., Vikhor L.M., Kotsur M.P., Kobylianskyi R.R., Kadeniuk T.Ya. (2016). Optimal control of time dependence of cooling temperature in thermoelectric devices. *J.Thermoelectricity,* 5, 5-11.
12. Anatychuk L.I., Kobylianskyi R.R., Kadeniuk T.Ya. (2017). Computer simulation of local thermal effect on human skin. *J. Thermoelectricity*, 1, 66 – 75.
13. Anatychuk L.I., Vikhor L.M., Kobylianskyi R.R., Kadeniuk T.Ya. (2017). Computer simulation and optimization of the dynamic operating modes of thermoelectric device for treatment of skin diseases. *J.Thermoelectricity*, 2, 44-57.

14. Anatychuk L.I., Vikhor L.M., Kobylianskyi R.R., Kadeniuk T.Ya., Zvarych O.V. (2017). Computer simulation and optimization of the dynamic operating modes of thermoelectric reflexotherapy device. *J.Thermoelectricity*, 3, 68-78.
15. L. Anatychuk, L. Vikhor, M. Kotsur, R. Kobylianskyi, T. Kadeniuk. (2018). Optimal control of time dependence of temperature in thermoelectric devices for medical purposes. *International Journal of Thermophysics*. 39:108. https://doi.org/10.1007/s10765-018-2430-z.
16. Pennes H.H. (1948). Analysis of tissue and arterial blood temperatures in the resting forearm *J. Appl. Physiol*. 1 (2), 93 – 122.
17. COMSOL Multiphysics User's Guide // COMSOLAB. 2010. 804 p.
18. Anatychuk L.I., Denisenko O.I., Kobylianskyi R.R., Kadeniuk T.Ya. (2015). On the use of thermoelectric cooling in dermatology and cosmetology. *J.Thermoelectrcity*, 3, 57-71.
19. Kobylianskyi R.R., Kadeniuk T.Ya. (2016 Pro perspektyvy vykorystannia termoelektryky dlia likuvannia zakhvoriuvan shkiry kholodom [On the prospects of using thermoelectricity for treatment of skin diseases with cold]. *Naukovy visnyk Chernivetskogo universitetu: zbirnyk naukovykh ptrats. Fizyka. Elektronika - Scientific Bulletin of Chernivtsi University: Collection of Scientific Papers. Physics. Electronics,* 5, 1, 67 – 72 [in Ukrainian].
20. Anatychuk L.I., Denisenko O.I., Kobylianskyi R.R., Kadeniuk T.Ya., Perepichka M.P. (2017). Modern methods of cryotherapy in dermatological practice. *Klinichna ta etsperymentalna patologiia- Clinical and Experimental Pathology,* XVI, 1 (59), 150-156 [in Ukrainian].

Submitted 16.05.2018

Anatychuk L.I. *Acad. National Academy of Sciences of Ukraine*[1,2],
Maksimuk M.V.[1], **Prybyla A.V.** *Candidate Phys.-math. Sciences*[1,2],
Rozver Yu.Yu.[1]

[1]Institute of Thermoelectricity of the NAS and MES of Ukraine,
1, Nauky str., Chernivtsi, 58029, Ukraine;
[2]Yu.Fedkovych Chernivtsi National University,
2, Kotsiubynskyi str., Chernivtsi, 58000, Ukraine,
e-mail: anatych@gmail.com

THERMOELECTRIC GENERATORS WITH FLAME HEAT SOURCES OF VARIABLE POWER AND TEMPERATURE STABILIZERS FOR THERMOPILES

In this paper, the calculations of the dynamic power of a thermoelectric generator with flame heat sources of variable power are made. The results of experimental studies of temperature operating modes of furnaces using solid fuels are presented, as well as an assessment of the possibilities of increasing the output power of a thermoelectric generator. Bibl. 8, Fig. 5.
Key words: thermoelectric generator, computer design, physical model.

Introduction

General characterization of the problem. For powering various low-power equipment chemical sources of current are generally used. However, along with the undeniable advantages, their use is associated with certain disadvantages - the presence of a self-discharge, a small service life, a limited shelf life and operation at low temperatures, as well as problems of their utilization [1, 2].

These deficiencies are lacking in thermoelectric generators (TEG) with flame heat sources on solid fuels, in particular, on firewood and pressed briquettes, which are widely used for space heating and cooking, especially in rural areas and remote regions [2, 3].

Serial production of thermoelectric generators with flame sources of heat on solid fuels is carried out by many manufacturers, including the Russian companies Kryotherm and Termofor [4, 5] who developed thermoelectric furnaces with an electrical power of 25 – 50 W designed for illuminating and powering low-power household appliances, battery charging, as well as space heating up to 50 m^2 [4, 5]. The Chinese company Thermonamic Electronics (Jiangxi) Corp., Ltd. developed a series of thermal generators with a capacity of 15 – 45 W [6]. The general approach in the development of such thermal generators is the use of thermoelectric modules made of materials based on bismuth telluride with a maximum “hot” temperature of 300 °C. However, the temperature of the surfaces of solid-fuel heat sources on which TEG is installed reaches 600 °C and constantly changes over time. This leads to a decrease in the life of the TEG and, as a result, to a rapid generator failure. To eliminate this, the thermal generator design assumes the presence of a temperature stabilizer for the hot surface of the furnace that cuts temperatures exceeding 300 °C. It is clear that this leads to a decrease in the electrical power of the TEG, because it already does not use the entire thermal power of the furnace.

In addition, as shown by temperature analysis, when designing a TEG, physical models with a constant temperature of the heat source are used, which does not correspond to the real situation. During operation

of the furnace, its surface temperature changes dynamically, which is reflected in the output power of the TEG.

The purpose of this work is to develop the theory and methods of designing a thermoelectric generator with unstable heat sources of variable power, in particular on wood.

Physical model

The calculations used a physical model of a thermoelectric generator unit (Fig. 1), which contains a heated surface of a heat source of variable power 1, a temperature stabilizer that cuts off temperatures on the hot surface of a thermoelectric generator above 300 °C 2, heat exchangers for supply 3 and removal 6 of heat flux to/from thermoelectric module 4, thermal insulation 5, electric voltage stabilizer 7 and electric energy battery 8.

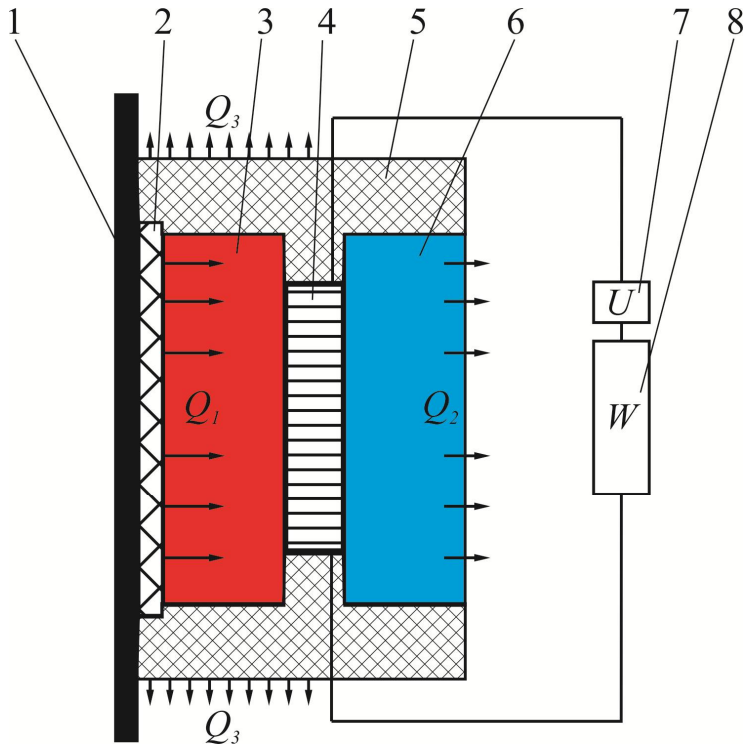

Fig. 1. Physical model of thermoelectric generator unit: 1 – heated surface; 2 – temperature stabilizer; 3 – hot heat exchanger; 4 –thermoelectric module; 5 – thermal insulation; 6 – cold heat exchanger; 7 – voltage stabilizer; 8 – electric energy battery.

Since the generator is installed on a heated surface, the model does not consider the processes of heat transfer from the actual source of combustion of fuel to this surface. Instead, to determine the temperature of the heated surface 1, the experimental temporal dependence of its temperature in the real cycle of using the solid fuel heat source is used (Fig. 3).

Mathematical and computer descriptions of the model

Thus, the equation of heat balance is used to calculate the thermoelectric generator in accordance with the physical model (Fig. 1).

On the hot side there is a heat source of variable power $Q_1[T_1(t)]$.Its thermal power depends on the temperature of this surface T_1 which, in turn, changes with time t (Fig. 3), and is given in the form of some function $f[T_1(t)]$.

$$Q_1 = f\left[\mathrm{T_1(t)}\right], \tag{1}$$

Heat supply from the heated surface to the hot side of the thermoelectric module and heat removal to the cold heat exchanger is described by the equations:

$$Q_1 = \chi_1[T_1(t) - T_H], \tag{2}$$

$$Q_2 = \chi_2[T_C - T_2], \tag{3}$$

where χ_1, χ_2 are thermal resistances of the hot and cold heat exchangers; T_H, T_C are the hot and cold side temperatures of thermoelectric module, respectively; T_2 is the temperature of the external surface of the cold heat exchanger.

Thermal power Q_2 is removed from the cold heat exchanger by forced convection of air to the environment:

$$Q_2 = \alpha(T_2 - T_0)S_m, \tag{4}$$

where α is coefficient of convective heat exchange between the surface of the heat exchanger and the environment; S_m is the area of heat exchange surface; T_0 is ambient temperature.

The electrical power generated by thermoelectric module is proportional to $Q_1[T_1(t)]$ and its efficiency η:

$$W = Q_1[T_1(t)] \cdot \eta, \tag{5}$$

The main losses of heat Q_3 occur due to thermal insulation:

$$Q_3 = \chi_4(T_M - T_0), \tag{6}$$

where χ_4 is thermal resistance of insulation, T_M is temperature of the internal surface of thermal insulation.

Thus, the equation of heat balance for the chosen model of the thermoelectric generator can be written as:

$$Q_1 = W + Q_2 + Q_3. \tag{7}$$

For the computer representation of the TEG mathematical model, the Comsol Multiphysics software package [7] was used. For this it is necessary to present our equations in the following form.

To describe the flows of heat and electricity, we will use the laws of conservation of energy

$$div\vec{E} = 0 \tag{8}$$

and electrical charge

$$div\vec{j} = 0, \tag{9}$$

where

$$\vec{E} = \vec{q} + U\vec{j}, \tag{10}$$

$$\vec{q} = \kappa\nabla T + \alpha T\vec{j}, \tag{11}$$

$$\vec{j} = -\sigma\nabla U - \sigma\alpha\nabla T. \tag{12}$$

Here $\vec{E}$ is energy flux density, $\vec{q}$ is heat flux density, $\vec{j}$ is electrical current density, U is electrical

potential, T is temperature, α, σ, κ are the Seebeck coefficient, electrical conductivity and thermal conductivity.

With regard to (10) – (12), one can obtain

$$\vec{E} = -(\kappa + \alpha^2\sigma T + \alpha U\sigma)\nabla T - (\alpha\sigma T + U\sigma)\nabla U. \quad (13)$$

Then the laws of conservation (8), (9) will take on the form:

$$-\nabla\left[(\kappa + \alpha^2\sigma T + \alpha U\sigma)\nabla T\right] - \nabla\left[(\alpha\sigma T + U\sigma)\nabla U\right] = 0, \quad (14)$$

$$-\nabla(\sigma\alpha\nabla T) - \nabla(\sigma\nabla U) = 0. \quad (15)$$

From the solution of equation (14) - (15) we obtain the distribution of physical fields, as well as the integral values of the efficiency and power of the TEG.

Experimental investigations of thermal modes of variable power heat source

To determine the actual temperature conditions on the heated surfaces of furnaces with flame heat sources on solid fuels (wood), experimental studies were carried out using the furnace shown in Fig.2.

In the course of the experiment, the dependences of the temperatures of the heated furnace surfaces on the time during which the equal amount of firewood was added at identical intervals were determined. The total experiment time was 3.2 hours. Firewood in the amount of 5 kg of willow wood was added with a time interval of 50 minutes.

Fig. 3 shows the results of measurements of the temperature of the hot surfaces of the furnace. Curves 1 and 2 in Fig. 3 correspond to the temperature of the side surfaces of the furnace, and curve 3 - the rear surface of the furnace. I, II, III, IV - intervals of time during which the addition of firewood in the furnace occurred.

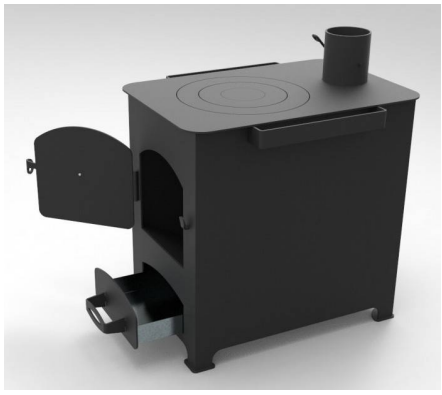

Fig. 2. External view of the furnace

As can be seen from Fig. 3, the temperature of the furnace surfaces cyclically changed according to the intervals of addition of firewood. Moreover, the temperature of the side surfaces (curves 1 and 2 in Fig. 3) does not exceed 430 ° C, and the temperature of the rear surface of the furnace (curve 3 in Fig. 3) reaches values of ~ 600 ° C.

The obtained data are processed in the form of functional temporal dependences of the temperatures of heated surfaces of the furnace and used in the calculations of characteristics of a thermoelectric generator with flame heat sources of variable power on solid fuels.

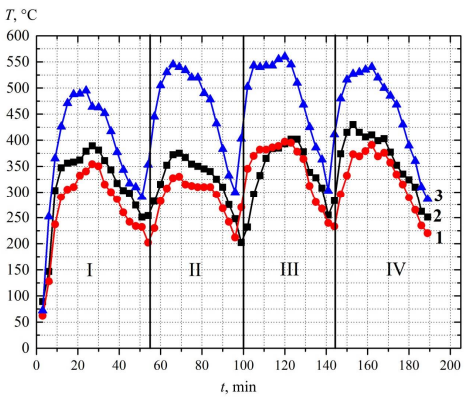

Fig. 3. Experimental temporal dependences of the temperature of heated furnace surfaces: 1, 2 – temperatures of the lateral furnace surfaces, 3 – temperature of the rear furnace surface

Description of the dynamic surfaces of TEG

Thus, using computer methods, the calculation of the dynamic powers of a TEG in terms of its installation on the lateral and rear surfaces of the furnace was carried out (Fig. 4, 5).

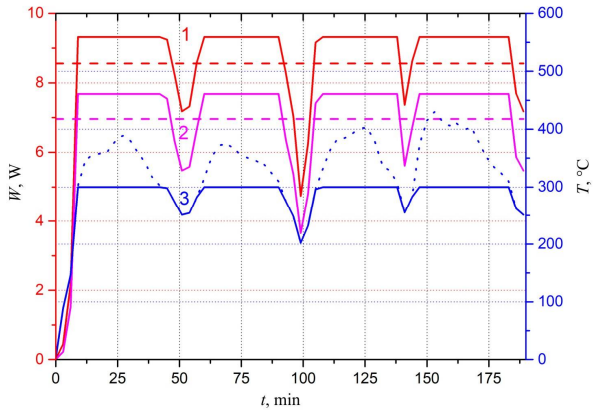

Fig. 4. Temporal dependence of the power of TEG located on the lateral surface of the furnace: 1 – TEG power at T_X=30°C , 2 – TEG power at T_X=50°C; 3 – the surface temperature of the furnace.

As thermoelectric converters for TEG, 1 ALTEC - 1061 thermoelectric module made of a material based on bismuth telluride (Bi_2Te_3) was used. The characteristics of such a module are given in [8]. Its maximum "hot" temperature is 300 ° C. Therefore, according to the physical model (Fig. 1), there is a temperature stabilizer between the surface of the hot wall and the TEG, which cuts off temperatures exceeding 300 °C.

Fig. 4 shows the temporal dependence of the power of TEG placed on the lateral surface of the furnace for the cold side temperatures of TEG T_c = 30 °C (1 in Fig. 4) and T_c = 50 °C (2 in Fig. 4). The hot side temperature of TEG is shown by the solid curve 3 in Fig. 4, and the temperature of the lateral surface of the furnace is shown by the dotted curve in Fig. 4.

As can be seen from Fig. 4, the type of the temporal dependence of the dynamic power in general reproduces the dependences of the surface temperature of the furnace. For the case of the cold side temperatures, T_c = 30 °C, the average power of a TEG consisting of one thermoelectric module for a selected period of time is 8.6 W, and for T_c = 50 ° C -7 W. At the same time, the energy generated by TEG per 1 hour is ~ 30 kJ for T_c = 30 °C and ~ 25 kJ for T_c = 50 °C.

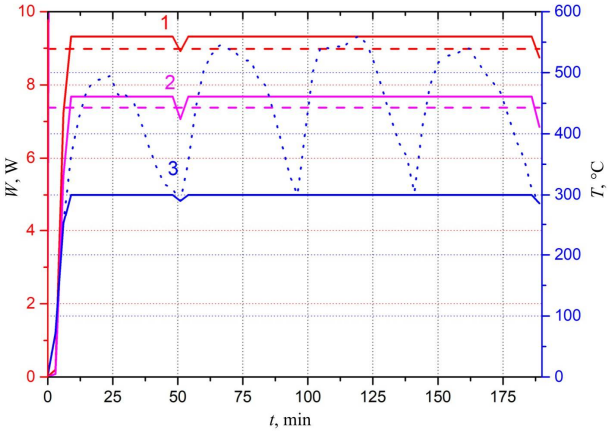

Fig. 5. Temporal dependence of a TEG located on the rear surface of the furnace: 1 – TEG power at T_X=30°C , 2 – TEG power at T_X=50°C; 3 – the surface temperature of the furnace.

Fig. 5 shows a similar dependence of the power of TEG located on the rear surface of the furnace for the cold side temperatures of TEG T_c = 30 °C (1 in Fig. 5) and T_c = 50 °C (2 in Fig. 5). The hot side temperature of the TEG is shown by the solid curve 3 in Fig. 4, and the temperature of the rear surface of the furnace is shown by the dotted curve in Fig. 4.

As can be seen from Fig. 5, the type of the temporal dependence of the dynamic power in general reproduces the dependences of the surface temperature of the furnace. For the case of the cold side temperatures, T_c = 30 °C, the average power of a TEG, consisting of one thermoelectric module, is 9 W for a selected period of time, and for T_c = 50 °C, it is -7.4 W. At the same time, the energy generated by TEG per 1 hour is ~ 32 kJ for T_c = 30 °C and ~ 27 kJ for T_c = 50 °C.

Thus, despite the significant differences between the temperatures of the side and rear walls of the furnace, the power of the TEG for the first and second cases differ only by ~ 5 %, which is associated with the use of the temperature stabilizer of the hot side of the TEG.

However, if we analyze curves 3 in Fig. 4 and 5, it becomes clear that such forced stabilization of the surface temperature of the furnace leads to significant power losses in the TEG. These losses can be estimated, because, as already noted, the type of the temporal dependence of the dynamic power in general reproduces the dependences of the surface temperature of the furnace. And if we assume that instead of the stabilized temperature (solid blue line 3 in Fig. 4 and 5) we use the entire temperature of the furnace surface (dotted blue line 3 in Fig. 4 and 5), the gain in TEG output power will be ~ 30 – 40 %.

Therefore, in order to further improve the quality of thermoelectric generators using flame heat sources of variable power for solid fuels, it is important to study the direction in which to search for opportunities to use the total heat capacity of furnaces, in particular the development of TEM from high-temperature materials, as well as the use of cascade generators optimized for necessary temperature intervals.

Conclusion

1. The experimental dependences of the dynamic temperature of the hot surfaces of the furnace for burning wood in the mode of its cyclic use have been determined.
2. Based on the experimental data, the dynamic power of TEG with flame heat sources on solid fuel with thermopile temperature stabilizers has been calculated. The average power of a TEG consisting of one thermoelectric module installed on the rear surface of the furnace, in given time interval is 9 W (at its cold side temperature T_c = 30°C).
3. It has been established that the forced stabilization of the surface temperature of the furnace leads to significant losses in the power of TEG, which reach ~ 30 – 40 %.
4. The possibilities of enhancing the quality of thermoelectric generators using flame heat sources of variable power on solid fuels, in particular, due to the development of TEG from high-temperature materials, as well as the use of cascade generators optimized for required temperature ranges have been analyzed.

References

1. Bubnov Yu.I., Orlov S.B. (2005). Germetichnyiie kmicheskiie istochniki toka: *Elementy i akkumuliatory. Oborudovaniie dlia ispytanii i ekspluatatsii. [Sealed chemical sources of current: Elements and batteries. Testing and operating equipment]*. Saint-Petersburgr: Khimizdat [in Russian].
2. Anatychuk L.I., Mocherniuk R.M., Havryliuk M.V., Andrusiak I.S. (2017). Thermoelectric generator using the heat of heated surfaces. *J.Thermoelectricity*, 2, C 84 – 95.
3. Vikhor L.M., Maksimuk M.V. (2017). Design of thermoelectric cascade modules for solid fuel TEG. *J.Thermoelectricity*, 4, 40 – 48.

4. http://www.energopech.ru
5. http://kryothermtec.com/ru
6. Thermonamic electronic (Jiangxi) Corp. Ltd. Retrieved from: http://www.thermonamic.com (application date: 05.09.2018).
7. COMSOL Multiphysics User's Guide // COMSOLAB. – 2010. – 804 p.
8. http://www.ite.inst.cv.ua

Submitted 30.04.2018

Анатичук Л.І. *акад. НАН України* [1,2],
Максимук М.В.[1], **Прибила А.В.** *канд. фіз.-мат. наук* [1,2],
Розвер Ю.Ю.[1]

[1]Інститут термоелектрики НАН і МОН України,
вул. Науки, 1, Чернівці, 58029, Україна;
[2]Чернівецький національний університет
ім. Юрія Федьковича, вул. Коцюбинського 2,
Чернівці, 58000, Україна,
e-mail: anatych@gmail.com

ТЕРМОЕЛЕКТРИЧНІ ГЕНЕРАТОРИ З ПОЛУМ'ЯНИМИ ДЖЕРЕЛАМИ ТЕПЛА ЗМІННОЇ ПОТУЖНОСТІ І СТАБІЛІЗАТОРАМИ ТЕМПЕРАТУРИ ТЕРМОБАТАРЕЙ

У роботі виконано розрахунки динамічної потужності термоелектричного генератора з полум'яними джерелами тепла змінної потужності. Наводяться результати експериментальних досліджень температурних режимів роботи печей, що використовують тверде паливо, а також оцінки можливостей підвищення вихідної потужності термоелектричного генератора. Бібл. 8, рис. 5.
Ключові слова: термоелектричний генератор, комп'ютерне проектування, фізична модель.

Анатычук Л.И. *акад. НАН Украины* [1,2],
Максимук Н.В.[1], **Прибыла А.В.** *канд. физ.-мат. наук* [1,2],
Розвер Ю.Ю.[1]

[1]Институт термоэлектричества НАН и МОН Украины,
ул. Науки, 1, Черновцы, 58029, Украина;
[2]Черновицкий национальный университет
им. Юрия Федьковича, ул. Коцюбинского 2,
Черновцы, 58012, Украина,
e-mail: anatych@gmail.com

ТЕРМОЭЛЕКТРИЧЕСКИЕ ГЕНЕРАТОРЫ С ПЛАМЕННЫМИ ИСТОЧНИКАМИ ТЕПЛА ПЕРЕМЕННОЙ МОЩНОСТИ И СТАБИЛИЗАТОРАМИ ТЕМПЕРАТУРЫ ТЕРМОБАТАРЕЙ

В работе выполнены расчеты динамической мощности термоэлектрического генератора с пламенными источниками тепла переменной мощности. Приведены результаты экспериментальных исследований температурных режимов работы печей, использующих твердое топливо, а также оценки возможностей повышения выходной мощности термоэлектрического генератора. Библ. 8, рис. 5.

Ключевые слова: термоэлектрический генератор, компьютерное проектирование, физическая модель.

References

1. Bubnov Yu.I., Orlov S.B. (2005). Germetichnyiie kmicheskiie istochniki toka: *Elementy i akkumuliatory. Oborudovaniie dlia ispytanii i ekspluatatsii. [Sealed chemical sources of current: Elements and batteries. Testing and operating equipment]*. Saint-Petersburgr: Khimizdat [in Russian].
2. Anatychuk L.I., Mocherniuk R.M., Havryliuk M.V., Andrusiak I.S. (2017). Thermoelectric generator using the heat of heated surfaces. *J.Thermoelectricity*, 2, C 84 – 95.
3. Vikhor L.M., Maksimuk M.V. (2017). Design of thermoelectric cascade modules for solid fuel TEG. *J.Thermoelectricity*, 4, 40 – 48.
4. http://www.energopech.ru
5. http://kryothermtec.com/ru
6. Thermonamic electronic (Jiangxi) Corp. Ltd. Retrieved from: http://www.thermonamic.com (application date: 05.09.2018).
7. COMSOL Multiphysics User's Guide // COMSOLAB. – 2010. – 804 p.
8. http://www.ite.inst.cv.ua

Submitted 30.04.2018

V.P.Zaykov[1], *Candidate of Tech. science*,
V.I.Mescheryakov[2], *Doctor of Tech. science*,
Yu. I. Zhuravlov[3], *Candidate of Tech. science*

[1]SHTORM Research Institute, 27, Tereshkova str., Odesa, Ukraine
[2]Odesa State Ecological University, 15, Lvivskastr,, Ukraine
[3]NationalUniversity "Odesa Maritime Academy", 8, Didrikhson str., Ukraine
e-mail: anatych@gmail.com

EFFECT OF THE VOLUMETRIC AVERAGE TEMPERATURE OF THERMOELEMENT LEG ON THE BASIC PARAMETERS, RELIABILITY INDICATORS AND DYNAMICS OF THERMOELECTRIC HEAT PUMP OPERATION

The effect of the volumetric average temperature of thermoelement leg on the basic parameters, reliability indicators and dynamics of thermoelectric heat pump operation at a given thermal load for different geometry of thermoelement legs is considered. The ratio has been determined to estimate the volumetric average temperature depending on the relative operating current corresponding to the maximum cooling capacity. It is shown that with regard to the volumetric average temperature, the cooling capacity per one thermoelement decreases, the relative temperature difference, the number of thermoelements at a given thermal load, the failure rate, the time to reach steady-state mode of operation increase. Bibl. 12, Fig. 9, Table 5.
Key words: thermoelectric cooler, volumetric average temperature, dynamics of thermoelement operation, reliability indicators, temperature difference.

Introduction

The promising outlook for thermoelectric heat pumps is due to the absence of moving parts, the independence of operation from the spatial arrangement of the product, resulting in increased reliability indicators compared to steam generator and absorption machines [1]. Small dimensions and mass, the principle of energy conversion and electrical control give a significant gain in the dynamic characteristics of thermoelectric devices [2]. At the same time, lower conversion efficiency leads to the fact that the main field of application of thermoelectric pumps are the areas of heat loaded electronics, where the requirements to weight and size and dynamic characteristics, reliability indicators of thermal mode support systems are most critical [3]. The constant toughening of requirements to onboard information systems is also transmitted to thermal mode support systems which are the inseparable part of them [4]. The operational reliability indicators of thermoelectric devices depend on the influence of external climatic [5], mechanical [6] factors, thermal load [7], design parameters [8], current operating modes [9]. Jointly addressing the issues of improving reliability and dynamic performance is a problem, since the increase in temperature gradients over time is in conflict with reliability indicators [10]. The relevance of the analysis of this problem is evident from the considerations that accelerated testing of thermoelectric devices to identify reliability indicators is carried out in switching modes, whereby the operation time is reduced by an order of magnitude. The operating conditions of high-speed thermoelectric systems ensuring the thermal conditions of heat-loaded radioelectronic elements can quickly approach these conditions.

The purpose of this work is development and analysis of mathematical model relating reliabilityindicators and dynamics of thermoelement leg to design parameters and energy indicators of thermoelectric heat pump.

Model of interrelation of reliability indicators, thermoelement leg dynamics with design and energy parameters in the heat pump mode

In some cases of thermoelectric cooling devices (TEC) design, especially in the heat pump mode ($\Delta T = 0$), it becomes necessary to estimate the volumetric average temperature of thermoelement leg that exceeds the temperature of heat-releasing junction T, which significantly affects the basic parameters, reliability indicators and dynamics of thermoelement operation.

Consider a nonlinear temperature distribution along thermoelement leg $T(x) = T$ at $x = 0$ and $T(x) = T_0$ at $x = l$ [11] which can be represented as:

$$\overline{T} = \frac{1}{l}\int_0^l \left\{ T + \frac{\Delta T_{\max}}{l} x \left[B_{\text{K}}^2 \left(1 - \frac{x}{l} \right) - \Theta \right] \right\} dx, \tag{1}$$

where $B_{\text{K}} = I/I_{\max\text{K}}$ is the relative operating current at τ, A;

I is the value of operating current at τ, A;

$I_{\max\text{K}} = \overline{e}\, T_0 / R$ is maximum operating current, A;

T_0 is the temperature of heat- absorbing layer, K;

$\overline{e}$ is the average thermoEMF of thermoelement leg, V/K;

$R = l/(\overline{\sigma}\, S)$ is the electrical resistance of thermoelement leg, Ohm;

$\overline{\sigma}$ is the average electrical conductivity of thermoelement leg, S/cm;

l, S is the height, cm, and cross-section area, cm^2, of thermoelement leg;

$\Delta T_{\max} = 0{,}5 \overline{z}\, T_0^2$ is maximum temperature difference, K;

$\overline{z}$ is the average thermoelectric material efficiency in a module, 1/K;

$\Theta = (T - T_0)/\Delta T_{\max}$ is the relative temperature difference.

Integrating expression (1), we obtain the ratio to determine the volumetric average temperature in a simpler form:

$$\overline{T} = \frac{T + T_0}{2} + \frac{B_{\text{K}}^2 I_{\max\text{K}}^2 R}{12K}, \tag{2}$$

where $K = \dfrac{\overline{æ} S}{l}$ – is heat transfer coefficient, W/K;

$\overline{æ}$ is the average thermal conductivity coefficient, W/(cm·K).

The ratio (2) can be represented as

$$\overline{T} = \frac{T_0 + T}{2} + \frac{B_{\text{K}}^2 \Delta T_{\max}}{6}. \tag{3}$$

With increasing the relative operating current B_{K}, the volumetric average temperature $\overline{T}$ increases for different geometry of thermoelement legs at $T = 300$ K in the heat pump mode (Figs. 1, 2).

From expression (2) one can determine the relative temperature difference

$$\Theta = B_{\text{K}}^2 \frac{I_{\max\text{K}}^2 R}{12K\Delta T_{\max}} = \frac{B_{\text{K}}^2}{6}. \tag{4}$$

With increasing the relative operating current B_K, the relative temperature difference for different geometry of thermoelement legs at $T = 300$ K in the heat pump mode increases (Fig. 3).

The ratio for the cooling capacity of a single-stage TEC can be written as

$$Q_0 = n I_{\max}^2 R \left(2B_{\text{K}} - B_{\text{K}}^2 - \Theta \right), \tag{5}$$

where n is the number of thermoelements.

In expression (5) instead of Θ we substitute (4) and find

$$K = \frac{Q_0}{nI^2_{\max K}R} = 2B_K - B_K^2 - B_K^2 \frac{I^2_{\max K}R}{12K\Delta T_{\max}}. \quad (6)$$

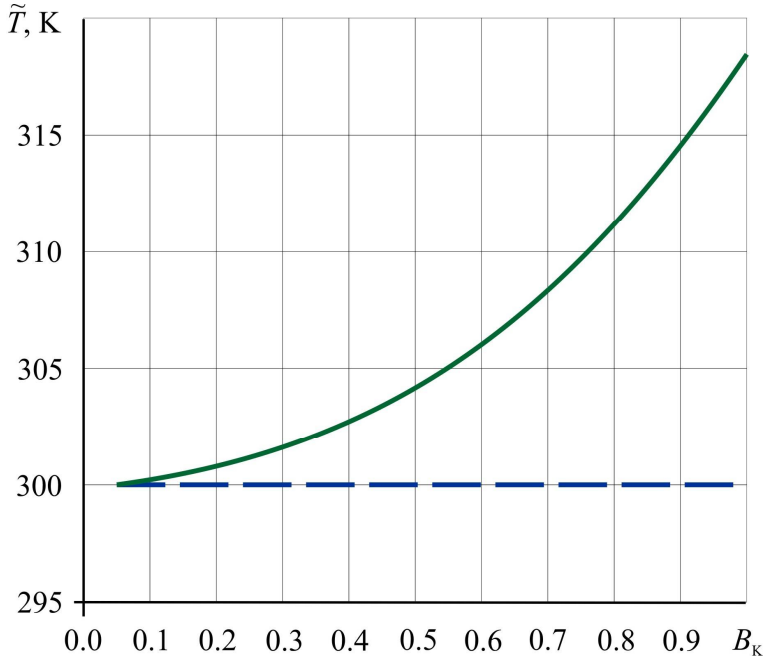

Fig. 1. Dependence of the volumetric average temperature $\tilde{T}$ of a single-stage TEC leg in the heat pump mode on the relative operating current B_K at T = 300 K: solid line– with regard to overheating; dashed line – without regard to overheating.

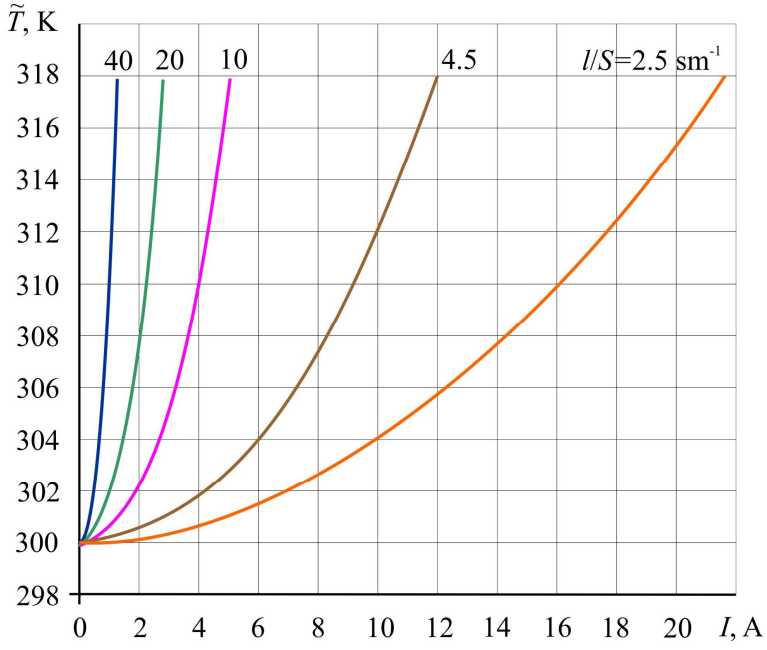

Fig. 2. Dependence of the volumetric average temperature $\tilde{T}$ of a single-stage TEC leg in the heat pump mode on the operating current I at T = 300 K for different geometry of thermoelement legs.

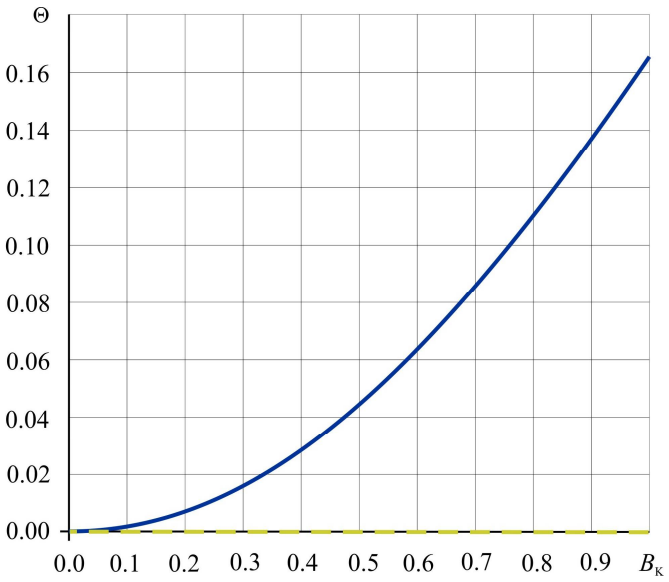

Fig. 3. Dependence of the relative temperature difference Θ of a single-stage TEC leg in the heat pump mode on the relative operating current B_K at T = 300 K: solid line – with regard to overheating; dashed line – without regard to overheating.

From the condition $\frac{dK}{dB_K} = 0$ we obtain the ratio for the optimal relative operating current B_{opt}, corresponding to maximum cooling capacity in the heat pump mode:

$$B_{\text{îïò}} = \left(1 + \frac{I^2_{\max K} R}{12 K \Delta T_{\max}}\right)^{-1} = \frac{6}{7}. \tag{7}$$

The optimal value of the relative operating current B_{opt} does not depend on the geometry of thermoelement legs.

Fig. 4 represents the dependences of cooling capacity on the relative operating current B_K with and without regard to overheating for different geometry of thermoelement legs at T = 300 K, with a given number of thermoelements n = 5.

With increasing the relative operating current B_K, functional dependence of cooling capacity Q_0 on the relative operating current B_K with regard to overheating of thermoelement legs has a maximum (Fig. 4)

In conformity with [12], the time τ to reach the steady-state operating mode of a single-stage TEC can be determined from the expression:

$$\tau = \frac{\sum_i m_i C_i}{K_K \left(1 + 2B_K \frac{\Delta T_{\max}}{T_0}\right)} \ln \frac{\gamma B_H (2 - B_H)}{2B_K - B_K^2 - \Theta}, \tag{8}$$

where $\gamma = \frac{I^2_{\max H} R_H}{I^2_{\max K} R_K}$;

$I_{maxH} = e_H T/R_H$ is maximum operating current at $\tau_H = 0$ at the beginning of the process of thermal power output, A;

$I_{maxK} = e_K T_0/R_K$ is maximum operating current at τ_K at the end of the process of thermal power output, A;

e_H, e_K is the Seebeck coefficient of thermoelement leg at the beginning and end of the process of thermal power output, respectively, V/K;

R_H, R_K is the electrical resistance of thermoelement leg at the beginning and end of the process of thermal power output, respectively, Ω;

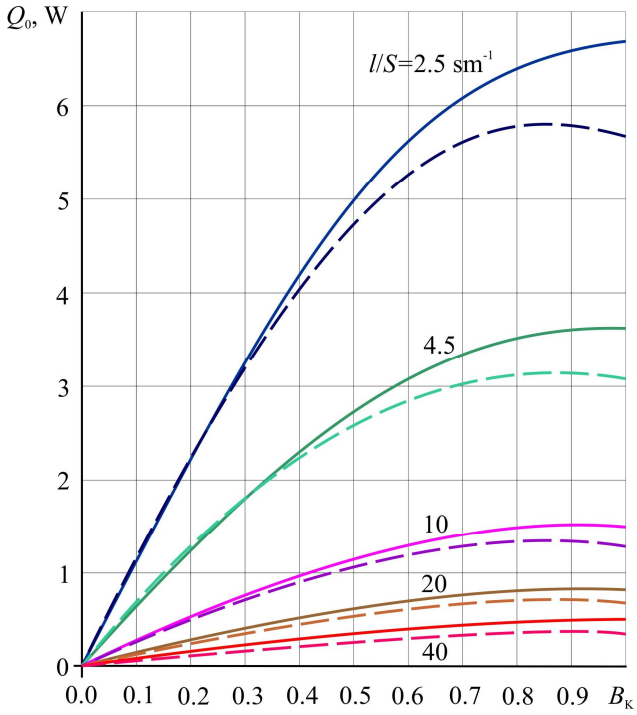

Fig. 4. Dependence of cooling capacity Q_0 of a single-stage TEC in the heat pump mode on the relative operating current B_K for different geometry of thermoelement legs at T = 300 K, n = 5: solid lines – with regard to overheating; dashed lines – without regard to overheating.

$B_H = I/I_{maxH}$ is the relative operating current at $\tau = 0$ at the beginning of the process of thermal power output;

$B_K = I/I_{maxK}$ is the relative operating current at τ_K at the end of the process of thermal power output;

$\Theta = \dfrac{\Delta T}{\Delta T_{max}}$ – is the relative temperature difference;

$\Delta T = T - T_0$ is the operating temperature difference in TEC, K;

$\sum_i m_i C_i$ – is the total value of the product of heat capacity and the mass of the components of design and technological elements of TEC.

With equal currents at the beginning and end of the process of thermal power output

$$I = B_H I_{maxH} = B_K I_{maxK}. \quad (9)$$

The number of thermoelements n can be determined from the ratio

$$n = \frac{Q_H}{I^2_{max\,K} R_K \left(2B_K - B_K^2 - \Theta\right)}, \quad (10)$$

where Q_H is thermal power output, W.

Power consumption W_K of TEC can be determined from the ratio

$$W_K = 2nI^2_{max\,K} R_K B_K \left(B_K + \frac{\Delta T_{max}}{T_0}\Theta\right). \quad (11)$$

Voltage drop U_K can be determined from the ratio

$$U_K = W_K/I. \quad (12)$$

Thermal coefficient μ can be calculated from the formula

$$\mu = Q_{\text{H}}/W_{\text{K}}. \tag{13}$$

The relative value of failure rate λ/λ_0 can be determined from the ratio [11]:

$$\lambda/\lambda_0 = nB_{\text{K}}^2\left(\Theta + C\right)\left(\frac{B_{\text{K}} + \frac{\Delta T_{\max}}{T_0}\Theta}{1 + \frac{\Delta T_{\max}}{T_0}\Theta}\right)^2 K_{T_1}, \tag{14}$$

where $C = \dfrac{Q_{\text{i}}}{nI_{\max\text{K}}^2 R_{\text{K}}}$ is the relative thermal load;

K_{T1} is the significant temperature coefficient.

The probability of failure-free operation P of TEC can be determined from the formula

$$P = \exp[-\lambda t], \tag{15}$$

where t is specified life, h.

Analysis of the model of interrelation of reliability indicators, dynamics of thermoelement legs with design energy parameters

The results of calculations of the basic parameters and reliability indicators in operation of TEC with different geometry of thermoelement legs (l/S) in the heat pump mode at given thermal load Q_0 = 5.5 W, l/S = 2.5; 4.5; 10; 20; 40 cm^{-1} and for different current operating modes are given in Tables 1–5.

Table 1

T = 300 K; $\Delta T_{\max}$ = 108 K; Q_0 = 5.5 W; $\Sigma m_i C_i = 1140\cdot10^{-4}$ J/K; $R_{\text{H}} = 2.78\cdot10^{-3}$ Ω; $R_{\text{K}} = 2.91\cdot10^{-3}$ Ω; $I_{\max\text{H}}$ = 22.0 A; $I_{\max\text{K}}$ = 21.3 A; K = $6.16\cdot10^{-3}$ W/K; l/S= 2.5 sm^{-1}

ΔT, K	B_{K}	$\overline{T}$, K	Θ	μ	W, W	U, V	n, pcs.	τ, s	I, A	B_{H}	λ/λ_0	$\lambda\cdot10^8$, 1/h	P
18.0	1.0	318*	0.167	0.393	14.0	0.66	5.0	2.16	21.3	0.969	5.0	15.0	0.9985
		300	0,0	0.417	13.2	0.62	4.17				4.17	12.5	0.99875
15.0	0.916	315*	0.139	0.444	11.4	0.59	4.88	1.83	19.5	0.886	3.45	10.3	0.99897
		300	0.0	0.466	9.3	0.48	4.20				2.53	7.58	0.99924
13.0	0.853	313*	0.120	0.480	9.8	0.54	4.85	1.62	18.2	0.827	2.55	7.65	0.99923
		300	0.0	0.500	8.2	0.45	4.27				1.94	5.83	0.99942
10.0	0.748	310*	0.093	0.546	7.62	0.48	4.94	1.31	16.0	0.724	1.48	4.44	0.99956
		300	0.0	0.626	6.57	0.41	4.45				1.174	3.52	0.99965
5.0	0.529	305*	0.046	0.680	4.30	0.38	5.70	0.80	11.3	0.512	0.360	1.07	0.999893
		300	0.0	0.735	3.95	0.35	5.35				0.306	0.92	0.999908
3.0	0.410	303*	0.028	0.750	3.05	0.35	6.70	0.55	8.7	0.397	0.127	0.38	0.999962
		300	0.0	0.795	2.84	0.33	6.40				0.112	0.337	0.999966
1.0	0.237	301*	0.009	0.860	1.53	0.31	10.20	0.18	5.0	0.229	0.014	0.041	0.9999960
		300	0.0	0.881	1.48	0.30	9.97				0.013	0.039	0.9999961

* the data obtained with regard to overheating.

Table 2

T = 300 K; ΔT_{max} = 108 K; Q_0 = 5.5 W; $\Sigma m_i C_i$ = 451.7·10^{-4} J/K; R_H = 5.0·10^{-3} Ω; R_K = 5.23·10^{-3} Ω; I_{maxH} = 12.24 A; I_{maxK} = 11.9 A; K = 3.42·10^{-3} W/K; l/S = 4.5 sm^{-1}

ΔT, K	B_K	$\overline{T}$, K	Θ	μ	W, W	U, V	n, pcs	τ, s	I, A	B_H	λ/λ_0	$\lambda\cdot10^8$, 1/h	P
18.0	1.0	318*	0.167	0.393	14.0	1.17	8.9	1.47	11.9	0.972	8.9	22.3	0.9973
		300	0,0	0.50	11.0	0.925	7.4				7.4	22.3	0.99777
15.0	0.912	315*	0.139	0.445	11.3	1.04	8.7	1.25	10.9	0.886	6.0	18.0	0.9982
		300	0.0	0.544	9.23	0.85	7.5				4.42	13.3	0.99867
13.0	0.825	313*	0.120	0.465	9.82	0.97	8.75	1.10	10.1	0.825	4.47	13.4	0.9987
		300	0.0	0.575	8.18	0.80	7.66				3.37	10.1	0.9990
10,0	0,744	310*	0,093	0,547	7,56	0,85	8,83	0,90	8,9	0,724	2,58	7,75	0,99923
		300	0,0	0,63	6,52	0,74	8,0				2,05	6,15	0,99939
5,0	0,526	305*	0,046	0,68	4,31	0,69	10,2	0,53	6,3	0,512	0,62	1,87	0,99981
		300	0,0	0,74	3,93	0,63	9,6				0,534	1,60	0,99984
3,0	0,410	303*	0,028	0,75	3,0	0,63	12,0	0,30	4,85	0,40	0,22	0,664	0,99993
		300	0,0	0,80	2,81	0,58	11,4				0,20	0,590	0,99994
1,0	0,235	301*	0,0093	0,86	1,52	0,54	18,3	0,09	2,80	0,23	0,022	0,066	0,999993
		300	0,0	0,88	1,46	0,52	17,9				0,022	0,066	0,999994
0,5	0,166	300,5*	0,0046	0,90	1,114	0,56	24,8	0,05	1,98	0,16	0,0076	0,023	0,999997
		300	0,0	0,903	1,0	0,50	24,4				0,0056	0,017	0,999998

* the data obtained with regard to overheating.

Table 3

T = 300 K; ΔT_{max} = 108 K; Q_0 = 5.5 W; $\Sigma m_i C_i$ = 175·10^{-4} J/K; R_H = 11.1·10^{-3} Ω; R_K = 11.63·10^{-3} Ω; I_{maxH} = 5.51 A; I_{maxK} = 5.34 A; K = 1.54·10^{-3} W/K; l/S = 10 sm^{-1}

ΔT, K	B_K	$\overline{T}$, K	Θ	μ	W, W	U, V	n, pcs	τ, s	I, A	B_H	λ/λ_0	$\lambda\cdot10^8$, 1/h	P
18.0	1.0	318*	0.167	0.393	14.0	2.62	19.9	1.29	5.34	0.969	19.9	59.7	0.9940
		300	0.0	0.50	11.0	2.0	16.6				16.6	41.5	0.9959
15.0	0.914	315*	0.139	0.445	11.3	2.32	19.4	1.10	4.90	0.886	13.6	40.8	0.9959
		300	0.0	0.542	9.25	1.90	16.7				9.96	29.9	0.9970
13.0	0.851	313*	0.120	0.480	9.74	0.96	19.3	0.97	4.54	0.827	10.0	30.0	0.9970
		300	0.0	0.575	8.12	0.80	16.9				7.62	22.9	0.9977
10.0	0.746	310*	0.093	0.547	7.60	1.90	19,7	0.78	4.0	0.723	5.8	17.4	0.9983
		300	0.0	0.627	6.53	1.63	17,7				4.6	13.8	0.9986
5.0	0.528	305*	0.046	0.68	4.33	1.54	22.7	0.46	2.8	0.512	1.41	4.23	0.99958
		300	0.0	0.74	3.94	1.40	21.3				1.29	3.63	0.99964
3.0	0.410	303*	0.028	0.75	3.04	1.39	26.6	0.30	2.2	0.40	0.50	1.50	0.99985
		300	0.0	0.80	2.83	1.29	25.4				0.47	1.40	0.99986
1.0	0.236	301*	0.0093	0.86	1.52	1.21	40.7	0.10	1.3	0.23	0.054	0.162	0.999984
		300	0.0	0.882	1.41	1.12	39.8				0.053	0.159	0.999984
0.5	0.167	300,5*	0.0046	0.90	1.03	1.15	55.0	0.02	0.89	0.16	0.0134	0.040	0.9999960
		300	0.0	0.916	1.0	1.13	54.2				0.0129	0.039	0.9999961

* the data obtained with regard to overheating.

Table 4

T = 300 K; ΔT_{max} = 108 K; Q_0 = 5.5 W; $\Sigma m_i C_i$ = 85.8·10^{-4} J/K; R_H = 22.2·10^{-3} Ω; R_K = 23.26·10^{-3} Ω; I_{maxH} = 2.76 A; I_{maxK} = 2.67 A; K = 0.77·10^{-3} W/K; l/S= 20 sm^{-1}

ΔT, K	B_K	$\overline{T}$, K	Θ	μ	W, W	U, V	n, pcs	τ, s	I, A	B_H	λ/λ_0	$\lambda\cdot10^8$, 1/h	P
18.0	1.0	318*	0.167	0.393	14.0	5.24	39.8	1.30	2.67	0.967	39.8	119.4	0.9881
		300	0.0	0.50	11.0	4,12	33.2				33.2	99.6	0.9900
15.0	0.914	315*	0.139	0.410	11.37	4.66	38.9	1.10	2.44	0.884	27.2	81.6	0.99187
		300	0.0	0.543	9.25	3.79	33.4				23.1	69.4	0.9931
13.0	0.851	313*	0.120	0.480	9.74	4.29	38.6	0.97	2.27	0.823	20.1	60.4	0.9940
		300	0.0	0.575	8.14	3.59	33.9				17.4	52.2	0.9948
10.0	0.741	310*	0.093	0.547	7.60	3.80	39.4	0.80	2.0	0.722	11.66	35.0	0.99650
		300	0.0	0.627	6.53	3.27	35.4				10.26	30.8	0.99692
5.0	0.528	305*	0.046	0.680	4.33	3.10	45.4	0.48	1.40	0.511	2.82	8.46	0.99915
		300	0.0	0.736	3.95	2.82	42.7				2.58	7.74	0.99923
3.0	0.410	303*	0.028	0.754	3.03	2.78	53.1	0.34	1.09	0.397	1.0	3.0	0.99970
		300	0.0	0.795	2.84	2.61	51.0				0.938	2.81	0.99972
1.0	0.236	301*	0.0093	0.860	1.52	2.41	81.5	0.16	0.63	0.229	0.108	0.324	0.9999676
		300	0.0	0.880	1.41	2.24	79.7				0.106	0.318	0.999968
0.5	0.167	300,5*	0.0046	0.900	1.03	2.31	110.0	0.07	0.45	0.162	0.027	0.080	0.9999920
		300	0.0	0.916	1,0	2.25	108.4				0.026	0.77	0.9999923

* the data obtained with regard to overheating.

Table 5

T = 300 K; ΔT_{max} = 108 K; Q_0 = 5.5 W; $\Sigma m_i C_i$ = 36.1·10^{-4} J/K; R_H = 44.4·10^{-3} Ω; R_K = 45.45·10^{-3} Ω; I_{maxH} = 1.378 A; I_{maxK} = 1.35 A; K = 0.385·10^{-3} W/K; l/S= 40 sm^{-1}

ΔT, K	B_K	$\overline{T}$, K	Θ	μ	W, W	U, V	n, pcs	τ, s	I, A	B_H	λ/λ_0	$\lambda\cdot10^8$, 1/h	P
18.0	1.0	318*	0.167	0.393	14.0	10.4	79.7	1.09	1.35	0.967	79.7	239.1	0.9764
		300	0.0	0.50	11.0	8.15	66.4				66.4	199.2	0.9803
15.0	0.914	315*	0.139	0.410	11.4	9.32	77.8	0.92	1.22	0.884	54.4	163.2	0.9838
		300	0,0	0.543	9.25	7.58	66.8				46.2	138.6	0.9862
13.0	0.851	313*	0.120	0.480	9.74	8.6	77.2	0.81	1.14	0.823	40.2	120.6	0.9880
		300	0.0	0.575	8.14	7.2	67.8				34.8	104.4	0.9895
10.0	0.746	310*	0.093	0.547	7.60	7.6	78.8	0.66	1.0	0.722	23.3	70.0	0.9930
		300	0.0	0.627	6.53	6.54	70.8				20.5	61.6	0.9939
5.0	0.528	305*	0.046	0.680	4.33	6.19	90.8	0.40	0.7	0.511	5.64	16.9	0.9983
		300	0.0	0.736	3.95	5.64	85.4				5.16	15.5	0.99845
3.0	0.410	303*	0.028	0.754	3.03	5.51	106.2	0.31	0.55	0.397	2.0	6.0	0.99940
		300	0.0	0.795	2.84	5.16	102.0				1.88	5.63	0.99944
1.0	0.236	301*	0.0093	0.860	1.52	4.90	163.0	0.12	0.31	0.229	0.22	0.65	0.999935
		300	0.0	0.880	1.41	4.55	160.0				0.21	0.64	0.999936
0.5	0.167	300.5*	0.0046	0.900	1.03	4.64	220.0	0.04	0.22	0.162	0.054	0.161	0.999984
		300	0.0	0.916	1.0	4.50	216.8				0.052	0.155	0.999985

* the data obtained with regard to overheating.

For a single-stage TEC in the heat pump mode at a given thermal load Q_0 = 5.5 W and different geometry of thermoelement legs l/S= var the functional dependence of the number of thermoelements on the relative operating current $n = f(B_K)$ when calculating with regard to overheating of thermoelement legs has a minimum at B_{opt} = 0.856; if, however, overheating is not taken into account, the extremum of function $n = f(B_K)$ is not observed (Fig. 5).

For a given value of the relative operating current B_K, the number of thermoelements n when calculating with regard to overheating of thermoelement legs increases in comparison with n, obtained without such account. For different geometry of thermoelement legs in the maximum for B_K= 1, this difference (Δn/n, %) averages 20%. At the same time, as the relative operating current decreases, the value of Δn / n decreases also.

With decreasing the relative operating current B_K:

– the value of thermal coefficient μ when calculating both with and without regard to overheating of thermoelement legs (Fig. 6). At B = 1, Δμ/μ is 22%, i.e. thermal coefficient when calculating with regard to overheating decreases by 22%. With a decrease in B_K, the value Δμ/μ decreases also. In so doing, it should be noted that the value Δμ/μ does not depend on the geometry of thermoelement legs;

– the relative value of failure rate λ/λ_0 increases (Fig. 7). With a given value of the relative operating current B, the value λ/λ_0 increases when calculating with regard to overheating. For different l/S this difference ($[\Delta\lambda/\lambda_0]/[\lambda/\lambda_0]$, %) for B = 1 is about 20%. With increasing l/S, the value λ/λ_0 increases. With decreasing the relative operating current B, the value $[\Delta\lambda/\lambda_0]/[\lambda/\lambda_0]$ decreases also;

– the probability of failure-free operation P decreases (Fig. 8). With a given value of the relative operating current B, the probability of failure-free operation P decreases when calculating with regard to overheating for different l/S. With increasing l/S, the probability of failure-free operation P decreases;

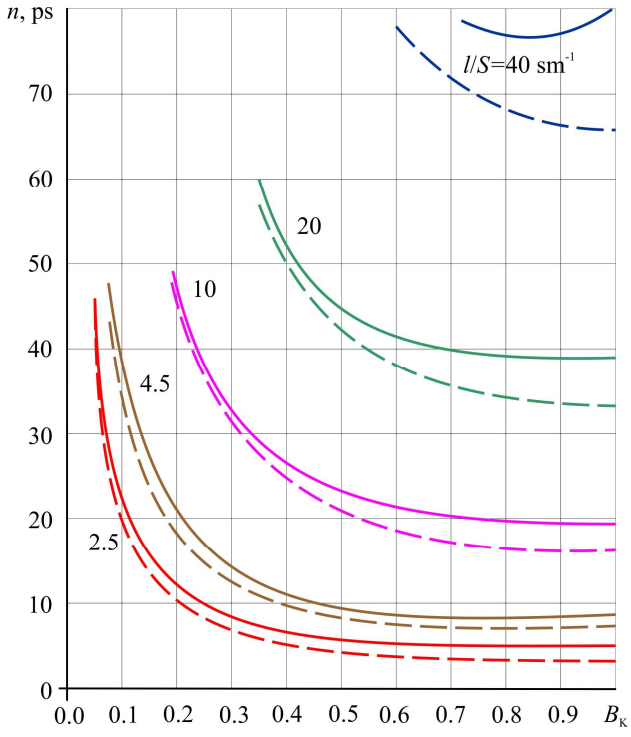

Fig. 5. Dependence of the number of thermoelements n of a single-stage TEC in the heat pump mode on the relative operating current B_K for different geometry of thermoelement legs at T = 300 K, Q_0 = 5.5 W: solid lines– with regard to overheating; dashed lines– without regard to overheating.

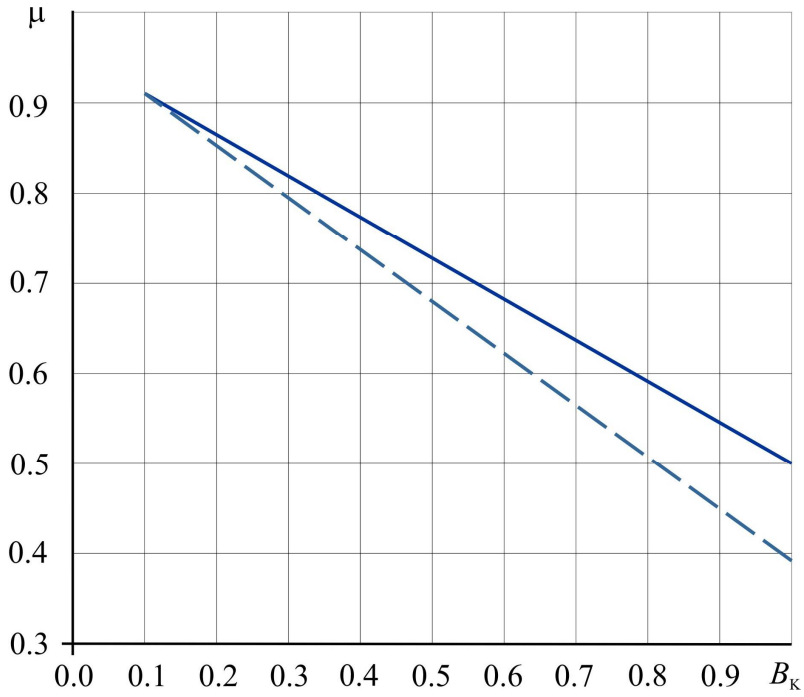

Fig. 6. Dependence of thermal coefficient μ of a single-stage TEC in the heat pump mode on the relative operating current B_K at T = 300 K, Q_0 = 5.5 W: solid line – with regard to overheating; dashed line – without regard to overheating.

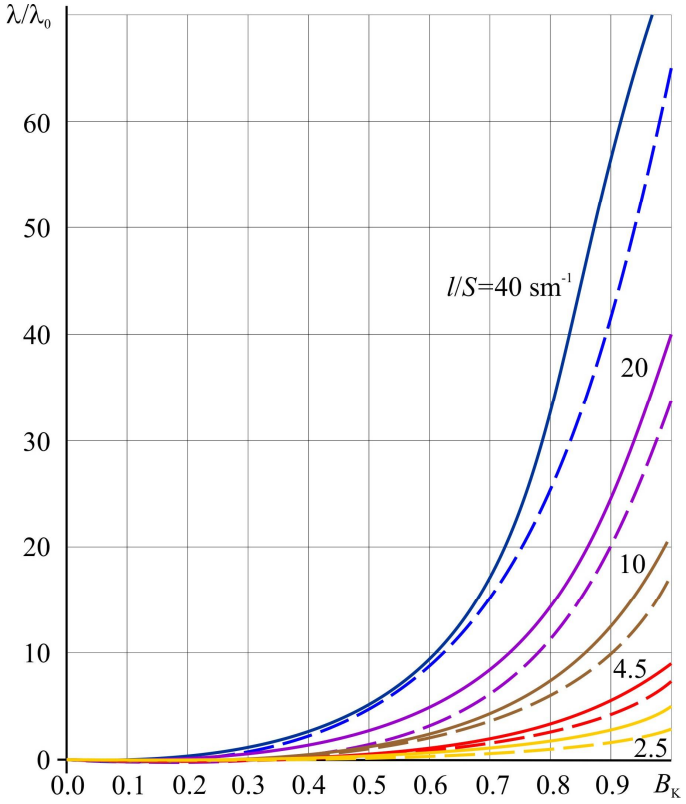

Fig 7. Dependence of relative value of failure rate λ/λ_0 of a single-stage TEC in the heat pump mode on the relative operating current B_K for different geometry of thermoelement legs at T = 300 K, Q_0 = 5.5 W: solid lines– with regard to overheating; dashed lines– without regard to overheating.

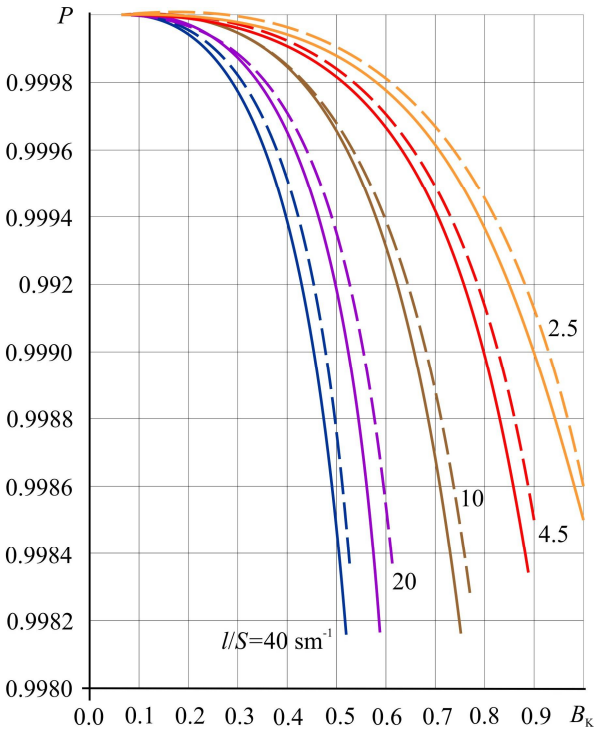

Fig. 8. Dependence of the probability of failure-free operation P of a single-stage TEC in the heat pump mode on the relative operating current B_K for different geometry of thermoelement legs at T = 300 K, Q_0 = 5.5 W, t = 10^4 h: solid lines– with regard to overheating; dashed lines– without regard to overheating.

- the time to reach the steady-state mode τ (Fig. 9) for different geometry of thermoelement legs l/S increases. For a given value of the relative operating current B_K with increasing *l/S*, the time to reach the steady-state mode τ decreases.

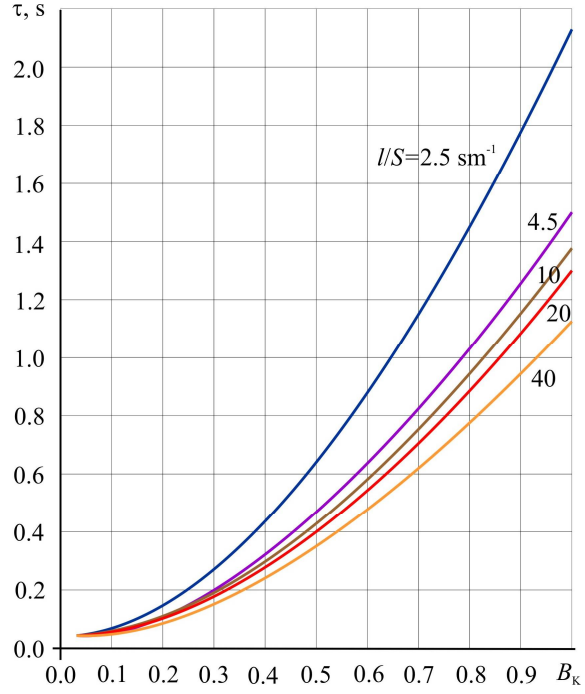

Fig. 9. Dependence of the time to reach the steady-state mode τ of a single-stage TEC in the heat pump mode on the relative operating current B_K for different geometry of thermoelement legs at T = 300 K, Q_0 = 5.5 W: solid lines– with regard to overheating; dashed lines - with regard to overheating.

Discussion of the results of analysis of the model of interrelation of reliability indicators, dynamics of thermoelement legs with design energy parameters

1) The optimum value of the relative operating current B_{opt}, corresponding to the maximum cooling capacity with regard to overheating, has been determined.

2) With increasing the volumetric average temperature at a given thermal load Q_0 = 5.5 W:

– the relative operating current B_K increases;

– the relative temperature difference Θ increases;

– the thermal coefficient μ decreases;

– the power consumption W_K increases;

– the voltage drop U_K increases;

– the number of thermoelements n decreases;

– the operating current I increases;

– the time to reach the steady-state operating mode τ increases;

– the relative value of failure rate λ/λ_0 increases;

– the probability of failure-free operation P decreases.

3) With increasing the ratio l/S characterizing the geometry of thermoelement legs, at a given value of the relative operating current B_K and heat load Q_H:

– the time to reach the steady-state operating mode τ decreases;

– the number of thermoelements n increases;

– the relative value of failure rate λ/λ_0 increases;

– the probability of failure-free operation P decreases.

4) The volumetric average temperature $\overline{T}$, the relative temperature difference Θ, the thermal coefficient μ do not depend on the geometry of thermoelement legs (l/S).

Conclusion

1. The interrelation between the volumetric average temperature $\overline{T}$ of thermoelement leg and the relative operating current B_K for various geometry of thermoelement legs is determined which allows determining the reliability indicators and the time to reach the steady-state mode.
2. It is shown that when designing thermoelectric cooling devices in the heat pump mode, it is necessary to take into account the influence of the volumetric average temperature on the basic parameters, reliability indicators and dynamics of operation.

References

1. Anatychuk L.I. (2007). The current state and some perspectives of thermoelectricity. *J.Thermoelectricity,* 2,7–20.
2. Rowe D. M. (2012). *Thermoelectrics and its Energy Harvesting. Materials, Preparation, and Characterization in Thermoelectrics*. Boca Raton: CRC Press.
3. Jurgensmeyer A. L. (2011). *High efficiency thermoelectric devices fabricated using quantum well confinement techniques*. Colorado State University.
4. Tsarev A.V., Chugunkov V.V. (2008). Investigation of thermoelectric devices characteristics for temperature control systems launch facilities. *Actual problems of Russian cosmonautics: Materials of XXXII Academic Conference on Astronautics, Moscow: The Board of RAS.*
5. Hyoung –Seuk Choi. (2011). Prediction of reliability on thermoelectric module through accelerated
6. life test and Physics –of –failure. *Electronic Materials Letters,* 7, 271.

7. Wereszczak A. A., Wang H. (2011). Thermoelectric mechanical reliability. *Vehicle Technologies Annual Merit Review and Peer Evaluation Meeting. – Arlington.*
8. Singh, R. (2008). *Experimental characterization of thin film thermoelectric materials and film deposition via molecular beam epitaxial.* University of California.
9. Ping Yang. (2010). Approach on thermoelectricity reliability of board–level backplane based on the orthogonal experiment design. *International Journal of Materials and Structural Integrity,* 4(2–4), 170–185.
10. Zaykov V., Mescheryakov V., Zhuravlov Yu. (2017). Analysis of the model of interdependence of thermoelement branch geometry and reliability indicators of the single–stage cooler. *Eastern – European Journal of Enterprise Technologies,* 1/1 (85), 26–33.
11. Zaykov V., Mescheryakov V., Zhuravlov Yu. (2018). Analysis of relationship between the dynamics of a thermoelectric cooler and its design and modes of operation. *Eastern –European Journal of Enterprise Technologies,*1/8 (91),12–24.
12. Zaikov V.P., Kinshova L.A., Moiseev V.F. (2009). *Prediction of reliability figures of thermoelectric cooling devices. Vol.1. Single-state devices.* Odessa: Politekhperiodica.
13. Zaykov V., Mescheryakov V., Zhuravlov Yu., Mescheryakov D. (2018). Analysis of dynamics and prediction of reliability indicators of a cooling thermoelement with the predefined geometry of branches. *Eastern –European Journal of Enterprise Technologies,* 5/8 (95), 41–51.

Submitted 19.04.2018

Зайков В.П. *канд. техн. наук.*[1]**,**
Мещеряков В.І. *доктор техн. наук.*[2]**,**
Журавльов Ю.І. *канд. техн. наук*[3]

[1]Науково-дослідний інститут ШТОРМ,
вул. Терешкової, 27, Одеса, Україна;
e-mail: grand@i.ua;
[2]Одеський державний екологічний університет,
вул. Львівська, 15, Україна; *e-mail: grand@ua.fm;*
[3]Національний університет «Одеська морська академія»,
вул. Дідріхсона, 8, Україна;
e-mail: zhuravlov.y@ya.ru.

ВПЛИВ СЕРЕДНЬОБ'ЄМНОЇ ТЕМПЕРАТУРИ ГІЛОК ТЕРМОЕЛЕМЕНТА НА ОСНОВНІ ПАРАМЕТРИ, ПОКАЗНИКИ НАДІЙНОСТІ ТА ДИНАМІКУ ФУНКЦІОНУВАННЯ ТЕРМОЕЛЕКТРИЧНОГО ТЕПЛОВОГО НАСОСА

Розглянуто вплив середньооб'ємної температури гілок термоелемента на основні параметри, показники надійності та динаміку функціонування термоелектричного теплового насоса за заданого теплового навантаження для різної геометрії гілок термоелементів. Визначено співвідношення для оцінки середньооб'ємної температури залежно від відносного робочого струму и відносного робочого струму, який відповідає максимуму холодопродуктивності. Показано, що з врахуванням середньооб'ємної температури зменшується холодопродуктивність на один

термоелемент, збільшується відносний перепад температури, кількість термоелементів за заданого теплового навантаження, інтенсивність відмов, збільшується час виходу на стаціонарний режим роботи. Бібл. 12, Рис. 9, Табл. 5.

Ключові слова: термоелектричний охолоджувач, середньооб'ємна температура, динаміка функціонування термоелемента, показники надійності, перепад температур.

Зайков В.П. *канд. техн. наук.*[1],
Мещеряков В.И. *доктор техн. наук.*[2],
Журавлев Ю.И.[3] *канд. техн. наук.*

[1]Научно-исследовательский институт ШТОРМ,
ул. Терешковой, 27, Одесса, Украина;
e-mail: grand@i.ua;
[2]Одесский государственный экологический университет,
ул. Львовская, 15, Одесса, Украина; *e-mail: grand@ua.fm;*
[3]Национальный университет «Одесская морская академия»,
ул. Дидрихсона, 8, Одесса, Украина;
e-mail: zhuravlov.y@ya.ru.

ВЛИЯНИЕ СРЕДНЕОБЪЕМНОЙ ТЕМПЕРАТУРЫ ВЕТВИ ТЕРМОЭЛЕМЕНТА НА ОСНОВНЫЕ ПАРАМЕТРЫ, ПОКАЗАТЕЛИ НАДЕЖНОСТИ И ДИНАМИКУ ФУНКЦИОНИРОВАНИЯ ТЕРМОЭЛЕКТРИЧЕСКОГО ТЕПЛОВОГОНАСОСА

Рассмотрено влияние среднеобъемной температуры ветви термоэлемента на основные параметры, показатели надежности и динамику функционирования термоэлектрического теплового насоса при заданной тепловой нагрузке для различной геометрии ветвей термоэлементов. Определено соотношение для оценки среднеобъемной температуры в зависимости от относительного рабочего тока и относительного рабочего тока, соответствующего максимуму холодопроизводительности. Показано, что с учетом среднеобъемной температуры уменьшается холодопроизводительность на один термоэлемент, увеличивается относительный перепад температуры, количество термоэлементов при заданной тепловой нагрузке, интенсивность отказов, увеличивается время выхода на стационарный режим работы. Библ. 12, Рис. 9, Табл. 5

Ключевые слова: термоэлектрический охладитель, среднеобъемная температура, динамика функционирования термоэлемента, показатели надежности, перепад температур.

References

1. Anatychuk L.I. (2007). The current state and some perspectives of thermoelectricity. *J.Thermoelectricity,* 2,7–20.
2. Rowe D. M. (2012). *Thermoelectrics and its Energy Harvesting. Materials, Preparation, and Characterization in Thermoelectrics*. Boca Raton: CRC Press.
3. Jurgensmeyer A. L. (2011). *High efficiency thermoelectric devices fabricated using quantum well confinement techniques*. Colorado State University.

4. Tsarev A.V., Chugunkov V.V. (2008). Investigation of thermoelectric devices characteristics for temperature control systems launch facilities. *Actual problems of Russian cosmonautics: Materials of XXXII Academic Conference on Astronautics, Moscow: The Board of RAS.*
5. Hyoung –Seuk Choi. (2011). Prediction of reliability on thermoelectric module through accelerated life test and Physics –of –failure. *Electronic Materials Letters,* 7, 271.
6. Wereszczak A. A., Wang H. (2011). Thermoelectric mechanical reliability. *Vehicle Technologies Annual Merit Review and Peer Evaluation Meeting. – Arlington.*
7. Singh, R. (2008). *Experimental characterization of thin film thermoelectric materials and film deposition via molecular beam epitaxial.* University of California.
8. Ping Yang. (2010). Approach on thermoelectricity reliability of board–level backplane based on the orthogonal experiment design. *International Journal of Materials and Structural Integrity,* 4(2–4), 170–185.
9. Zaykov V., Mescheryakov V., Zhuravlov Yu. (2017). Analysis of the model of interdependence of thermoelement branch geometry and reliability indicators of the single–stage cooler. *Eastern – European Journal of Enterprise Technologies,* 1/1 (85), 26–33.
10. Zaykov V., Mescheryakov V., Zhuravlov Yu. (2018). Analysis of relationship between the dynamics of a thermoelectric cooler and its design and modes of operation. *Eastern –European Journal of Enterprise Technologies,*1/8 (91),12–24.
11. Zaikov V.P., Kinshova L.A., Moiseev V.F. (2009). *Prediction of reliability figures of thermoelectric cooling devices. Vol.1. Single-state devices.* Odessa: Politekhperiodica.
12. Zaykov V., Mescheryakov V., Zhuravlov Yu., Mescheryakov D. (2018). Analysis of dynamics and prediction of reliability indicators of a cooling thermoelement with the predefined geometry of branches. *Eastern –European Journal of Enterprise Technologies,* 5/8 (95), 41–51.

Submitted 19.04.2018

M.V.Maksimuk

M.V. Maksimuk

Institute of Thermoelectricity of the NAS and MES of Ukraine,
1, Nauky str, Chernivtsi, 58029, Ukraine;
e-mail: anatych@gmail.com

FIELD RESEARCH ON A THERMOELECTRIC STARTING PRE-HEATER FOR CARS

The results of research on a thermoelectric starting pre-heater for a car under low ambient temperatures are presented. The diagram of connecting the heater to the car cooling system and the arrangement of its functional components on a vehicle are described. The thermal modes of internal combustion engine and the operating modes of car battery which are provided by a thermoelectric starting pre-heater are considered. The results of research on the rationality of using thermoelectric starting pre-heaters during operation of vehicles in climatic zones with low air temperatures are given. Bibl. 15, Fig. 12.

Key words: starting pre-heater, thermoelectric generator.

Introduction

One of the promising methods of solving the problem of battery discharge during pre-start heat preparation of vehicle engines is the use of electric energy sources for pre-start heaters [1 – 6]. This idea is the basis of research performed at the Institute of Thermoelectricity aimed at creating thermoelectric starting pre-heaters for car engines [7 – 11]. As a result of the research, an experimental sample of a thermoelectric pre-heater on diesel fuel with a thermal power of 3 kW was developed for pre-heating internal combustion engines with a displacement of up to 4 liters.

The heater comprises a thermoelectric generator of electric power 80-100 W which operates from the heat of starting pre-heater and provides for power supply to its components. Moreover, the excess electric energy of thermal generator can be used to recharge the car battery which was proved by the experimental bench tests of the heater [12]. However, in the course of bench tests it is impossible to take into account a number of key factors which will inevitably take place during operation of the heater on a vehicle, namely impact of low temperatures on the structural elements and functional opportunities of the heater, heat removal from the engine, the loss of heat on the hydraulic system elements. Therefore, in order to confirm the efficiency of a thermoelectric heater in real operating conditions, field tests become relevant.

The purpose of this work is to study the thermal and electrical characteristics of a thermoelectric starting pre-heater on a car under low ambient temperatures.

Connection diagram and measurement procedure

The work of a thermoelectric starting pre-heater was studied on a “Mercedes” car with the engine displacement 2.8 l. The diagram of connecting a thermoelectric pre-heater to the car is shown in Fig. 1.

A thermoelectric heater was installed in the engine compartment between the wheel niche and the front bumper with a support bracket which was fixed to the car frame.

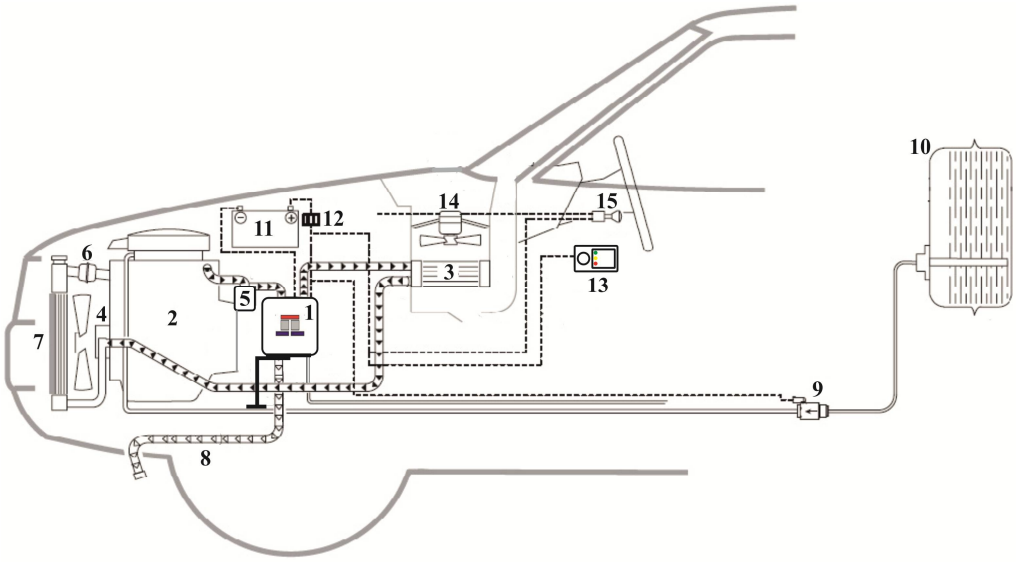

Fig.1. Diagram of connecting a thermoelectric starting pre-heater to the car:
1 – thermoelectric starting pre-heater; 2 – engine; 3 – heating system radiator;
4 – standard liquid car pump; 5 – circulating liquid heater pump;
6 – cooling liquid thermostat; 7 – radiator; 8 – collector of heater exhaust gases;
9 – heater fuel pump; 10 – fuel tank; 11 –battery;
12 – fuse block; 13 – heater control panel;
14 – heating system fan; 15 – circuit breaker for heating system fan.

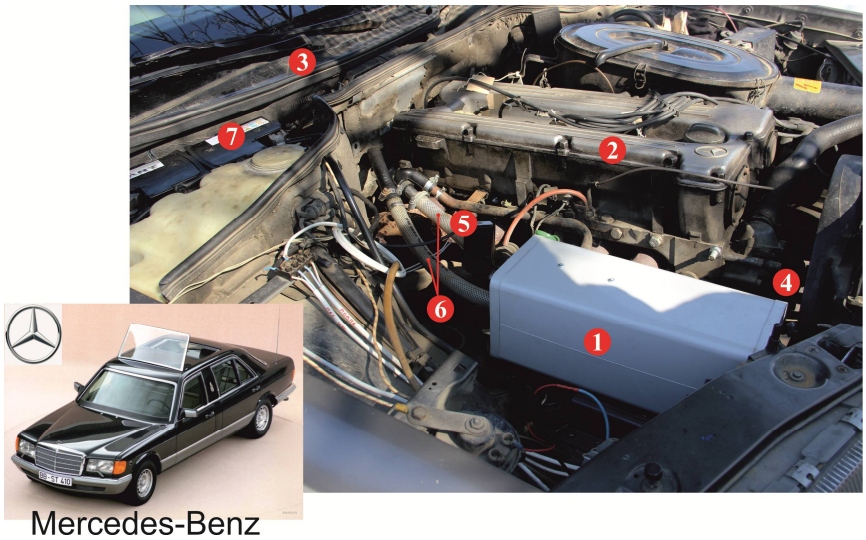

Fig.2. Thermoelectric starting pre-heater on a "Mercedes" car:
1 – thermoelectric starting pre-heater; 2 – engine; 3 – top panel of radiator heating system;
4 – standard liquid car pump; 5 – circulating liquid heater pump;
6 – connecting hoses; 7 – battery.

In the hydraulic circuit of the car, the heater was positioned between the engine and the compartment heating system, so that the liquid coolant, moving along the small cooling circuit ("engine-heating radiator-standard pump") from the heater outlet came to the engine entrance (Fig. 2). In this case, the circulating pump was connected by the side of injection to the engine entrance. Connection of the heater to the hydraulic system was carried out by gas-oil-resistant hoses.

Diesel fuel to the heater was fed from a separate tank, which, together with the fuel pump, was placed in the luggage compartment of the car (Fig. 3*a*). With the help of electric wires and fuel lines, the fuel pump was connected to the heater mounted under the hood (Fig.3*b*).

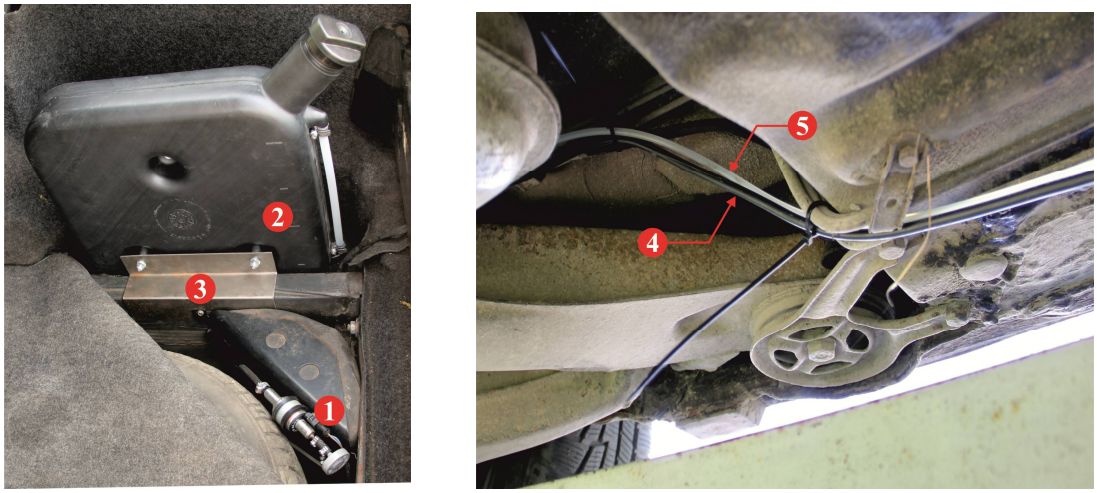

a) *b)*

Fig.3. Arrangement of fuel tank and fuel pump (a),electric wires and fuel lines (b):
1 – heater fuel pump; 2 – fuel tank;3 – mounting bracket; 4 – electrical wire; 5 – fuel line.

The heater control panel was placed in the passenger compartment under the on-board control panel (Fig. 4). The control panel was connected to the heater by an electric loop drawn from the engine compartment, from the place where the heater was installed, to the interior, past the lateral inner side of the car frame.

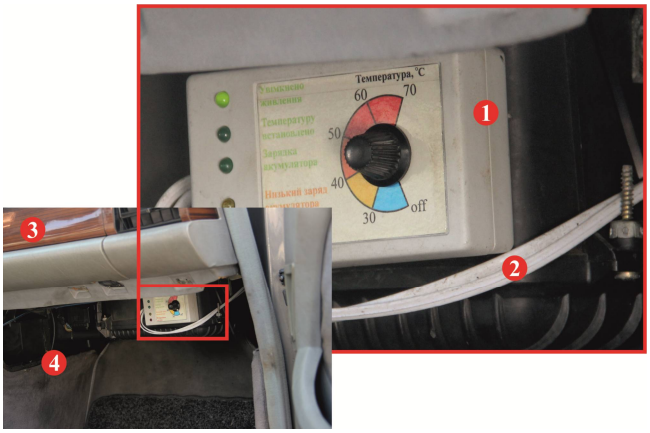

Fig.4. Arrangement of control panel:1 – heater control panel; 2 – electrical loop switch;
3 – onboard control system; 4 – car compartment.

A thermoelectric heater was connected to the car battery through the fuse block. The waste gas of the heater was carried outside the vehicle by the exhaust collector.

In the course of field research, the engine temperature and the voltage and current of the car battery were measured. Schemes of measurement of these values are shown in Fig. 5 – 6.

The engine temperature was measured by chromel-alumel thermocouples (TXA3), which were fixed under cylinder head. To determine the loss of heat on the hydraulic system elements, the temperature of the coolant at the outlet of the heater (thermocouple THA1) and at the entrance to the engine of the car (thermocouple THA2) were additionally measured. Thermal measurements were performed at ambient temperatures T_0 = (0; -5; -10) °C.

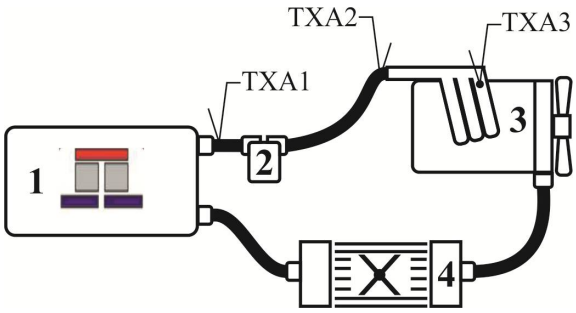

Fig. 5. Thermal measurement circuit:1 – thermoelectric heater; 2 – circulating liquid pump; 3 – internal combustion engine; 4 – heating system radiator.

The modes (charging / discharging) of the battery during the operation of a thermoelectric pre-heater were estimated at the output voltage of the battery, which was taken directly from its terminals and current strength in the "heater-battery" circuit. The moment of switching on battery charging mode was recorded by changing the direction of the current in the circuit and the corresponding LED signal on the heater control panel.

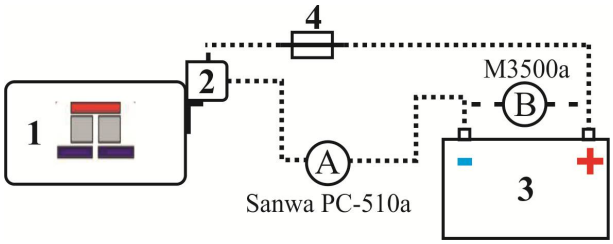

Fig. 6. Electrical measurement circuit: 1 – thermoelectric heater; 2 – heater electronic block;3 – battery; 4 – fuse block.

In order to determine fuel saving which is provided by engine pre-heating, fuel consumption studies were carried out when the vehicle was warmed up at idle speed.

Results

Fig.7 shows the experimentally determined dependences of engine warm-up temperature T_E on the operation time of a thermoelectric starting pre-heater t at ambient temperatures T_0 = (-10; -5; 0) °C.

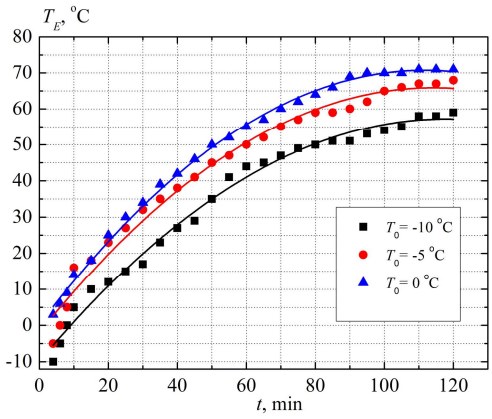

Fig.7. Dependence of car engine warm-up temperature T_E on the operation time t of a thermoelectric starting pre-heater at various ambient temperatures T_0.

From the above data it is clear that a thermoelectric heater provides pre-heating of engine car to temperature T_E = ~70 °C which is optimal for its start at ambient temperatures $T_0 \geq$ -5 °C in 100 - 110 minutes of its operation. Temperature loss in the "heater-engine" circuit of the hydraulic system is ~5 °C (Fig. 8).

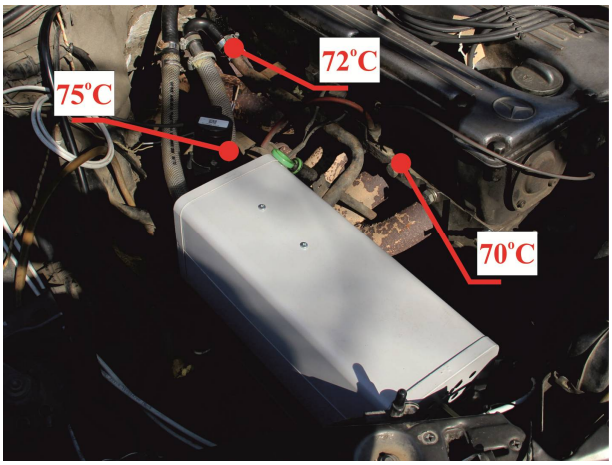

Fig.8. Temperature distribution in the "heater-engine" circuit. T_0 = -5 °C.

Fig. 9 shows the operating modes of a car battery that are assured by a thermoelectric heater in the pre-start period.

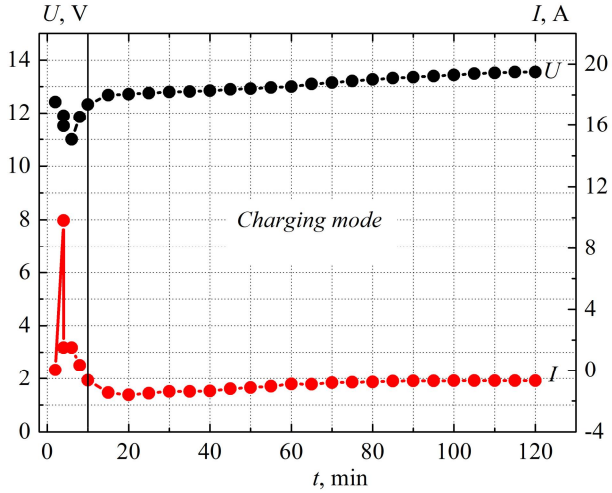

Fig.9. Dependence of voltage U on the battery and current I in "heater-battery" circuit on the operation time t of a thermoelectric starting pre-heater. T_0 = -5 °C.

As is seen from Fig. 9, after the heater is started, its components are powered from the battery. Battery discharge mode lasts until the moment when generator power output is equal to power consumption of the components. Following that, the electron control unit switches off battery power of components – the heater goes over to autonomous operating mode. As the electric power output of the generator increases, the electronic unit directs electric energy excess to recharge the battery [13, 14].

The charging mode of the battery is switched on in the tenth minute of operation of the heater, and already at the twentieth minute the charge current I reaches its maximum I = ~ 2 A. The voltage level on the car battery at the moment of charging is 12 V, and as the heater goes over to the steady-state mode, it rises to 14 V. Hence, the maximum power used to charge the battery in this case is 30 Watts. In the future, the level of electrical power of the thermal generator, which is consumed by the battery, is reduced to

10 W, which is due to both warm-up of the engine cooling liquid, and to the increase in the charge level of the battery itself.

It should be noted that for each particular application, the electric power used for recharging will be different, since it will be determined by the individual charge level of the battery (Fig. 10) [15].

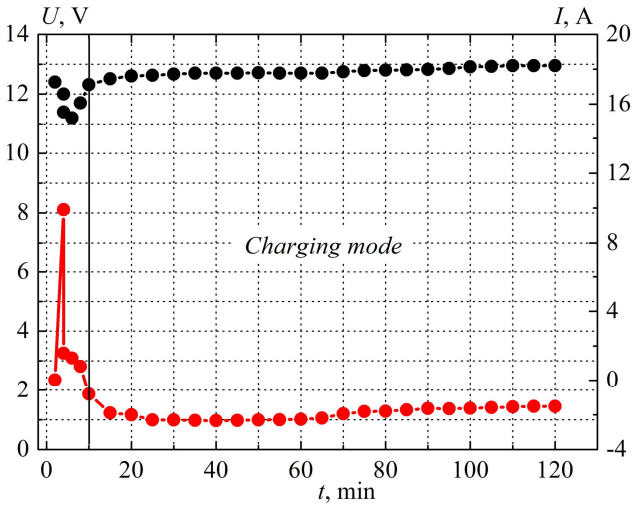

a)

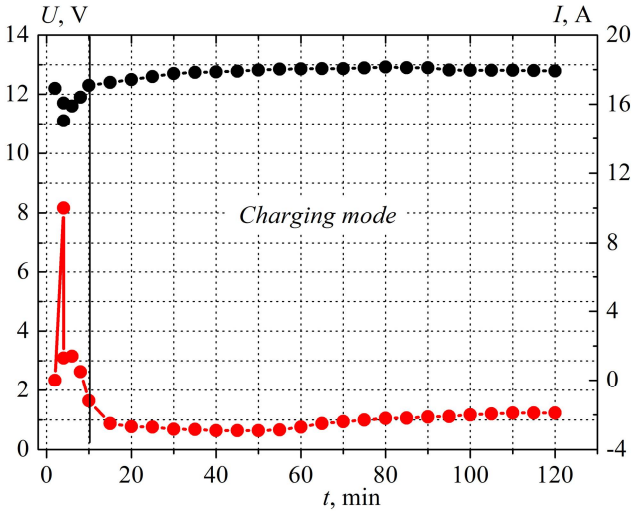

b)

Fig.10. Dependence of voltage U on the battery and current I in the "heater-battery" circuit on the operation time t of a thermoelectric starting pre-heater.
a) T_0 = -0 °C; b) T_0 = -10 °C.

In the course of field tests of the heater, the thermal modes of the engine and the operating conditions of the battery were investigated when setting lower temperatures of the engine coolant from the control panel - (30 ÷ 60) ° C. In such cases, the temperature sensor of overheating actuated and the heater started to work in the mode of maintaining the set temperature of the coolant. In this case, the behavior of temperature and electrical characteristics is similar to the results of bench studies described in [12], taking into account the temperature difference in the thermal distribution of the engine hydraulic circuit, which is practically unchanged.

Comparative dependences of fuel consumption with a car warm-up at “idle speed” and in the case of using a thermoelectric heater are given in Figs. 11 – 12.

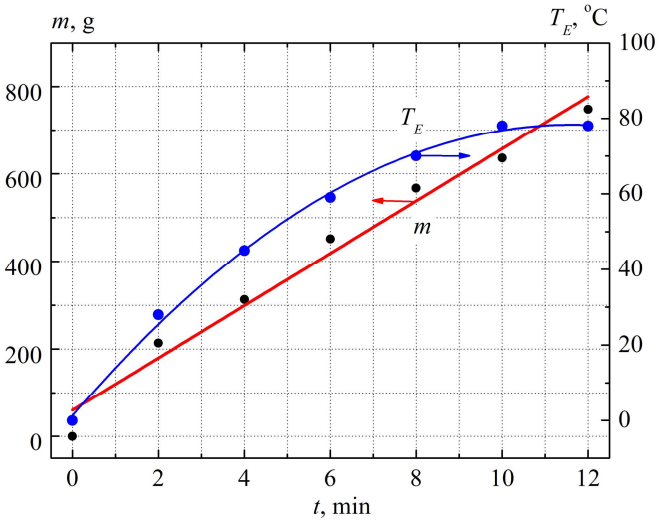

Fig.11. Dependence of the amount of spent fuel m and engine warm-up temperature T_E on the heating period t of a car “at idle speed". T_0 = 0 °C.

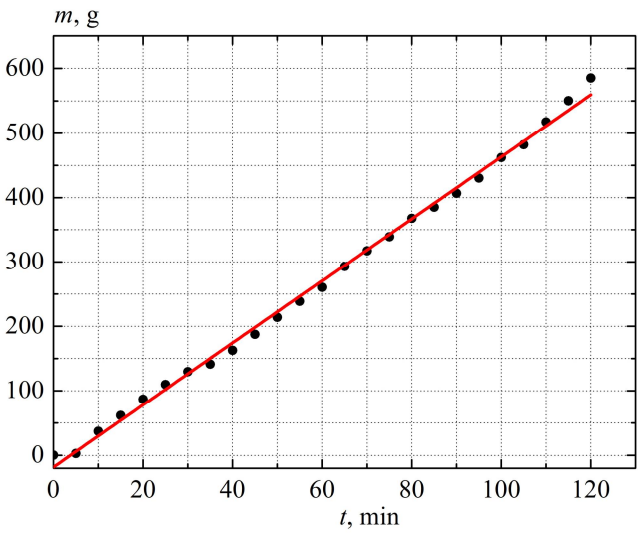

Fig.12. Dependence of the amount of spent fuel m on the operation time t of a thermoelectric starting pre-heater. T_0 = 0 °C.

As compared to warm-up through use of a thermoelectric heater, “idle run” already in the tenth minute assures engine temperature T_E= 80 °C optimal for a car start. However, in this case the weight of burnt fuel *m* is 700 g, which almost a factor of 2.5 exceeds the amount of spent fuel at pre-heating. Engine warm-up to minimum permissible temperatures for its start (T_E = 20 °C) allows significant reduction of fuel consumption at “idle speed” (*m* = 200 g). However, even then the advantages of pre-heating are evident, since to assure such thermal modes it is necessary to spend 3 times less fuel (*m* = 65 g, Fig. 7, Fig. 12).

Thus, the use of a heater only with one engine start can save (0.2 ÷ 0.5) l of fuel. If it is remembered that during one winter season (~100 days) a car makes on the average 4 cold starts per day, then fuel saving for a car with an engine displacement 2.8 l will be 120 – 150 l.

Conclusion

1. It is confirmed that the use of a thermoelectric generator in the design of starting pre-heaters solves the problem of battery discharge in the operation of pre-start equipment.
2. It is established that the use of a thermoelectric heater provides pre-heating of a car engine to the optimum temperatures for its start.
3. It is shown that the heater components are powered from the thermoelectric generator in the tenth minute from the moment of its activation. As the electric power output of thermal generator increases, the electronic unit directs the electric energy excess to recharge the automobile battery. In so doing, the electric power value used for recharging will be determined by the battery charge level.
4. It is established that the use of a thermoelectric starting pre-heater in the cars with engine displacement 2.8l provides saving (0.2÷0.5) l of oil as compared to one "cold start".

The author expresses gratitude to academician L.I. Anatychuk for the topic and the idea of scientific research, as well as valuable advice when writing the work.

References

1. *Patent of Ukraine № 102303* (2013). Anatychuk L.I., Mykhailovsky V.Ya. Thermoelectric power supply for automobile [in Ukrainian].
2. *Patent of Ukraine №72304* (2012). Anatychuk L.I., Mykhailovsky V.Ya. Automobile heater with thermoelectric power supply [in Ukrainian].
3. *Patent of Ukraine №124999* (2017). Maksimuk M.V. Automobile heater with thermoelectric power supply [in Ukrainian].
4. *Patent of US6527548B1* (2003). Aleksandr S. Kushch, Daniel Allen. Self powered electric generating space heater.
5. *Patent of US0115968A1* (2010). Jorn Budde, Jeans Baade, Michael Stelter. Heating apparatus comprising a thermoelectric device.
6. *Patent of Russia* 2268393 (2006). Prilepo Yu.P. A device to facilitate the start of internal combustion engine [in Russian].
7. Mykhailovsky V.Ya., Maksimuk M.V. (2014). Automobile operating conditions at low temperatures. The necessity of applying heaters and the rationality of using thermal generators for their work. *J.Thermoelectricity*, 3, 20-31.
8. Mykhailovsky V.Ya., Maksimuk M.V. (2015). Rational powers of thermal generators for starting pre-heaters of vehicles. *J. of Thermoelectricity,* 4, 65–74.
9. Maksimuk M.V. (2017). On the optimization of thermoelectric modules of automobile starting pre-heater. *J.Thermoelectricity*, 1, 57–67.
10. Maksimuk M.V. (2017). Design of automobile starting pre-heater with a thermoelectric generator. Diesel version. *J.Thermoelectricity*, 2, 32-43.
11. Maksimuk M.V. (2017). Design of automobile starting preheater with a thermoelectric generator. *Herald of the National Technical University of Ukraine "Kyiv Polytechnic Institute". Series INSTRUMENTATION*, 54(2), 53-60 [in Ukrainian].
12. Maksimuk M.V. (2018). Bench tests of a thermoelectric starting preheater for cars. *J.Thermoelectricity*, 1, стор. ?
13. Maksimuk M.V., Andrusiak I.S. (2016). Electronic control unit for thermoelectric automobile starting pre-heater. *J. of Thermoelectricity,* 5, 65–74.
14. *Patent of Ukraine № 90764* (2014). Mykhailovsky V.Ya., Zvozdetsky P.V., Maksimuk M.V.

System of control of starting liquid pre-heater for internal combustion engines [in Ukrainian].
15. Bubnov Yu.I., Orlov S.B. (2005). *Germetichnyie khimicheskiie istochniki toka: elementy i akkumuliatory. Oborudovaniie dlia ispytanii i ekspluatatsii. – Spravochnik [Sealed chemical current sources: elements and batteries. Testing and operating equipment*. - *Handbook*]. Saint-Petersburg: Khimizdat [in Russian].

Submitted 03.05.2018

Максимук М.В.

Інститут термоелектрики НАН і МОН України, вул. Науки, 1,
Чернівці, 58029, Україна,
e-mail: anatych@gmail.com

НАТУРНІ ДОСЛІДЖЕННЯ ТЕРМОЕЛЕКТРИЧНОГО ПЕРЕДПУСКОВОГО ДЖЕРЕЛА ТЕПЛА ДЛЯ АВТОМОБІЛІВ

Наведено результати досліджень термоелектричного передпускового джерела тепла на автомобілі в умовах понижених температур навколишнього середовища. Описано схему підключення нагрівника до системи охолодження автомобіля та розташування його функціональних компонент на транспортному засобі. Розглянуто теплові режими двигуна внутрішнього згорання та режими роботи акумуляторної батареї автомобіля, які забезпечуються передпусковим термоелектричним нагрівником. Представлено результати досліджень раціональності використання термоелектричних передпускових джерел тепла під час експлуатації транспортних засобів в кліматичних зонах з пониженими температурами повітря. Библ. 15, Рис. 12.

Ключевые слова: передпусковий нагрівник, термоелектричний генератор.

Максимук Н.В.

Институт термоэлектричества, ул. Науки, 1,
Черновцы, 58029, Украина
e-mail: anatych@gmail.com

НАТУРНЫЕ ИССЛЕДОВАНИЯ ТЕРМОЭЛЕКТРИЧЕСКОГО ПРЕДПУСКОВОГО ИСТОЧНИКА ТЕПЛА ДЛЯ АВТОМОБИЛЕЙ

Приведены результаты исследований термоэлектрического предпускового источника тепла на автомобиле в условиях пониженных температур окружающей среды. Описана схема подключения нагревателя к системе охлаждения автомобиля и размещение его функциональных компонент на транспортном средстве. Рассмотрены тепловые режимы двигателя внутреннего сгорания и режимы работы аккумуляторной батареи автомобиля, которые обеспечиваются предпусковым термоэлектрическим нагревателем. Представлены результаты исследований рациональности использования термоэлектрических предпусковых источников тепла во время эксплуатации транспортных средств в климатических зонах с пониженными температурами воздуха. Библ. 15, Рис. 12.

Ключевые слова: предпусковой нагреватель, термоэлектрический генератор.

References

1. *Patent of Ukraine № 102303* (2013). Anatychuk L.I., Mykhailovsky V.Ya. Thermoelectric power supply for automobile [in Ukrainian].
2. *Patent of Ukraine №72304* (2012). Anatychuk L.I., Mykhailovsky V.Ya. Automobile heater with thermoelectric power supply [in Ukrainian].
3. *Patent of Ukraine №124999* (2017). Maksimuk M.V. Automobile heater with thermoelectric power supply [in Ukrainian].
4. *Patent of US6527548B1* (2003). Aleksandr S. Kushch, Daniel Allen. Self powered electric generating space heater.
5. *Patent of US0115968A1* (2010). Jorn Budde, Jeans Baade, Michael Stelter. Heating apparatus comprising a thermoelectric device.
6. *Patent of Russia* 2268393 (2006). Prilepo Yu.P. A device to facilitate the start of internal combustion engine [in Russian].
7. Mykhailovsky V.Ya., Maksimuk M.V. (2014). Automobile operating conditions at low temperatures. The necessity of applying heaters and the rationality of using thermal generators for their work. *J.Thermoelectricity*, 3, 20-31.
8. Mykhailovsky V.Ya., Maksimuk M.V. (2015). Rational powers of thermal generators for starting pre-heaters of vehicles. *J. of Thermoelectricity,* 4, 65–74.
9. Maksimuk M.V. (2017). On the optimization of thermoelectric modules of automobile starting pre-heater. *J.Thermoelectricity*, 1, 57–67.
10. Maksimuk M.V. (2017). Design of automobile starting pre-heater with a thermoelectric generator. Diesel version. *J.Thermoelectricity*, 2, 32-43.
11. Maksimuk M.V. (2017). Design of automobile starting preheater with a thermoelectric generator. *Herald of the National Technical University of Ukraine "Kyiv Polytechnic Institute". Series INSTRUMENTATION*, 54(2), 53-60 [in Ukrainian].
12. Maksimuk M.V. (2018). Bench tests of a thermoelectric starting preheater for cars. *J.Thermoelectricity*, 1, стор. ?
13. Maksimuk M.V., Andrusiak I.S. (2016). Electronic control unit for thermoelectric automobile starting pre-heater. *J. of Thermoelectricity,* 5, 65–74.
14. *Patent of Ukraine № 90764* (2014). Mykhailovsky V.Ya., Zvozdetsky P.V., Maksimuk M.V. System of control of starting liquid pre-heater for internal combustion engines [in Ukrainian].
15. Bubnov Yu.I., Orlov S.B. (2005). *Germetichnyie khimicheskiie istochniki toka: elementy i akkumuliatory. Oborudovaniie dlia ispytanii i ekspluatatsii. – Spravochnik [Sealed chemical current sources: elements and batteries. Testing and operating equipment. - Handbook*]. Saint-Petersburg: Khimizdat [in Russian].

Submitted 03.05.2018

O.S. Kshevetsky

O.S. Kshevetsky, *Candidate in Phys-math Science, assistant professor*

Chernivtsi Institute of Trade and Economics
of Kyiv National University of Trade and Economics,
7, Tsentralna Square, Chernivtsi, 58002, Ukraine
e-mail: kshevos@gmail.com

ESTIMATION OF THE EFFICIENCY OF PARTIAL CASE OF HEAT AND MASS TRANSFER PROCESSES BETWEEN HEAT PUMPS AND MOVING SUBSTANCE, PART 2

Theoretical analysis is made of the peculiarities of using compression and thermoelectric heat pumps in the partial case of heat and mass transfer between moving substance and heat pumps, whereby moving substance (or at least part of this moving substance) is brought into thermal contact with the heat absorbing and heat releasing heat-exchange parts of at least two heat pumps. Examples of corresponding calculations are given. Some variants of respective possible technical solutions are described. Bibl. 11, Fig. 9, Table 2.

Key words: heat pump, moving substance, heat and mass transfer, efficiency, energy efficiency, compression heat pump, thermoelectric heat pump, thermoelectric module.

Introduction

This paper (part 2) is a continuation of the previous work [1] (part 1). In this part 2 we will use abbreviations that were introduced in [1], in the same sense as in [1]. In [1], mathematical expressions were obtained for estimating the efficiency of the *investigated method of heat and mass transfer*. These mathematical expressions are general in nature and they do not directly take into account the specific features of certain individual types of HPs. At the same time, it is well known that different types of HPs have different properties.

The purpose of this work is to create theoretical prerequisites for the approximate quantitative estimation of the efficiency (primarily, energy efficiency) *of* the *investigated method of heat and mass transfer* with the use of compression heat pumps (CHPs) and thermoelectric heat pumps (THPs). To accomplish this goal, *the task of this work* is to analyze the corresponding specificity of CHPs and THPs. Also, *the task of this work* is to analyze the peculiarities of using CHPs and THPs in the *investigated method of heat and mass transfer* and to obtain mathematical expressions that could be used to estimate the efficiency of the *investigated method of heat and mass transfer* with employment of CHPs and THPs. Another *task of this work* is to obtain examples of respective estimated calculations.

CHPs in the investigated method of heat and mass transfer

For the CHPs, calculations in the initial approximation use the average value of the heating coefficient, which has a value of about 0.5 from that of the corresponding Carnot cycle [2, 3]. We use it here for the appropriate further estimated calculations. Let us assume:

$$\mu_i^{KTH} = B_i^{KTH}\mu_{K,i},\ B_i^{KTH} = const = 0.5, \qquad (2.1)$$

where μ_i^{KTH} is heating coefficient of the i^{th} CHP; B_i^{KTH} is dimensionless factor taking into the difference of the heating coefficient of the i^{th} CHP from the heating coefficient of the ideal HP which, under the same

conditions, operates on the Carnot cycle; $\mu_{K,i}$ is heating coefficient of the ideal HP which works on the Carnot cycle under the same conditions as the i^{th} CHP.

Let us consider the case of the *investigated method of heat and mass transfer* where all HPs are CHPs; moving substance in its input flow is cooled by all separate CHPs according to Fig. 2 [1], so that all changes in the moving substance temperature as a result of its thermal contact with each individual HE of CHP in the input flow of its moving substance are identical (assumption 9 [1]). For this case $\Delta T_{1,i}^{PP} = \Delta T_{cool,i}^{PP}$, $\Delta T_{1}^{PP} = \Delta T_{cool}^{PP}$, $\Delta T_{2,i}^{PP} = \Delta T_{hot,i}^{PP}$, $\Delta T_{2}^{PP} = \Delta T_{hot}^{PP}$. To determine total temperature difference of moving substance in its output flow ΔT_{2}^{PP}, in this case one can use expressions (43) [1] and (2.1). Table 2.1 gives an example of the results of corresponding calculations.

Table 1

Example of the results of estimated calculations of the efficiency of the investigated method of heat and mass transfer with the use of CHPs for the case of cooling of moving substance in its input flow by all separate CHPs in conformity with assumption 9 [1] *according to Fig. 2* [1]; $T_{2.n}^{PP} = T_{1.n}^{PP}$ $B_i^{KTH} = const = 0.5$)

Total amount of THPs n	Inlet temperature of moving substance $T_{1.0}^{PP}$, K	Total temperature difference of moving substance in its input flow ΔT_1^{PP}, K	Total temperature difference of moving substance in its output flow ΔT_2^{PP}, K	$\frac{\Delta T_1^{PP}}{\Delta T_2^{PP} - \Delta T_1^{PP}}$
1	303.15	24	29.719	4.1965
2	303.15	24	26.443	9.8241

THPs in the investigated method of heat and mass transfer

THPs can be manufactured on the basis of thermoelectric modules (TM). Coefficient of performance and heating coefficient of THPs can be less than coefficient of performance and heating coefficient of TM, respectively [4 – 6]. In order to take this into account, we assume that for the *i*-th THP its coefficient of performance ε_i^{TTH} and its heating coefficient μ_i^{TTH} are determined by the relations:

$$\varepsilon_i^{TTH} = C_i^{TTH} \cdot \varepsilon_i^{TM},\ C_i^{TTH} \le 1; \tag{2.2}$$

$$\mu_i^{TTH} = D_i^{TTH} \cdot \mu_i^{TM},\ D_i^{TTH} \le 1, \tag{2.3}$$

where C_i^{THP} is a dimensionless factor taking into account the difference of coefficient of performance of the *i*-th THP from the coefficient of performance of TM (on which basis this THP is made), which works under the same conditions as this THP; D_i^{THP} is a dimensionless factor taking into account the difference of heating coefficient of the *i*-th THP from the heating coefficient of TM (on which basis this THP is made), which works under the same conditions as this THP; ε_i^{TM} is coefficient of performance of TM (on which basis the *i*-th THP is made), which works under the same conditions as the *i*-th THP; μ_i^{TM} is heating coefficient of TM (on which basis the *i*-th THP is made) which works under the same conditions as the *i*-th THP.

For *the investigated method of heat and mass transfer*, the operation of a heat pump at possibly higher values of heating coefficient and coefficient of performance may be desirable. This may be especially true for

THPs. Let us analyze under what operating modes THPs may have relatively high values of heating coefficient and coefficient of performance. In THP, which is made on the basis of TM, TM plays a significant role. In this regard, let us analyze under what operating modes TM (typical TM, in which all thermoelement legs are electrically connected in series, and from the point of view of heat flows - in parallel: for example, TM TEC1-12706) can have relatively high values of heating coefficient and coefficient of performance. To do this, we use the well-known ratio to determine the coefficient of performance of TM ε^{TM} and the heating coefficient of TM μ^{TM} [4, 7]:

$$\varepsilon^{TM} = \frac{\alpha I T_{cool}^{TM} - \frac{1}{2} I^2 r - k\left(T_{hot}^{TM} - T_{cool}^{TM}\right)}{I^2 r + \alpha\left(T_{hot}^{TM} - T_{cool}^{TM}\right) I}, \tag{2.4}$$

$$\mu^{TM} = \frac{\alpha I T_{hot}^{TM} + \frac{1}{2} I^2 r - k\left(T_{hot}^{TM} - T_{cool}^{TM}\right)}{I^2 r + \alpha\left(T_{hot}^{TM} - T_{cool}^{TM}\right) I}, \tag{2.5}$$

where ε^{TM} is coefficient of performance of TM; α is differential Seebeck coefficient of material; I is strength of current flowing through TM; r is total electrical resistance of TM; k is thermal conductivity of TM; T_{hot}^{TM} is the temperature of the heat-releasing HE of TM; T_{cool}^{TM} is the temperature of the heat-absorbing HE of TM; μ^{TM} is heating coefficient of TM.

Let us designate:

$$T_{hot}^{TM} - T_{cool}^{TM} = \Delta T^{TM}. \tag{2.6}$$

On the basis of Eqs (2.4) and (2.6) we obtain:

$$\Delta T^{TM} = \frac{\alpha I T_{cool}^{TM} - I^2 r\left(\varepsilon^{TM} + \frac{1}{2}\right)}{\varepsilon^{TM} \alpha I + k}. \tag{2.7}$$

On the basis of Eqs (2.5) and (2.6) we obtain:

$$\Delta T^{TM} = \frac{\alpha I T_{hot}^{TM} + I^2 r\left(\frac{1}{2} - \mu^{TM}\right)}{\mu^{TM} \alpha I + k}. \tag{2.8}$$

Using Eq.(2.7), one can obtain the plots of ΔT^{TM} versus I for fixed values of ε^{TM}. An example of such plots is shown in Fig. 2.1. From these plots, for instance, it can be seen that a respective TM can have the values of coefficient of performance higher than 10 ($\varepsilon^{TM} > 10$) only at sufficiently low values of temperature difference ΔT^{TM} and current strength I (the respective plotted points are restricted by the curve for $\varepsilon^{TM} = 10$ and are below this curve).

Similar plots can be also obtained for the fixed values of heating coefficient with the use of Eq. (2.8).

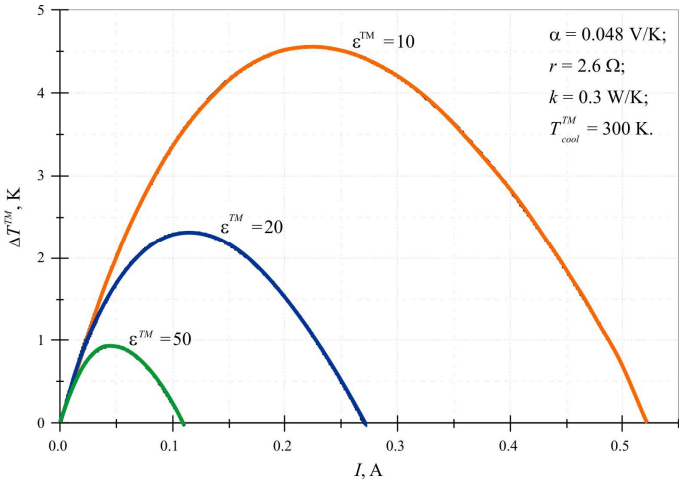

Fig. 2.1. Theoretical dependences of temperature difference ΔT^{TM} *on current strength I at fixed values of coefficient of performance* ε^{TM} *for TM which works at* $T_{cool}^{TM} = 300\ K$ *and has the following parameters: α = 0.048 V/K; r = 2.6 Ohm; k = 0.3 W/K.*

The case of using TM-based THPs in maximum energy efficiency modes

Let us assume that all THPs that are used in the *investigated method of heat and mass transfer* are based on standard TMs (based on standard thermoelements). And these TMs work in maximum energy efficiency modes. To estimate the efficiency of the *investigated method of heat and mass transfer,* for this case we will use a well-known expression for the definition of coefficient of performance of thermoelement working in maximum energy efficiency mode [8]:

$$\varepsilon_{\max}^{TM} = \frac{\sqrt{1+0.5Z\left(T_{hot}^{TM}+T_{cool}^{TM}\right)}-T_{hot}^{TM}/T_{cool}^{TM}}{\sqrt{1+0.5Z\left(T_{hot}^{TM}+T_{cool}^{TM}\right)}+1}\frac{T_{cool}^{TM}}{T_{hot}^{TM}-T_{cool}^{TM}}, \tag{2.9}$$

where $\varepsilon_{\max}^{TM}$ is coefficient of performance of TM working in maximum energy efficiency mode; Z is thermoelectric figure of merit of TM material; T_{hot}^{TM} is the temperature of the heat-releasing HE of TM; T_{cool}^{TM} is the temperature of the heat-absorbing HE of TM.

Let us designate:

$$\frac{\sqrt{1+0.5Z\left(T_{hot}^{TM}+T_{cool}^{TM}\right)}-T_{hot}^{TM}/T_{cool}^{TM}}{\sqrt{1+0.5Z\left(T_{hot}^{TM}+T_{cool}^{TM}\right)}+1} = A_{\max}^{TM}, \tag{2.10}$$

where $A_{\max}^{TM}$ is a dimensionless factor taking into account the difference of the coefficient of performance of TM (working in maximum energy efficiency mode) from the coefficient of performance of the ideal HP that operates on the Carnot cycle under the same conditions as TM.

Let us assume that

$$A_{\max}^{TTH} = C^{TTH} A_{\max}^{TM},\ C^{TTH} \le 1, \text{ за умови, що } T_{cool}^{TTH} = T_{cool}^{TM} \text{ і } T_{hot}^{TTH} = T_{hot}^{TM}, \tag{2.11}$$

where $A_{\max}^{TTM}$ is a dimensionless factor (generally introduced into [1]), taking into account the difference of coefficient of performance of TM-based THP (working in maximum energy efficiency mode) from the coefficient of performance of the ideal HP that operates the Carnot cycle under the same conditions as THP; C^{TTH} is a dimensionless factor taking into account possible difference of the coefficient of

performance of THP from the coefficient of performance of TM (on which basis this THP is made), working under the same conditions as THP; $A_{\max}^{TM}$ is a dimensionless factor taking into account the difference of coefficient of performance of TM (which works in maximum energy efficiency mode and is the basis of THP) from the coefficient of performance of the ideal HP that operates on the Carnot cycle under the same conditions as TM; T_{cool}^{TTH} is the temperature of the heat-absorbing HE of THP; T_{hot}^{TTH} is the temperature of the heat-releasing HE of THP.

For a fixed value of thermoelectric figure of merit Z the $A_{\max}^{TM}$ value depends on temperatures T_{hot}^{TM} and T_{cool}^{TM}.

Using Eqs (2.10) and (2.11), one can obtain the plots of $A_{\max}^{TM}$ values versus temperature T_{cool}^{TM} (in particular, at a fixed value of T_{hot}^{TM}) and $A_{\max}^{TTM}$ values versus temperatures T_{cool}^{TTH} (in particular, at a fixed value of T_{hot}^{TTH}). An example of such plots is given in Fig. 2.2.

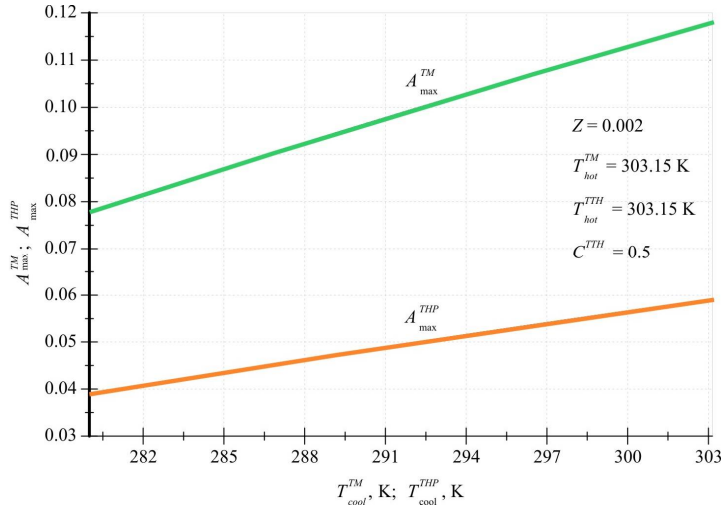

Fig. 2.2.The plots of $A_{\max}^{TM}$ value versus temperature T_{cool}^{TM} for the case when $Z = 0.002$, $T_{hot}^{TM} = 303.15\,\mathrm{K}$ and $A_{\max}^{TTM}$ versus temperature T_{cool}^{TTH} for the case when $Z = 0.002$, $T_{hot}^{TTH} = 303.15\,\mathrm{K}$ and $C^{TTH} = const = 0.5$ (the plots obtained on the basis of Eqs (2.10)and (2.11)).

In connection with the information on the values $A_{\max}^{TM}$ and $A_{\max}^{TTM}$ given here, on the basis of Eqs (2), (4), (7), (8) [1], (2.2), (2.9), (2.10), (2.11) we obtain the following equation for determining the temperature operating mode of the i-th THP based on TM, which works in the mode of maximum energy efficiency:

$$\frac{\Delta T_{cool,i}^{PP}}{\Delta T_{hot,i}^{PP} - \Delta T_{cool,i}^{PP}} = C_i^{TTH} \frac{\sqrt{1+0.5Z_i\left(T_{hot,i}^{TTH} + T_{cool,i}^{TTH}\right)} - T_{hot,i}^{TTH} / T_{cool,i}^{TTH}}{\sqrt{1+0.5Z_i\left(T_{hot,i}^{TTH} + T_{cool,i}^{TTH}\right)} + 1} \frac{T_{cool,i}^{TTH}}{T_{hot,i}^{TTH} - T_{cool,i}^{TTH}}, \qquad (2.12)$$

where $\Delta T_{cool,i}^{PP}$ is change in moving substance temperature due to its thermal contact with the heat-absorbing HE of the *i*-th THP; $\Delta T_{hot,i}^{PP}$ is a change in moving substance temperature due to its thermal contact with the heat-releasing HE of the *i*-th THP; Z_i is thermoelectric figure of merit of material of the *i*-th TM (which is the basis of the *i*-th THP); $T_{hot,i}^{TTH}$ is the temperature of the heat-releasing HE of the *i*-th THP; $T_{cool,i}^{TTH}$ is the temperature of the heat-absorbing HE of the *i*-th THP.

Such equations can be solved by numerical methods.

Let us consider the case of the *investigated method of heat and mass transfer where all HPs are THPs*, in each of which TM (which is the basis of corresponding THP) works in maximum energy efficiency mode; moving substance in its input flow is cooled by all separate THPs according to Fig. 2 [1] and assumption 9 [1]. Table 2.2 gives an example of the results of calculations to estimate the efficiency of this case of the *investigated method of heat and mass transfer* using the solution of appropriate Eqs.(2.12) by numerical methods.

Table 2

Example of the results of estimated calculations of the efficiency of the investigated method of heat and mass transfer with the use of THPs for the case of cooling of moving substance in its input flow by all separate THPs according to Fig.2 and assumption 9 [1] $T_{2.n}^{PP} = T_{1.n}^{PP}$ (with the use of Eq. (2.12); $C_i^{THP} = const = 0.5$; $Z_i = const = 0.002$)

Total amount of THPs n	Inlet temperature of moving substance $T_{1.0}^{PP}$, K	Total temperature difference of moving substance in its input flow ΔT_1^{PP}, K	Total temperature difference of moving substance in its output flow ΔT_2^{PP}, K	$\frac{\Delta T_1^{PP}}{\Delta T_2^{PP} - \Delta T_1^{PP}}$
1	303.15	2	2.2628	7.6092
2	303.15	2	2.1249	16.016
16	303.15	24	29.926	4.0502
17	303.15	24	29.502	4.3618

Some possible options for the technical implementation of the investigated method of heat and mass transfer

The technical implementation of the *investigated method of heat and mass transfer* with the use of several THPs can be somewhat complicated, especially with a large number of THPs. The solution to this issue may be associated with the development and creation of specialized TM. For example, such TM may contain at least one thermoelement, which is separated (in one way or another), in terms of possible heat flows (thermally) from at least one other thermoelement of the same TM. This, according to assumption 1 [1], will allow the TM thermoelements to operate in separated thermal modes from the point of view of possible heat flows. The corresponding THPs based on such TM thermoelements (which are separated in terms of possible heat flows relative to each other) can be considered as individual THPs. HPs in *the investigated method of heat and mass transfer* work in different thermal conditions. In this regard, it may be appropriate that the relevant specialized TM contain thermoelements or groups of thermoelements with different properties. It may also be advisable that the TM be made with the possibility of individual electrical connection of their parts to the electrical circuits (for example, appropriate wires or terminals can be used for connecting individual thermocouples or thermoelement groups to electric circuits).

Fig. 2.3 provides a simplified scheme of such specialized TM, which can be considered as a modified typical TM (for example, TEC1-12706). This specialized TM (Fig. 2.3) contains 16 parts based on thermoelement groups with heat-conducting insulating elongated plates (for example, ceramic) 1 which are separated in terms of possible heat flows (thermally) relative to each other using 15 layers of thermal insulation 2. Parts of this specialized TM 1 have different properties, as conventionally shown in Fig. 2.3 with different shades of grey. In terms of electrical connections, this specialized module has 8 parts, of which there are 9 electrical wires 3 for connecting these parts to electric circuits. Fig. 2.3 also conventionally reflects the moving

substance and its possible direction of movement 4. Specialized TM (Fig. 2.3) differs from typical TM, in particular, by the fact that its thermoelements are connected into a single design not by two heat-conducting electrically insulating ceramic plates of square shape (as in typical TM), but by 32 elongated heat-conducting electrically insulating plates (16 pcs. on each side of the module) and layers of thermal insulation (for example, based on foamed insulating material). To use a specialized TM (Fig. 2.3) in the *investigated method of heat and mass transfer*, it may be necessary to install separate additional heat exchangers (radiators) on this module. This is shown in Fig. 2.4 (Fig. 2.4 also conventionally reflects the moving substance and its possible direction of movement). This specialized TM can also be used without such heat exchangers (for example, with direct thermal contact of the moving substance (for example, water) with 32 elongated heat-conducting insulating plates).

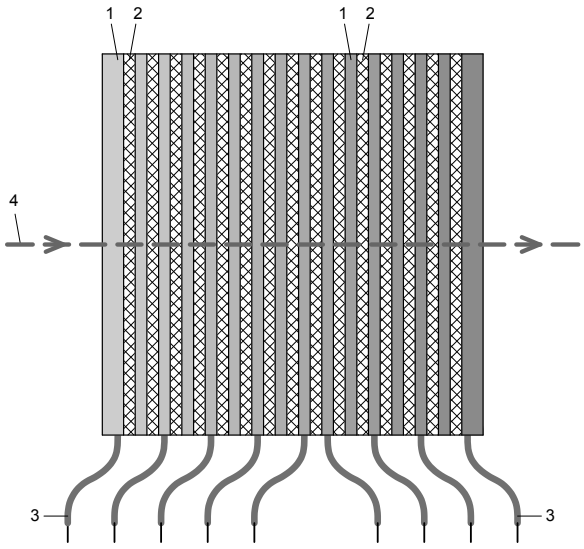

Fig. 2.3. Simplified schematic of possible specialized TM (modified standard TM), which comprises 16 parts with different properties based on thermoelement groups with heat-conducting electrically insulating elongated plates separated relative to each other in terms of possible heat flows. 1 –parts of specialized TM based on thermoelement groups with heat conducting electrically insulating elongated plates; 2 –heat insulating layers; 3 –electrical wires; 4 –moving substance and possible direction of its movement.

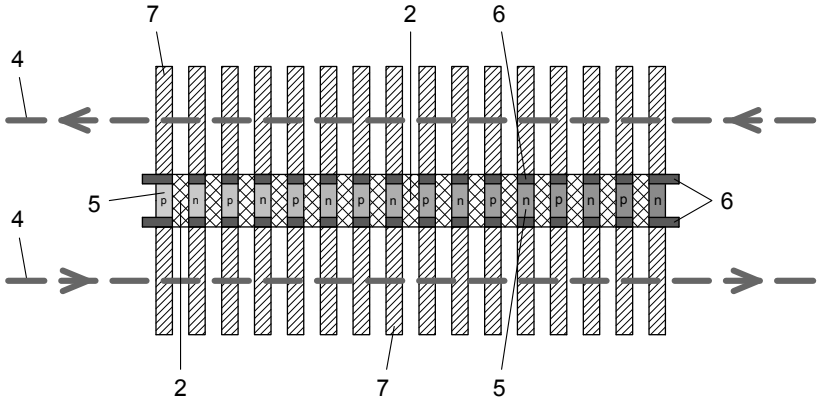

Fig. 2.4. Simplified schematic of possible specialized TM (shown in Fig.2.3) with 32 separate heat exchangers (radiators) installed on it. 2 – heat insulating layers; 4 – moving substance and possible direction of its movement; 5 – thermoelement legs; 6 – heat conducting electrically insulating elongated plates (cross view); 7 – heat exchangers (radiators) installed on plates 6.

In particular, to reduce thermal resistance between the TM thermoelements and moving substance in the *investigated method of heat and mass transfer (*as well as in other applications), such specialized TMs

can be used whose thermoelement legs are electrically connected by heat exchangers (for example, copper) that have a thermal contact with a moving substance. Through heat exchangers a specialized TM can be connected to the electrical circuit. If necessary, heat exchangers can be protected from corrosion (in particular, due to contact with the moving substance) and / or electrical insulation. An example of such possible specialized TM is presented in Fig. 2.5. Among other things, this specialized TM has thermal insulation from the environment. In particular, with the use of thermal insulation in this specialized TM, two channels for the movement of moving substance are implemented.

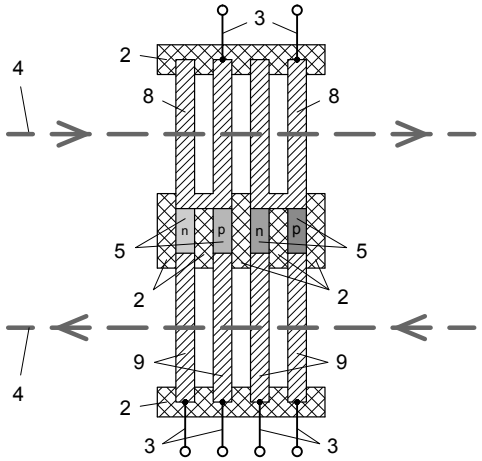

Fig. 2.5. Simplified schematic of possible specialized TM with the use of heat exchangers for electrical connections, heat insulation from the environment and channels for motion of moving substance. 2 – heat insulationя; 3 – elements for connection to electrical circuits (for instance, wires or terminals); 4 – moving substance and possible direction of its movement; 5 – thermoelement legs; 8 – heat exchangers (radiators), in particular, used for electrical connection of thermoelement legs and connection of these legs to electrical circuits; 9 –heat exchangers (radiators), in particular, used for connection of thermoelement legs 5 to electrical circuits.

To some extent, it is possible to increase the efficiency of using standard TM in the *investigated method of heat and mass transfer* (as well as in other applications, for example, such when thermoelements of a typical TM work under different conditions) compared to the case when one heat exchanger –radiator is installed on each individual HE of TM (ceramic plate) (as shown in Fig. 2.6), if several, rather than one, individual heat exchangers (radiators) are installed on at least one individual HE of TM (thermally conductive ceramic plate of a typical TM). An example is shown in Fig. 2.7.

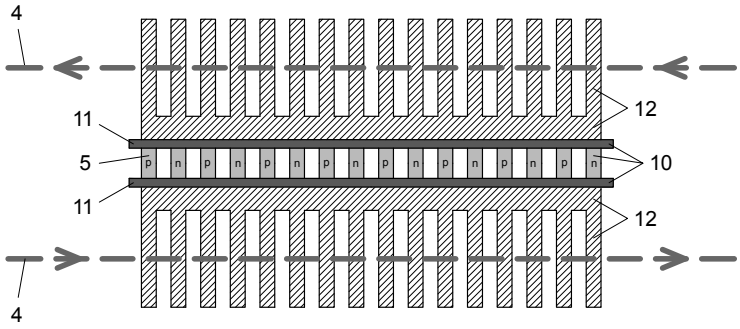

Fig. 2.6. Simplified schematic of a typical TM having on each of its opposite HEs (heat conducting ceramic plates) only one heat exchanger ; 4 – moving substance and possible direction of its movement; 5 – thermoelement legs of a typical TM; 10 – typical TM; 11 –heat conducting ceramic plates of a typical TM; 12 –heat exchangers (radiators), which are common for all thermoelemeents of a typical TM.

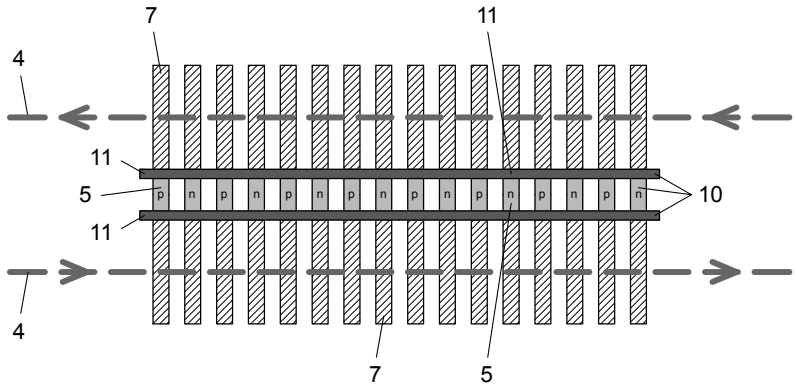

Fig. 2.7. Simplified schematic of a typical TM 10 with 32 heat exchangers (radiators) 7 installed on it (16 pcs on each side of a typical TM), which to some extent are individual for the respective 16 parts of this typical TM (these parts to some extent are connected in terms of possible heat flows by 2 heat conducting electrically insulating ceramic plates 11). 4 – moving substance and possible direction of its motion; 5 – thermoelement legs.

Also, in the investigated method of heat-mass transfer, such specialized TMs can be used, which can also be considered as modified typical TMs, whose thermoelements are similar to the design of typical TMs from opposite sides, coupled by two thermal conductive plates (having a structure similar to the design of typical TMs), but differ from the typical TMs in that they contain parts (based on at least one thermoelement) with different properties and / or are made with the possibility of separate electrical connection of their parts to electrical circuits. Simplified schemes of examples of such specialized TMs are presented in Fig. 2.8 and in Fig. 2.9. Fig. 2.8 shows a simplified scheme of an example of specialized TM with additional individual heat exchangers installed on it. In this example, the thermoelements have different properties which are conventionally shown in Fig. 2.8 with different shades of grey. Fig. 2.9 is a simplified schematic of a specialized TM that has 9 electrical wire leads for connecting parts of this specialized TM to electrical circuits.

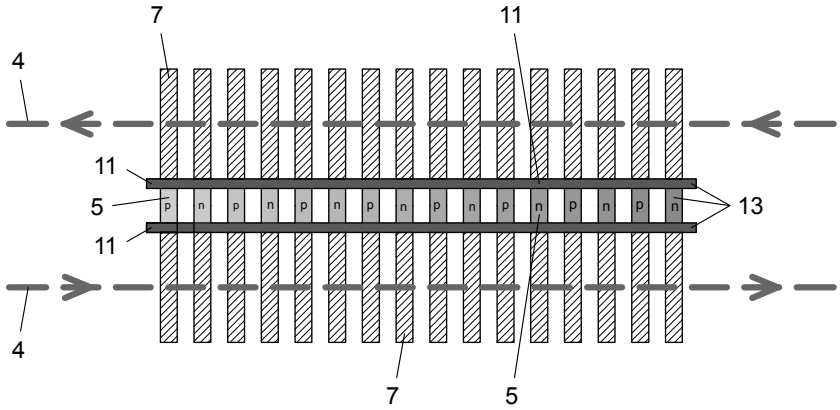

Fig. 2.8. Simplified schematic of possible specialized TM (modified typical TM) comprising 16 parts based on thermoelements with different properties. 4 –moving substance and possible direction of its motion; 5 – legs of thermoelements with different properties; 7 – individual heat exchangers (radiators); 11 –heat conducting electrically insulating plates; 13 – specialized TM.

Other specialized TMs for the investigated method of heat and mass transfer are also possible, which may have the features of the above-described specialized TMs in various combinations. The above-described specialized TMs, besides being used in the investigated method of heat and mass transfer, may have other applications (assignments). Similar to those described above or fundamentally similar technical solutions are possible with the use of other types of HP with a modular design.

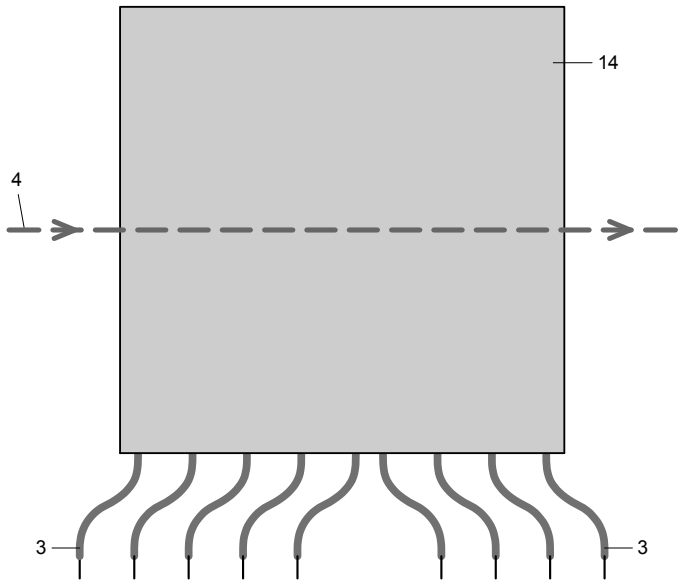

Fig. 2.9. Simplified schematic of possible specialized TM (modified typical TM) comprising 9 electrical wires 3 – electrical wires; 4 – moving substance and possible direction of its motion; 14 –part of TM based on thermoelements which on the opposite sides are connected by two heat conducting plates.

Conclusion

The examples of estimated calculations given in this work for the cases of CHPs and THPs use in the *investigated method of heat and mass transfer* confirm the fundamental possibility of increasing the energy efficiency of the corresponding processes due to the increase in the number of HPs used in this process [1, 9 – 11].

Some possible options for the technical implementation of the *investigated method of heat-mass transfer* are described.

At the same time, in order to make decisions regarding the practical applications of the *investigated method of heat and mass transfer*, further theoretical and / or experimental studies may be required.

References

1. Kshevetsky O.S. (2017). Estimation of the efficiency of partial case of heat and mass transfer processes between heat pumps and moving substance, part 1. *J.Thermoelectricity, 6,* 41–56.
2. Bonin J. (2015). *Heat Pump Planning Handbook*. London and New York: Routledge.
3. Snezhkin Yu.F., Chalaiev D.M., Dabizha N.O. (2017). Analiz energetychnykh pokaznykiv protsesu teplonasosnoho sushinnia [Analysis of energy performance of heat pump drying]. *Promyshlennaia teplotekhnika – Industrial Heat Engineering,* 39, 47–52 [in Ukrainian].
4. Anatychuk L.I., Prybyla A.V. (2016). Comparative analysis of thermoelectric and compression heat pumps for individual air-conditioners. *J. Thermoelectricity,* 2, 33–42.
5. Anatychuk L.I., Prybyla A.V. (2017). The influence of quality of heat exchangers on the properties of thermoelectric liquid-liquid heat pumps. *J. Thermoelectricity,* 5, 59–64.
6. Anatychuk L.I.., Prybyla A.V. (2017). On the coefficient of performance of thermoelectric liquid-liquid heat pumps with regard to energy loss for heat carrier transfer. *J.Thermoelectricity,* 6, 34–40.
7. Ioffe A.F. (1960). *Semiconductor Thermoelements. Moscow*- Leningrad: USSR Academy of Sciences.

8. Anatychuk L.I. (2005). *Thermoelectricity. Vol. 2. Thermoelectric Power Converters*. Kyiv, Chernivtsi: Institute of Thermoelectricity.
9. Kshevetsky O.S. (2017). Otsinka energoefektyvnosti sposobu teplomasoobminu mizh rukhomoiu rechovynoiu i tepolvymy nasosamy [Estimation of energy efficiency of a method for heat and mass transfer between moving substance and heat pumps]. *Materialy Vseukrainskoi naukovo-praktychnoi konferentsii "Innovatsiini tekhnolohii v hotelno-restorannomu biznesi" – Proc. of All-Ukrainian scientific and practical conference "Innovation technologies in hotel and restaurant business"* (Ukraine, Kyiv, March 22–23). Kyiv: NUFT [in Ukrainian].
10. Kshevetsky O.S. (2017). Pro mozhlyvist pidvyshchennia enerhoefektyvnosti procesiv teplomasoobminu, yaki peredbachaiiut nahrivannia ta okholodzhennia rukhomoi rechovyny [On the possibility of increasing the energy efficiency of heat and mass transfer processes which involve heating and cooling of moving substance]. *Khimichna tekhnologiia ta inzheneriia: zbirnyk tez dopovidei Mizhnarodnoi naukovo-praktychnoi konferentsii - Chemical Technology and Engineering: collection of abstracts of International scientific and practical conference* (Ukraine, Lviv, June 26–30, 2017). Lviv: Lvivska Politekhnika [in Ukrainian].
11. Kshevetsky O.S., Shtangeieva N.I. (2017). Pro mozhlyvist vykorystannia dekilkokh teplovykh nasosiv dlia pidvyshchennia enerhoefektyvnosti deiakykh procesiv teplomasoobminu [On the possibility of using several heat pumps for increasing energy efficiency of some heat and mass transfer processes]. Tezy dopovidei X Mizhnarodnoi konferentsii "Problemy teplofizyky ta teploenerhetyky" – Abstracts of X International conference "Problems of thermophysics and heat power engineering" (Ukraine, Kyiv, May 23–26, 2017). *Promyshlennaia teploteknika – Industrial Heat Engineering,* 39(7), 79–80 [in Ukrainian].

Submitted 15.05.2018

Кшевецький О.С. *канд. фіз.- мат. наук, доцент*

Чернівецький торговельно-економічний інститут
Київського національного торговельно-економічного університету,
Центральна площа, 7, м. Чернівці, 58002, Україна
e-mail: kshevos@gmail.com

ОЦІНКА ЕФЕКТИВНОСТІ ЧАСТИННОГО ВИПАДКУ ПРОЦЕСІВ ТЕПЛОМАСООБМІНУ МІЖ ТЕПЛОВИМИ НАСОСАМИ І РУХОМОЮ РЕЧОВИНОЮ, ЧАСТИНА 2

Теоретично проаналізовані особливості використання компресійних та термоелектричних теплових насосів у частинному випадкові способу тепломасообміну між рухомою речовиною і тепловими насосами, при якому рухому речовину (або принаймні частину цієї рухомої речовини) приводять у тепловий контакт з теплопоглинаючою і тепловиділяючою теплообмінними частинами принаймні двох теплових насосів. Наведені приклади відповідних розрахунків. Описані деякі варіанти відповідних можливих технічних рішень. Бібл. 11, рис. 9, табл. 2.

Ключові слова: тепловий насос, рухома речовина, тепломасообмін, ефективність, енергоефективність, компресійний тепловий насос, термоелектричний тепловий насос, термоелектричний модуль.

Кшевецкий О.С. *канд. физ.- мат наук, доцент*

Черновицкий торгово-экономический институт
Киевского национального торгово-экономического университета,
Центральная площадь, 7, г. Чернівці, 58002, Украина
e-mail: kshevos@gmail.com

ОЦЕНКА ЭФФЕКТИВНОСТИ ЧАСТНОГО СЛУЧАЯ ПРОЦЕССОВ ТЕПЛОМАСООБМЕНА МЕЖДУ ТЕПЛОВЫМИ НАСОСАМИ И ПОДВИЖНЫМ ВЕЩЕСТВОМ, ЧАСТЬ 2

Теоретически проанализированы особенности использования компрессионных и термоэлектрических тепловых насосов в частном случайные способа тепломассообмена между движущимся веществом и тепловыми насосами, при котором движущееся вещество (или хотя бы часть этого движущегося вещества) приводят в тепловой контакт с теплопоглощающей и тепловыделяющей теплообменными частями по крайней мере двух тепловых насосов. Приведены примеры соответствующих расчетов. Описаны некоторые варианты возможных технических решений. Библ. 11, рис. 9, табл. 2.

Ключевые слова: тепловой насос, движущееся вещество, тепломассообмен, эффективность, энергоэффективность, компрессионный тепловой насос, термоэлектрический тепловой насос, термоэлектрический модуль.

References

1. Kshevetsky O.S. (2017). Estimation of the efficiency of partial case of heat and mass transfer processes between heat pumps and moving substance, part 1. *J.Thermoelectricity, 6,* 41–56.
2. Bonin J. (2015). *Heat Pump Planning Handbook.* London and New York: Routledge.
3. Snezhkin Yu.F., Chalaiev D.M., Dabizha N.O. (2017). Analiz energetychnykh pokaznykiv protsesu teplonasosnoho sushinnia [Analysis of energy performance of heat pump drying]. *Promyshlennaia teplotekhnika – Industrial Heat Engineering,* 39, 47–52 [in Ukrainian].
4. Anatychuk L.I., Prybyla A.V. (2016). Comparative analysis of thermoelectric and compression heat pumps for individual air-conditioners. *J. Thermoelectricity,* 2, 33–42.
5. Anatychuk L.I., Prybyla A.V. (2017). The influence of quality of heat exchangers on the properties of thermoelectric liquid-liquid heat pumps. *J. Thermoelectricity,* 5, 59–64.
6. Anatychuk L.I.., Prybyla A.V. (2017). On the coefficient of performance of thermoelectric liquid-liquid heat pumps with regard to energy loss for heat carrier transfer. *J.Thermoelectricity,* 6, 34–40.
7. Ioffe A.F. (1960). *Semiconductor Thermoelements. Moscow*- Leningrad: USSR Academy of Sciences.
8. Anatychuk L.I. (2005). *Thermoelectricity. Vol. 2. Thermoelectric Power Converters*. Kyiv, Chernivtsi: Institute of Thermoelectricity.
9. Kshevetsky O.S. (2017). Otsinka energoefektyvnosti sposobu teplomasoobminu mizh rukhomoiu rechovynoiu i tepolvymy nasosamy [Estimation of energy efficiency of a method for heat and mass transfer between moving substance and heat pumps]. *Materialy Vseukrainskoi naukovo-praktychnoi konferentsii "Innovatsiini tekhnolohii v hotelno-restorannomu biznesi" – Proc. of All-Ukrainian*

scientific and practical conference "Innovation technologies in hotel and restaurant business" (Ukraine, Kyiv, March 22–23). Kyiv: NUFT [in Ukrainian].

10. Kshevetsky O.S. (2017). Pro mozhlyvist pidvyshchennia enerhoefektyvnosti procesiv teplomasoobminu, yaki peredbachaiiut nahrivannia ta okholodzhennia rukhomoi rechovyny [On the possibility of increasing the energy efficiency of heat and mass transfer processes which involve heating and cooling of moving substance]. *Khimichna tekhnologiia ta inzheneriia: zbirnyk tez dopovidei Mizhnarodnoi naukovo-praktychnoi konferentsii - Chemical Technology and Engineering: collection of abstracts of International scientific and practical conference* (Ukraine, Lviv, June 26–30, 2017). Lviv: Lvivska Politekhnika [in Ukrainian].
11. Kshevetsky O.S., Shtangeieva N.I. (2017). Pro mozhlyvist vykorystannia dekilkokh teplovykh nasosiv dlia pidvyshchennia enerhoefektyvnosti deiakykh procesiv teplomasoobminu [On the possibility of using several heat pumps for increasing energy efficiency of some heat and mass transfer processes]. Tezy dopovidei X Mizhnarodnoi konferentsii "Problemy teplofizyky ta teploenerhetyky" – Abstracts of X International conference "Problems of thermophysics and heat power engineering" (Ukraine, Kyiv, May 23–26, 2017). *Promyshlennaia teploteknika – Industrial Heat Engineering,* 39(7), 79–80 [in Ukrainian].

Submitted 15.05.2018

P. D. Mykytiuk

P.D.Mykytiuk[1, 2], *Candidate Phys.-math. Sciences*
O.Yu.Mykytiuk[3] *Candidate Phys.-math. Sciences, docent*

[1]Institute of Thermoelectricity of the NAS and MES of Ukraine, 1, Nauky str, Chernivtsi, 58029, Ukraine;
[2]Yu.Fedkovych Chernivtsi National University, 2, Kotsiubynskyi str., Chernivtsi, 58000, Ukraine
e-mail: anatych@gmail.com
[3]Higher State Educational Institution of Ukraine "Bukovinian State Medical University", 2, Theatre Square, Chernivtsi, 58002, Ukraine

O. Yu. Mykytiuk

TEMPERATURE DISTRIBUTION IN A HEATER WITH A RESISTANCE VARIABLE ALONG ITS LENGTH IN A THERMOELECTRIC CONVERTER

This paper studies temperature distribution in a heater with variable resistance along its length which is used in a semiconductor thermal converter. It is established that maximum localization of temperature at point of contact between the heater and the thermocouple junction allows increasing the temperature in its centre almost twice as compared to conventional heater variant that significantly increases the sensitivity of thermal converter. Bibl. 2, Fig. 1, Table. 1.
Key words: heater, thermal converter, temperature distribution.

Introduction

The authors of [1] note that it is advisable to consider the possibility of creating such a heater for a thermoelectric measuring thermal converter which might provide maximum temperature in its geometric centre, where, as a rule, the junctions of thermocouple legs are structurally arranged. This approach will significantly reduce heat loss in the thermal converter design, and, therefore, improve its operating efficiency.

The purpose of this paper is to estimate the boundary opportunities of such an option for optimizing the thermal converter design.

Model of a heater with a variable resistance along its length

Let us calculate the value of temperature in the centre of the heater, provided that all the heat is released in it. The calculation will be made for a manganin heater in glass insulation with a resistance of 16 ohms. The thermophysical properties of the glass will be taken into account by introducing "effective" values of thermal conductivity and other characteristics of the heater.

In the simplest variant, the loss of heat released in the heater is only due to its thermal conductivity. Then the formula [2] is valid:

$$\Delta T_{\max} = \frac{U_н^2}{8\kappa_н \rho_н}, \qquad (1)$$

where U_H is electric voltage on the heater, and κ_H, ρ_H is thermal conductivity and resistivity of the heater, respectively.

Substituting parameters for the heater, for current I_H = 5 mA we obtain that maximum temperature difference in the heater ΔT_{max} = 44 °C.

In real thermal converters, other mechanisms of heat loss have a significant impact. Taking into account heat loss due to thermal conductivity of the heater material and due to convective heat transfer, as shown in [1], can lead to temperature decrease in the centre of the heater by a factor of 1.5. Therefore, maximum concentration of heat in the centre of the heater, where the junction of the thermocouple legs is located, is expected to significantly increase the sensitivity of thermal converters.

Such a variant of the heater design can be realized in a heater with variable resistance along its length, the maximum of which falls on the point of thermal contact between the thermocouple and the heater.

To determine the appropriateness of such heater design, consider the heater model shown in Fig. 1, in which a change in the resistance of the heater along its length is achieved by varying its cross-section.

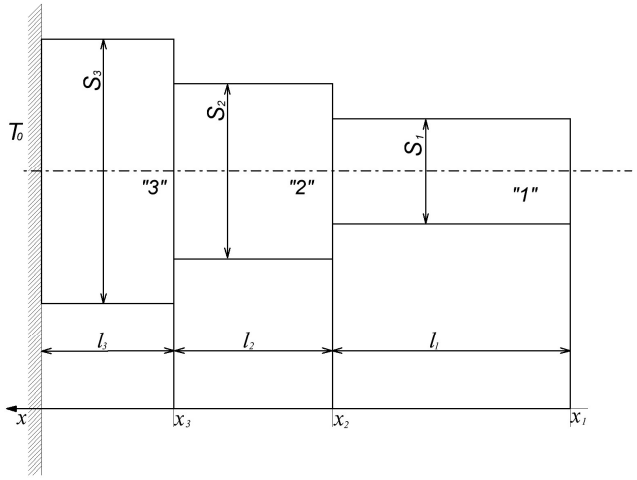

Fig. Model for the calculation of temperature distribution in a heater with variable cross-section.

Calculation of thermal balance of a heater with variable cross-section

Let us denote

$$\theta_H = T(x_H) - T_0, \tag{2}$$

$$a_H = \frac{\pi d_H C_{0H}}{\chi_H S_H}, \tag{3}$$

$$b_H = \frac{\rho_H I_H^2}{\kappa_H S_H^2}, \tag{4}$$

where x_H is heater coordinate along its length,

$T_{xH} - T_0$ is temperature difference on the heater,

d_H is heater diameter,

C_0 is coefficient of heat exchange with the environment,

ρ_H is heater resistivity,

S_H is heater cross-section,

I_H is current passing through the heater,

χ_H is thermal conductivity of the heater material.

Then the heat balance condition of the heater can be written as follows:

$$\frac{d^2\theta_i}{dx_i^2} - a_i\theta_i + b_i = 0, \tag{5}$$

where $i = 1, 2, 3\ldots$

Let us rearrange Eq. (5) by introducing a new variable

$$X_i = x - x_i \tag{6}$$

Since

$$\frac{d}{dx} = \frac{dX_i}{dx} \cdot \frac{d}{dX_i} = \frac{d}{dX_i}, \tag{7}$$

then (5) will be given by:

$$\frac{d^2\theta_i}{dX_i^2} - a_i\theta_i + b_i = 0 \tag{8}$$

Solution of (8) will be made for the boundary conditions summarized in Table 1.

Table

№	x	X_i	θ_i
1.	0	$X_3 = \ell_3$	$\theta_3(x = 0) = 0;\ \theta_3(x_3 - \ell_3) = 0$
2.	x_3	$X_3 = 0$ $X_2 = \ell_2$	$\theta_3(x_3) = \theta_2(x_3)$ $\theta_3(X_3 = 0) = \theta_2(X_2 = \ell_2)$ $\left[-\chi_3 S_3 \frac{\partial\theta_3}{\partial X_3}\Big\vert_{X_3=0} \cdot (+1)\right] + \left[-\chi_2 S_2 \frac{\partial\theta_2}{\partial X_2}\Big\vert_{X_2=\ell_2} \cdot (-1)\right] = 0$
3.	x_2	$X_2 = 0$ $X_1 = \ell_1$	$\theta_2(x_2) = \theta_1(x_2)$ $\theta_2(X_2 = 0) = \theta_1(X_1 = \ell_1)$ $\left[-\chi_2 S_2 \frac{\partial\theta_2}{\partial X_2}\Big\vert_{X_2=0} \cdot (+1)\right] + \left[-\chi_1 S_1 \frac{\partial\theta_1}{\partial X_1}\Big\vert_{X_1=\ell_1} \cdot (-1)\right] = 0$
4.	x_1	$X_1 = 0$	$\theta_1(x_1) = T_1 - T_0$ $\theta_1(x_1 = 0) = T_1 - T_0$ $-\chi_1 S_1 \frac{\partial\theta_1}{\partial X_1}\Big\vert_{X_1=0} = 0$

As a result of complex and cumbersome transformations that are not given in this paper, we obtain the formula for maximum temperature difference in a heater with variable cross-section:

$$T_1 - T_0 = \frac{b_1}{a_1} - \frac{\frac{b_3}{a_2} + (\frac{b_1}{a_1} - \frac{b_2}{a_2})\left[chL_2 \cdot chL_3 + K_{23} shL_2 \cdot shL_3\right] + (\frac{b_2}{a_2} - \frac{b_3}{a_3})chL_3}{(chL_1 \cdot chL_2 + K_{12} shL_1 \cdot shL_2)chL_3 + (K_{13} shL_1 \cdot chL_2 + K_{23} chL_1 \cdot shL_2)shL_3}, \quad (9)$$

where: $L_i = \sqrt{a_i}\,\ell_i$ (10)

$$K_{12} = \frac{S_1 \kappa_1 \sqrt{a_1}}{S_2 \kappa_2 \sqrt{a_2}}, \quad (11)$$

$$K_{23} = \frac{S_2 \kappa_2 \sqrt{a_2}}{S_3 \kappa_3 \sqrt{a_3}}, \quad (12)$$

Model of a heater with a variable resistance along its length

$$K_{13} = K_{12} \cdot K_{23} = \frac{S_1 \kappa_1 \sqrt{a_1}}{S_3 \kappa_3 \sqrt{a_3}}, \quad (13)$$

To check the theoretical calculations, in the paper we investigated a heater of thermal converter made of two segments of copper microwire and a central segment made of manganin microwire connected with each other. The length of the heater did not exceed 1.5 mm, and the length of its central part was 250 μm. The microwire diameter was 10 μm. The choice of copper and manganin was due not only to the difference in the specific layer but also to the minimization of the parasitic effects that occur in the areas of contact between dissimilar materials, since manganin coupled with copper has the lowest thermoelectric coefficient. To reduce the heat loss, the lateral surface of the thermocouple in the thermal converter was diminished. At a cross-section of 15x15 (μm^2), its length did not exceed 750 μm.

Taking into account in (9) the above numerical values of parameters and the thermophysical characteristics of materials for calculation in the air, we find that in a heater with variable cross-section, temperature gain in its centre nearly doubles, which is confirmed by the corresponding increase in the volt-watt sensitivity of a thermal converter with variable transverse resistance of the heater in the investigation of such thermal converters.

The use of heaters with variable resistance along their length yields good results in terms of volt-watt sensitivity increase, but such significant disadvantages as instability in time, low mechanical strength and the need to protect the surface of the heater from oxidation somewhat limit the use of such heaters in practice. A more technological solution that can drastically improve the quality of thermal converters might be the use for the heaters of a glass-insulated microwire with variable cross-section of its conductor. However, this is a serious topic in its own right.

Conclusion

1. The sensitivity of thermal converter can be significantly increased by maximum concentration of heat at point of contact between the heater and the thermocouple junction.

2. Due to the use in the thermal converter design of a heater with variable cross-section the temperature in its centre can be increased almost twice.
3. It is advisable to pursue research on creation and use of a glass-insulated microwire with variable cross-section as a heater of thermal converter.

References

1. Mykytiuk P.D., Mykytiuk O.Yu. (2018). Impact of thermocouple on temperature distribution in the heater of measuring thermal converter. *J.Thermoelectricity*, 1, 78-81
2. Anatychuk L.I. (1979). Termoelementy i termoelektricheskiye ustroistva: Spravochnik [Thermoelements and thermoelectric devices: Handbook]. Kyiv: Naukova Dumka [in Russian].

Submitted 05.04.2018

Микитюк П.Д. *канд. фіз.-мат. наук*[1,2]
Микитюк О.Ю. *канд. фіз.-мат. наук, доцент*[3]

[1]Інститут термоелектрики, вул. Науки, 1;Чернівці, 58029, Україна;
[2]Чернівецький національний університет імені Юрія Федьковича,
вул. Коцюбинського 2, Чернівці, 58012, Україна;
[3]Вищий державний навчальний заклад України «Буковинський державний
медичний університет», Театральна площа, 2, Чернівці, 58002, Україна

РОЗПОДІЛ ТЕМПЕРАТУРИ В НАГРІВНИКУ ЗІ ЗМІННИМ ПО ДОВЖИНІ ОПОРОМ У ТЕРМОЕЛЕКТРИЧНОМУ ПЕРЕТВОРЮВАЧІ

Досліджено розподіл температури у нагрівнику зі змінним опором по його довжині, що використовується у напівпровідниковому термоперетворювачі. Встановлено, що максимальна локалізація температури в точці контакту нагрівника зі спаєм термопари дозволяє збільшити температуру в його центрі майже в два рази в порівнянні зі звичайним варіантом нагрівника, що істотно збільшує чутливість термоперетворювача. Бібл. 2, Рис. 1, Табл. 1.
Ключові слова: нагрівник, термоперетворювач, розподіл температури.

Микитюк П.Д. *канд. физ.-мат. наук*[1,2]
Микитюк О.Ю. *канд. физ.-мат. наук, доцент*[3]

[1]Институт термоэлектричества, ул. Науки, 1;Черновцы, 58029, Украина;
[2]Черновицкий национальный университет имени Юрия Федьковича,
ул. Коцюбинского 2, Черновцы, 58012, Украина;
[3]Высшее государственное учебное заведение Украины «Буковинский государственный
медицинский университет», Театральная площадь, 2, Черновцы, 58002, Украина

РАСПРЕДЕЛЕНИЕ ТЕМПЕРАТУРЫ В НАГРЕВАТЕЛЕ С ПЕРЕМЕННЫМ ПО ДЛИНЕ СОПРОТИВЛЕНИЕМ В ТЕРМОЭЛЕКТРИЧЕСКОМ ПРЕОБРАЗОВАТЕЛЕ

Исследовано распределение температуры в нагревателе со сменным сопротивлением по его длине, который используется в полупроводниковом термопреобразователе. Установлено, что максимальная локализация температуры в точке контакта нагревателя со спаем термопары позволяет увеличить температуру в его центре почти в два раза по сравнению с обычным вариантом нагревателя, что существенным образом увеличивает чувствительность термопреобразователя. Библ. 2, Табл. 1, Рис. 1.
Ключевые слова: нагреватель, термопреобразователь, распределение температуры.

References

1. Mykytiuk P.D., Mykytiuk O.Yu. (2018). Impact of thermocouple on temperature distribution in the heater of measuring thermal converter. *J.Thermoelectricity*, 1, 78-81
2. Anatychuk L.I. (1979). Termoelementy i termoelektricheskiye ustroistva: Spravochnik [Thermoelements and thermoelectric devices: Handbook]. Kyiv: Naukova Dumka [in Russian].

Submitted 05.04.2018


Kokodiy N.G.

Kokodiy N.G. *Doctor phys.-mat. sciences, professor*[1,2],
Razinkov V.V *Cand. phys.-mat. sciences*[3].

[1]V.N.Karazin Kharkiv National University,
4 Svobody sq., Kharkiv, 61022, Ukraine
[2]National Pharmaceutical University, 53
Pushkinskaya str., 61002, Kharkiv, Ukraine;
e-mail: kokodiyng@gmail.com
[3]Institute of Thermoelectricity of the NAS and MES
of Ukraine, 1, Nauky str., Chernivtsi, 58029.
e-mail: anatych@gmail.com


Razinkov V.V.

THERMOELECTRIC MATRIX RECEIVER OF OPTICAL AND TERAHERTZ RADIATION

Matrix receiver of electromagnetic radiation is designed to work in the ultraviolet, visible, infrared and terahertz spectral ranges. The size of the receiver input window is 20 x 20 mm. The number of matrix elements is 36. The sensitivity of the receiver is 8 V/W in the optical range and 2-4 V/W in the terahertz range. The maximum intensity of radiation is 4 W. Bibl. 5, Fig. 13, Tables 2.
Key words: laser, radiation, receiver, thermoelectric, matrix.

Introduction

Currently, active efforts are underway to develop the middle and far regions of the infrared range (5-100 μm) and the adjacent region of the terahertz (submillimeter) range (100-1000 μm). Interest in them resumed after a long break. This is due to specific features that can be implemented in these spectral ranges:

1. Creation of very narrow radiation beams for radio communication and radar (with a beam width of a fraction of milliradians). In radiolocation, this provides spatial resolution up to several centimeters, in radio communication, the ability to transmit information without the risk of leakage.
2. The information capacity of communication channels is much larger than in the centimeter and millimeter ranges.
3. Use in security systems to detect plastic explosives and weapons.
4. To detect objects in space with a temperature of tens of kelvins emitting in the terahertz range, for instance, asteroids.
5. For the diagnostics of high-temperature plasma in controlled thermonuclear fusion facilities.

A very important characteristic of radiation beams is their profile (intensity distribution in cross section). Knowing it, it is possible to determine other parameters of the beam – the pulse energy, the radiation power, the beam diameter, the position of its energy center, the M^2 factor.

The problem of measuring the radiation beam profile is completely solved for the visible, near infrared and middle infrared spectral regions (0.4 – 10 μm). The firms COHERENT (USA), OPHIR (USA - Germany - Japan - Israel), PRIMES and PROMETEC (Germany) have developed devices using photoelectric arrays, matrices on heat receivers (thermocouples, pyroelectric receivers) and scanning receivers.

Photoelectric arrays are designed to work with narrow radiation beams (from 5 to 30 mm) and low powers (up to 1 W) in the spectral range from 0.2 to 1 μm. Matrices on thermal receivers are designed to work with radiation beams from 20 to 100 mm and radiation power from 1 mW to 10 kW in the spectral range from 0.2 μm to 10 μm. Scanning devices are designed to work in the focal region of the beam, as well as in beams with a diameter of up to 50 mm in the spectral range from 0.2 to 1 μm.

Measurement of the laser radiation characteristics in the terahertz range is still an unsolved problem of laser metrology. Known instruments for work in this range were developed by OPHIR - Pyrocam III HR and Pyrocam IV (Fig. 1) [1]. The cost of the instruments is high - about $ 30,000. The characteristics of the instruments are shown in Table 1.

Fig.1. Pyrocam III HR and Pyrocam IV instruments

Table 1

Characteristics of Pyrocam III HR and Pyrocam IV instruments

Instrument	**Pyrocam III HR**	**Pyrocam IV**
Spectral range	13-355 nm 1.06-3500 μm	13-355 nm 1.06-3500 μm
Input window	12.8 x 12.8 mm	25.6 x 25.6 mm
Number of elements	160 x 160	320 x 320

Institute of Thermoelectricity, NAS of Ukraine, developed matrix thermoelectric receivers for the visible and near infrared spectral ranges [2] (Fig. 2).

Fig.2. Matrix radiation energy receiver developed by Institute of Thermoelectricity, NAS of Ukraine

The matrix with an input window of 16 × 16 mm contains 256 elements - semiconductor thermocouples with dimensions of 1 x 1 mm. The spectral range of the receiver is from 0.4 μm to 10 μm,

the sensitivity is 100 mV/J. The receiver is designed to measure the energy of the radiation pulse. The power of continuous radiation is difficult to be measured by such a receiver. The reason for this is as follows.

From the theory of thermal measuring instruments it is known that their power sensitivity S_P and energy sensitivity S_E are related by:

$$S_P = S_E \tau,$$

where τ is thermal time constant. The receiver setting time is 4τ. With the energy sensitivity S_E = 100 mV/J and thermal time constant τ = 0.75 s, the power sensitivity turns out to be equal to S_P = 75 mV/W. If we assume that the signal level from the receiver should not be less than 1 mV, then the minimum measured power is about 15 mW, while many laser and LED sources have a much lower radiation power — a few milliwatts.

Matrix receiver for measurement of continuous power of laser radiation

To measure continuous power of laser radiation, at the Institute of Thermoelectricity of the National Academy of Sciences of Ukraine, a measuring transducer was developed in which semiconductor thermoelectric radiation receivers with power sensitivity in the optical range of about 8 V / W are matrix elements.

The general view of the receiver is shown in Fig. 3.

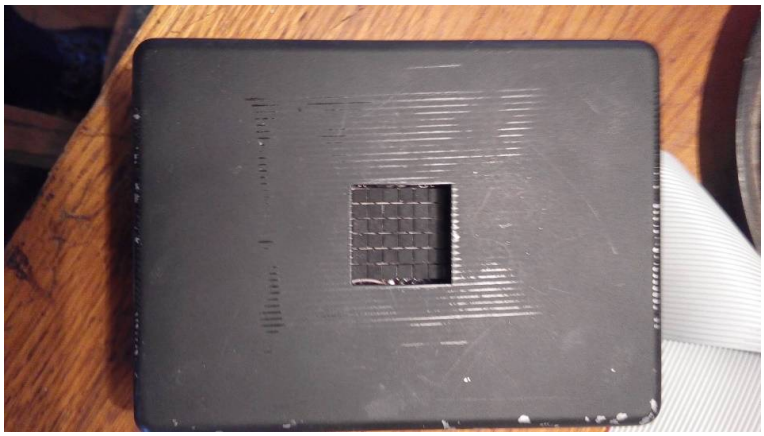

Fig. 3. Matrix thermoelectric receiver of continuous radiation

The receiver input window is 20 × 20 mm in size. The number of matrix elements – 36. The receiving element is schematically shown in Fig. 4. The receiving pad (1) is a plate of ferrite $Fe_2(V_{1-x}\ Ti_x)Al$ of size 3 × 3 mm and 0.3 mm thick. Through the layer of heat-conducting glue (2) 15-20 μm thick and the POS-61 solder layer (3) 50 μm thick, hot junctions of a battery of semiconductor thermocouples (4) based on *BiTe*, obtained by extrusion, are connected to the back side of the ferrite plate. The length of the thermoelectric element is 14.2 mm, the size of the end face of the *p-n* couple is 0.38 × 0.19 mm. The "cold junctions" of the battery through a layer of solder (5) and a layer of heat-conducting glue (6) are connected to a ceramic plate (7) 0.63 mm thick, which lies on the copper base (9). Thermal contact between the plate and the base is provided by a layer of solder (8) with a thickness of 50 μm.

Fig. 5*a* shows the numbering of matrix elements (view of the matrix from the front, along the laser beam). The analog-to-digital converter E14-140 used in the experiments has 32 channels. Therefore, the signals from the angular matrix elements were not measured (Fig. 5*b*). Their values were determined using interpolation.

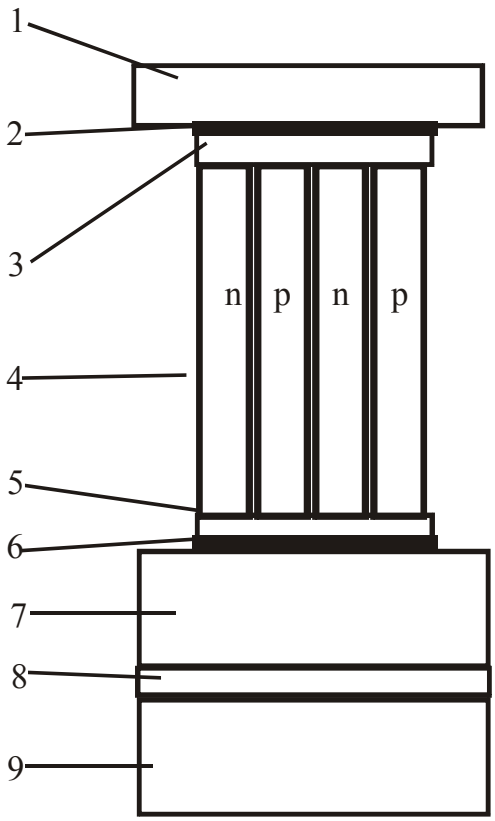

Fig. 4. Schematic of matrix receiving element

1	2	3	4	5	6
7	8	9	10	11	12
13	14	15	16	17	18
19	20	21	22	23	24
25	26	27	28	29	30
31	32	33	34	35	36

a)

	1	2	3	4	
5	6	7	8	9	10
11	12	13	14	15	16
17	18	19	20	21	22
23	24	25	26	27	28
	29	30	31	32	

b)

Fig. 5. Radiation receiver matrix
a – matrix elements, b – Numbers of ADC channels

STUDY OF THE RECEIVER

Irregularity of thermocouple sensitivity

A laser beam with a diameter of about 1 mm was induced on each of the matrix elements, and the electrical signal generated by the thermocouples of this element was measured. The laser power was controlled. The measurement results are shown in Fig. 6. The thermocouple numbers are plotted along the abscissa axis, and the power sensitivity of each of the thermopiles S_P is plotted along the ordinate axis.

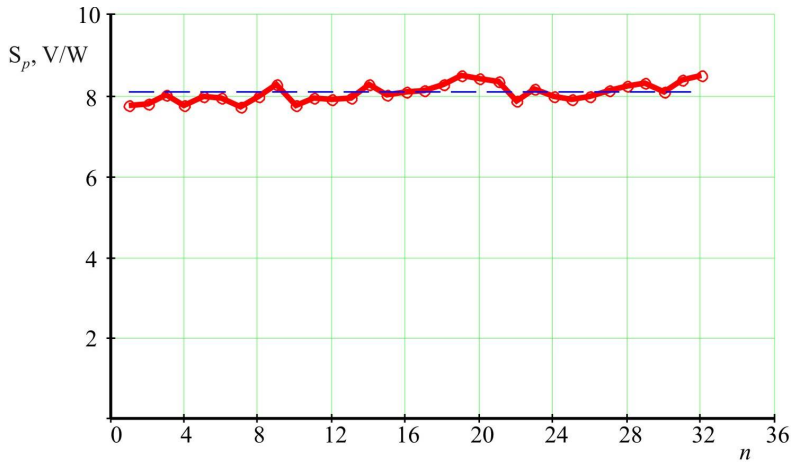

Fig. 6. Sensitivity of the receiver thermocouples

The spread of sensitivity is about 5 % of the average value:
$S_{P\,av}$ = 8.07 ± 0.01 V/W.

When processing the measurement results, the sensitivity of each thermocouple was taken into account.

Receiver dynamic range

Lower measurement limit

The lower measurement limit is determined by zero drift when the receiver is heated, zero offset with random changes in ambient temperature, pickups from the power supply network and other extraneous sources, internal noise of the analog-to-digital converter.

A typical view of a signal from a radiation receiver with a power near the lower measurement limit is shown in Fig. 7. For 60 seconds a "zero" signal was recorded. For the next 60 seconds, radiation was applied to the receiver, and then the radiation was blocked, and the receiver cooled down.

The width of the noise track, taking into account rare overshoots up and down, is about 2 mV, which, with a receiver sensitivity of 8 V / W, corresponds to a power of 0.25 mW. For confident measurement, it is necessary that the signal exceeds the noise at least 10 times. Fig. 6 presents something like this:

1. Noise: U_0 = -0.77 ± 0.07 mV.
2. Radiation: U_1 = 9.14 ± 0.09 mV.
3. Signal: $U = U_1 - U_0$ = 9.9 ± 0.1 mV.
4. Relative error of signal measurement: U = 1.4%.

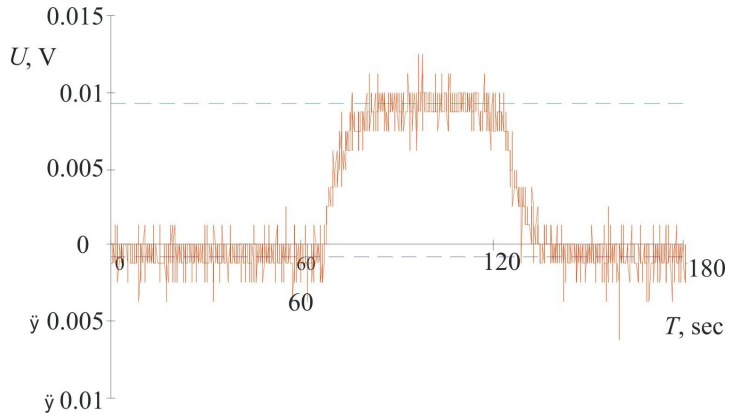

Fig. 7. Signal from matrix receiving element

Approximately the same will be the relative error in measuring the power of the radiation incident on a given matrix element, i.e.:
$P = 79 \pm 1$ mW.

The small error of the measurement result with a large noise level is due to averaging over a large number of data (from 400 to 600) when calculating the values of U_0 and U_1.

Thus, the lower measurement limit of matrix receiver with a noise corresponding to a radiation power of 0.25 mW is approximately 10 mW.

Upper measurement limit

The upper measurement limit is determined by the fracture threshold of ferrite plate, which serves as a radiation receiving element, and the melting point of solder in the joints of the "hot" junctions of thermocouples.

To evaluate it, the thermal problem was solved, which describes the heating of the matrix element [3]. The geometry of the problem is shown in Fig. 4. The layers of heat-conducting glue, solder and ceramics are very thin. Therefore, their presence can be ignored, and the matrix element can be considered to be a two-layer one, consisting of a ferrite plate and semiconductor thermocouples.

Laser radiation of intensity I falls on the ferrite plate. The "hot" thermopile junctions are adjacent to it. The "cold" junctions are on the ceramic plate and maintained at constant temperature.

The equation of thermal conductivity at steady-state temperature has the following form:

$$\frac{d^2T(x)}{dx^2} = 0, \tag{1}$$

where T is temperature at the point with coordinate x.

The initial temperature:

$$T_1 = T_2 = 0. \tag{2}$$

Here, T_1 and T_2 are the temperatures of ferrite and thermocouple, respectively.

The boundary condition on the surface of the receiving element with the coordinate $x = 0$ describes the situation when radiation is absorbed in an infinitely thin surface layer. Conductive heat removal into the body occurs (thermal conductivity coefficient k_1) and convective heat removal to the environment (heat transfer coefficient α):

$$k_1 \frac{dT_1(0)}{dx} = -I + \alpha T_1(0). \tag{3}$$

At the junction of thermocouples with the heat sink $(x = L)$, the initial temperature is maintained:

$$T_2(L) = 0. \tag{4}$$

At the point of contact between ferrite and thermocouple $(x = l)$, the boundary condition describes the continuity of temperature and heat flux:

$$T_1(l) = T_2(l), \tag{5}$$

$$k_1 \frac{dT_1(l)}{dx} = k_2 \frac{dT_2(l)}{dx}. \tag{6}$$

Here, T_1 and k_1 are the temperature in the ferrite plate and its thermal conductivity, T_2 and k_2 are the temperature in the thermocouple and its thermal conductivity.

The solution of Eq.(1) with the boundary conditions (3) - (6) looks like this:

$$T(x)=\begin{cases}T_1(x) & at \quad 0\le x\le l\\ T_2(x) & at \quad l<x\le L\end{cases}, \tag{7}$$

where

$$T_1(x)=I\frac{k_1(L-l)+k_2(l-x)}{k_1k_2+\alpha\left[k_1(L-l)+k_2l\right]}, \qquad T_2(x)=I\frac{k_1(L-x)}{k_1k_2+\alpha\left[k_1(L-l)+k_2l\right]}. \tag{8}$$

Fig. 8 shows a plot of temperature distribution along the x axis for the following parameter values:

$I = 5\cdot10^3$ W/m^2, $l = 0.3$ mm, $L = 14.5$ mm,

$k_1 = 4.2$ W/(m·K), $k_2 = 1.38$ W/(m·K), $\alpha = 20$ W/(m^2·K).

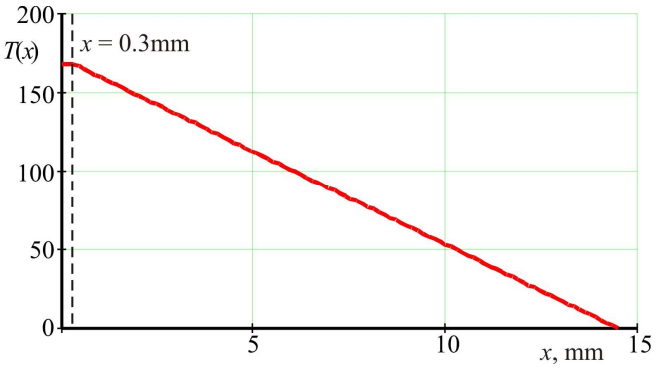

Fig. 8. Temperature distribution in matrix element

The intensity of radiation is chosen so that at the point of contact between thermocouples and the ferrite plate the heating temperature is 160 ° C, which at the ambient temperature of 20 ° C creates in this place the melting temperature of the POS-61 solder equal to 180 ° C.

In this case, the radiation intensity should be equal to $2\cdot10^4$ W/m^2. It is obtained when the radiation power incident on the receiver is 8 W. The surface temperature of the ferrite plate is about 200 ° C.

For safe operation of the receiver its surface temperature should not exceed 100° C. This will be at a radiation power of about 4 W.

Amplitude response

The radiation source was a projection incandescent lamp with a radiation power of up to 5 W. The dependence of the magnitude of the signal from the receiver on the radiation power is shown in Fig. 9. The ordinate is the sum of the signal values from all matrix elements. In this power range, the amplitude response of the receiver is linear.

The power sensitivity of the receiver in the visible range is – 6.2 ± 0.5 V/W.

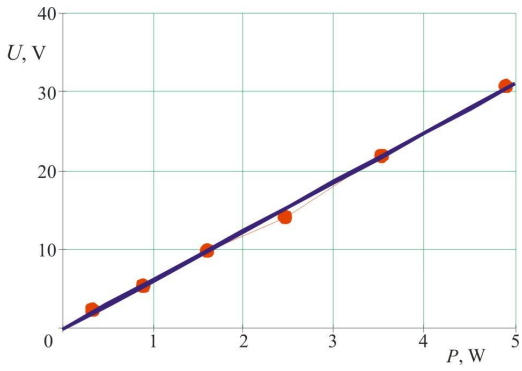

Fig. 9. Amplitude response of the matrix receiver

Time constant

Radiation from a projection incandescent lamp was applied to the receiver. Radiation power was 0.75 watts. The light spot is a horizontal ellipse with a major axis of 16 mm, a minor axis of 10 mm.

The time dependence of the thermocouple signal U was registered. The measurement results are shown by dots in Fig. 10. The solid line is the approximation of this dependence by the function

$$U(t) = U_0\left(1 - e^{-t/\tau}\right).$$

Least squares processing yields: τ = 4.3 s. The setting time t_{set} is 4.

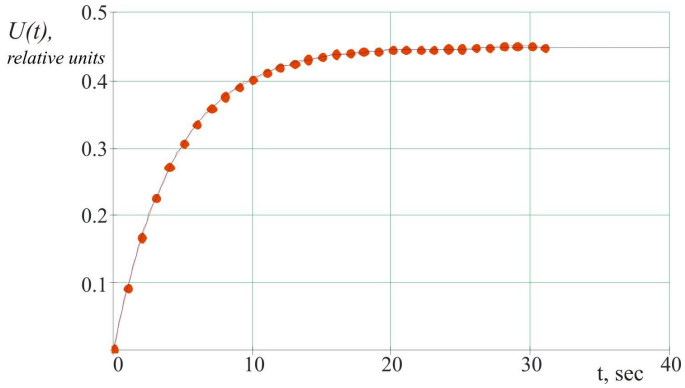

Fig. 10. Setting time of thermocouple signal

Thermal coupling between matrix elements

When measuring continuous power, a stationary thermal regime is set in the receiver after the time t_{set} . In this case, the heat from the more heated matrix elements can pass to less heated ones, as a result of which the temperature distribution over the surface of the receiver will be distorted, thus distorting the radiation beam profile.

To check the thermal coupling between the matrix elements, a narrow beam of radiation from a laser pointer was directed to one of them. The results of measurements are shown in Fig.11. The beam diameter is approximately equal to the size of the element – 3 × 3 mm.

The diagram in the form of columns shows that one element is very hot. It is shown in red.

The heating of neighboring elements in the diagram is almost unnoticeable. Matrix Mc shows the temperature distribution (in relative units) on the heated and adjacent elements. It is seen that the temperature of neighboring elements does not exceed 6 % of the temperature of the heated element. Thus, the thermal coupling between the elements is weak, and the error due to this cause is small. It is no more than the error caused by different thermocouples.

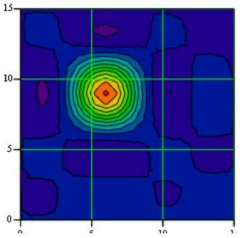

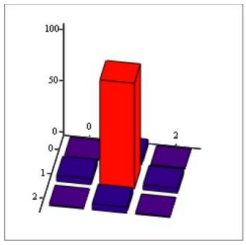

$$M_c := \begin{pmatrix} 0.691 & 5.891 & 0.846 \\ 5.610 & 103.102 & 4.832 \\ 0.893 & 6.097 & 0.743 \end{pmatrix}.$$

Radiation power P = 9 mW

X_c= 6.16 mm, Y_c= 8.66 mm, D_x= 2.19 mm, D_y= 4.02 mm, …D = 2.97 mm

Fig. 11. Thermal coupling between matrix elements

Spectral response

To measure the spectral response of the receiver, color LEDs covering the visible spectrum (blue, green, yellow and red), white LED, red and green semiconductor lasers, two incandescent lamps, an infrared laser and two terahertz lasers were used. The measurement results are shown in table 2.

Table 2

Receiver spectral response

Light source	Wavelength, µm	Sensitivity, V/W
Blue LED	0.460	6.8
Green LED	0.505	7.0
Yellow LED	0.590	6.5
Red LED	0.635	4.4
White LED	0.4 - 0.7	7.6
Lamp 1	0.4 – 0.7	6.4
Lamp 2	0.4 -0.7	6.2
Green laser	0.532	8.0
Red laser	0.650	6.4
IR laser	10.6	7.0
THz laser 1	119	4.9
THz laser 2	432	2.0

The same characteristic is shown in Fig. 12.

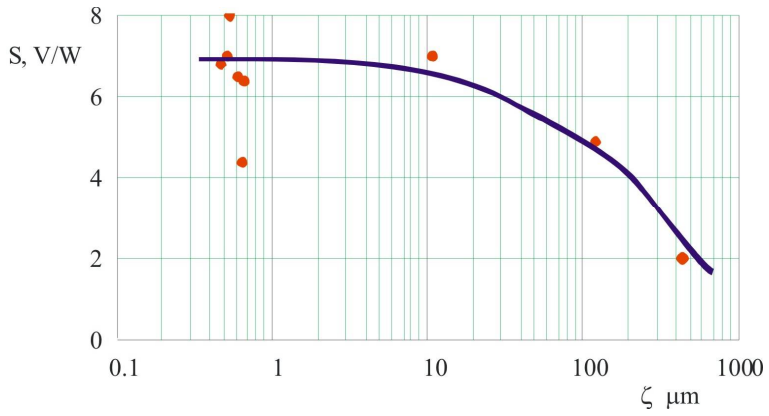

Fig. 12. Receiver spectral response

In the visible and infrared range up to 10 µm, the sensitivity is almost constant. The scatter of experimental points is explained by the measurement errors of the radiation power. In the terahertz range, the sensitivity is much lower. This is due to a decrease in the absorption capacity of ferrite at wavelengths close to the microwave range.

Measurement of radiation pulse energy

A flash lamp with the energy of 30 J (stored in a capacitor) served as a source of pulsed radiation. The pulse duration was about 1 ms. Fig. 13 shows the view of the signal from the receiver when exposed to a radiation pulse.

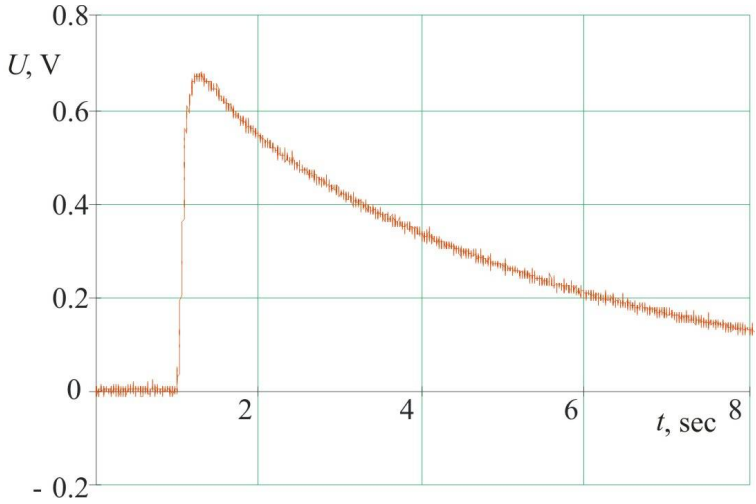

Fig. 13. Receiver response to optical pulse

With the receiver power sensitivity S_P = 8 V/W and time thermal constant τ = 4.3 s the energy sensitivity is

$$S_E = \frac{S_P}{\tau} = 1.86 \text{ V/J}.$$

The amplitude of the receiver signal is 0.7 V. This corresponds to radiation energy of about 1.3 J.

The energy sensitivity of the receiver under study is much greater than that of a matrix detector [2]. Therefore, it can be successfully used to measure the energy of a radiation pulse. It ranks below only in inertia - the time constant is 4.3, not 0.75 s, as in the receiver [2].

Measurement of the terahertz laser radiation parameters

Fig. 14 shows the results of measuring the beam profile of a gas laser operating on methanol vapor in the terahertz range. The radiation wavelength is 118.9 μm, the radiation power is 10 mW. The laser worked in TEM_{00} oscillation mode.

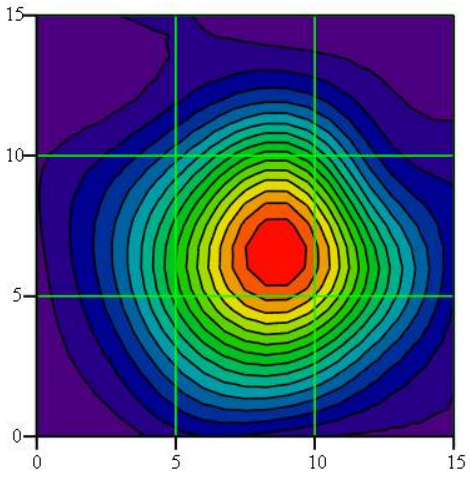

Fig. 14. The beam profile of a terahertz laser

The parameters of the radiation beam, calculated in accordance with the methodology described in the ISO / DIS 11146 standard [5], turned out to be as follows.

The coordinates of the energy center of the beam are determined by the relations:

$$x_c = \frac{\int\limits_S x\, I(x, y)\, dS}{\int\limits_S I(x, y)\, dS}, \qquad y_c = \frac{\int\limits_S y\, I(x, y)\, dS}{\int\limits_S I(x, y)\, dS}. \tag{9}$$

Here *I (x, y)* is the intensity distribution function in the beam cross section. Integration is done over its cross sectional area.

Calculations using these formulae yield:

$$x_c = -7.9 \text{ mm}, \quad y_c = 6.8 \text{ mm}.$$

The beam diameters along the axes *Ox* and *Oy* are determined as follows:

$$D_x = 4\sqrt{\frac{\int\limits_S (x - x_c)^2\, I(x, y)\, dS}{\int\limits_S I(x, y)\, dS}}, \quad D_y = 4\sqrt{\frac{\int\limits_S (y - y_c)^2\, I(x, y)\, dS}{\int\limits_S I(x, y)\, dS}}. \tag{10}$$

The geometric mean of the diameter is also used:

$$D = \sqrt{D_x D_y}. \tag{11}$$

The calculations give the following values of these quantities:

$$D_x = 14.1 \text{ mm}, \quad D_y = 14.0 \text{ mm}, \quad D = 14.0 \text{ mm}.$$

Conclusion

For the first time in Ukraine, a matrix laser radiation receiver was developed, which covers the visible, infrared and terahertz range with the following characteristics:

- spectral range – 0.4…500 μm;
- number of receiving matrix elements – 36;
- size of receiving element – 3 x 3 mm;
- receiver continuous power sensitivity – 8.07 V/W;
- receiver energy sensitivity – 1.86 V/J;
- setting time – 17 s.

References

1. Pyrocam III HR, Pyrocam IV // www. ophiropt.ru
2. Multielement laser radiation detector // www.it.inst.cv.ua
3. Lykov A.V. (1966). *Teoriia teploprovodnosti [Theory of thermal conductivity]*. Moscow: Vysshaia shkola [in Russian].
4. Goncharskii A.A., Nesterov A.V., Niziev V.G., Novikova L.V., Yakunin V.P. (2000). Opticheskiie elementy lasernogo resonatora dlia generatsii lucha s osesimmetrichnoi poliarizatsiei [Optical elements of laser resonator for generation of a beam with axisymmetric polarization]. *Optika i spectroskopiia – Optics and Spectroscopy*, 89(1), 160-164 [in Russian].
5. *Draft International Standard ISO/DIS 11146*. Optics and optical instruments – Laser and laser-related equipment - Test methods for laser beam parameters: beam widths, divergence angle and beam propagation factor. – 1995.

Submitted 20.04.2018

Кокодий Н.Г. *доктор фіз.-мат. наук, професор*[1,2]
Разіньков В.В. *канд. фіз.-мат. наук*[3]

[1]Харьківський національний університет
імені В.Н. Каразіна, пл. Свободи, 4,
Харьків, 61022, Україна,
e-mail: kokodiyng@gmail.com;
[2]Національний фармацевтичний університет,
вул. Пушкінська, 53, 61002, Харків, Україна;
[3]Інститут термоелектрики НАН і МОН України, вул. Науки, 1,
Чернівці, 58029, Україна, *e-mail: anatych@gmail.com*

ТЕРМОЕЛЕКТРИЧНИЙ МАТРИЧНИЙ ПРИЙМАЧ ОПТИЧНОГО Й ТЕРАГЕРЦЕВОГО ВИПРОМІНЮВАННЯ

Матричний приймач електромагнітного випромінювання призначений для роботи в ультрафіолетовому, видимому, інфрачервоному й терагерцовому діапазонах спектра. Розміри вхідного вікна приймача – 20× 20 мм. Кількість елементів матриці – 36. Чутливість приймача – 8 В/Вт в оптичному діапазоні й 2- Бібл. 5, рис. 13, табл. 2.
Ключові слова: лазер, випромінювання, приймач, термоелектричний, матриця.

Кокодий Н.Г. *доктор физ.-мат. наук, професор*[1,2]
Разиньков В.В. *канд. физ.-мат. наук*. [3]

[1]Харьковский национальный университет имени В. Н. Каразина,
пл. Свободы, 4, Харьков, 61022, Украина
[2]Национальный фармацевтический университет, ул. Пушкинская,
53, 61002, Харьков, Украина, *e-mail: kokodiyng@gmail.com;*
[3]Институт термоэлектричества НАН и МОН Украины,
ул. Науки, 1, Черновцы, 58029, Украина; *e-mail: anatych@gmail.com*.

ТЕРМОЭЛЕКТРИЧЕСКИЙ МАТРИЧНЫЙ ПРИЕМНИК ОПТИЧЕСКОГО И ТЕРАГЕРЦЕВОГО ИЗЛУЧЕНИЯ

Матричный приемник электромагнитного излучения предназначен для работы в ультрафиолетовом, видимом, инфракрасном и терагерцевом диапазонах спектра. Размеры входного окна приемника – 20 × 20 мм. Количество элементов матрицы – 36. Чувствительность приемника – 8 В/Вт в оптическом диапазоне и 2-4 В/Вт в терагерцевом диапазоне. Максимальная интенсивность излучения – 4 Вт. Библ. 5, рис. 13, табл. 2.
Ключевые слова: лазер, излучение, приемник, термоэлектрический, матрица.

References

1. Pyrocam III HR, Pyrocam IV // www. ophiropt.ru
2. Multielement laser radiation detector // www.it.inst.cv.ua

3. Lykov A.V. (1966). *Teoriia teploprovodnosti [Theory of thermal conductivity]*. Moscow: Vysshaia shkola [in Russian].
4. Goncharskii A.A., Nesterov A.V., Niziev V.G., Novikova L.V., Yakunin V.P. (2000). Opticheskiie elementy lasernogo resonatora dlia generatsii lucha s osesimmetrichnoi poliarizatsiei [Optical elements of laser resonator for generation of a beam with axisymmetric polarization]. *Optika i spectroskopiia – Optics and Spectroscopy*, 89(1), 160-164 [in Russian].
5. *Draft International Standard ISO/DIS 11146*. Optics and optical instruments – Laser and laser-related equipment - Test methods for laser beam parameters: beam widths, divergence angle and beam propagation factor. – 1995.

Submitted 20.04.2018

L.I. Anatychuk[1,2] *Acad. National Academy of Sciences of Ukraine*,
V.V.Lysko,[1,2] *Cand. Phys.- mat. Sciences*,
M.V. Havryliuk[1]
[1]Institute of Thermoelectricity, 1 Nauky Str., 58029, Chernivtsi, Ukraine
[2]Yu.Fedkovych Chernivtsi National University,
2, Kotsiubynskyi str., Chernivtsi, 58000, Ukraine,
e-mail: anatych@gmail.com

WAYS FOR QUALITY IMPROVEMENT IN THE MEASUREMENT OF THERMOELECTRIC MATERIAL PROPERTIES BY THE ABSOLUTE METHOD

The paper is concerned with the results of research on the errors in the measurement of thermoelectric material properties by the existing methods. It is established that the efficient measurement method is the absolute method which allows instrumental minimization of the majority of error sources. The results of research on the errors in the measurement of thermoelectric material properties by the absolute method obtained by object-oriented computer simulation are given. The effect of radiation, heat transfer by measuring electrodes, electrical and thermal field distortions on the contacts on the measurement accuracy is established. New methods for minimization of errors are described. The errors caused by deviations from the linear temperature distribution in the sample under study on the attainment of a steady-state are considered as well. Measurement rapidity is studied, and methods for its increase are developed. A description of two modifications of automated measurement equipment based on the elaborated methods – for temperature ranges from 30 to 500 °C and 30 to 900 °C is given. Bibl. 14, Fig. 17.
Key words: absolute method, measurement, electrical conductivity, thermoEMF, thermal conductivity, errors.

Introduction

It is known that recent decades have seen no considerable improvement of thermoelectric materials quality [1, 2]. As before, the best materials used in thermoelectric power converters for generation and refrigeration equipment are *Bi – Te*, *Pb – Te*, and *Ge – Si* compounds and, sometimes, others.

Various methods are used to devise new materials and improve the existing ones. Chemical composition is changed, various impurities are introduced and various material structures are used - inhomogeneous, nanostructures, powders and others. The influence of these effects on material is determined experimentally by measurement of electric conductivity σ, thermopower α, thermal conductivity κ and figure of merit *Z*.

Analysis of known methods and equipment for measurement of thermoelectric material properties has shown that the errors in determination of thermoelectric figure of merit *Z* achieve 10 to 15% [3 – 5]. The largest values of errors in the determination of figure of merit occur when measuring the electric conductivity, thermopower and thermal conductivity on different samples. Thus, the errors in the determination of the Seebeck coefficient are 2 to 5 % (steady-state method, Fig. 1; hot probe method, Fig. 2), electric conductivity – 2 to 3 % (two-probe method, Fig.3; four-probe method, Fig. 4), thermal conductivity - 3 to 7 %, relative method, Fig. 5; the Angstrom method, Fig. 6; laser flash method, Fig. 7) [4-13].

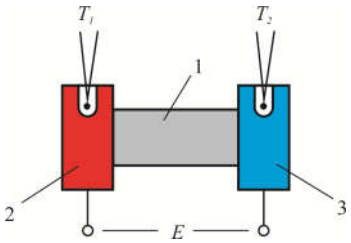

Fig. 1. Steady-state method of the Seebeck coefficient measurement.
1 – sample; 2, 3 – electrically conducting thermostats

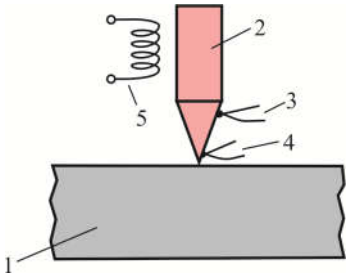

Fig. 2. Schematic of the Seebeck coefficient measurement by hot probe method.
1 – sample, 2 – probe, 3 and 4 – thermocouples, 5 – miniature furnace

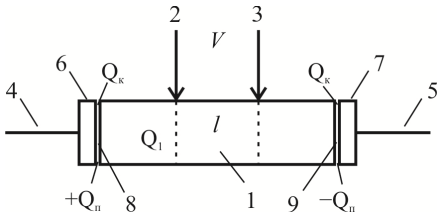

Fig. 3. Schematic of two-probe method of electric conductivity measurement.
1 – sample; 2, 3 – potential electrodes; 4, 5 – current conductors; 6, 7 – current electrodes; 8, 9 – contacts

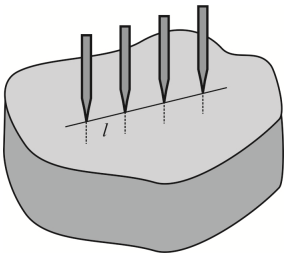

Fig. 4. Four-probe method of electrical conductivity determination

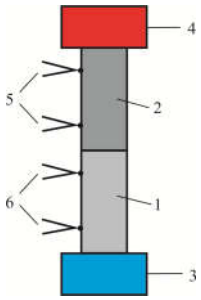

Fig. 5. Schematic of thermal conductivity measurement by the relative method.
1 – sample under measurement; 2 – reference sample; 3 – thermostat;
4 –electrical heater; 5, 6 – thermocouples used to measure temperature differences
in the reference and measured sample

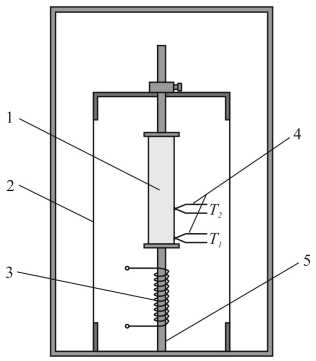

Fig. 6. Schematic of device for measurement of temperature diffusivity by the Angstrom method.
1 – sample under test; 2 – mica shield; 3 – heater; 4 –thermocouples; 5 – copper rod

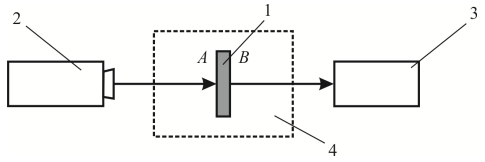

Fig. 7. Schematic of laser flash method.
1 – sample under study, 2 – laser, 3 – infrared detector, 4 – thermostat.

Thus, total error in the determination of figure of merit can reach 20%. Besides, as long as material is practically always slightly inhomogeneous, this leads to additional error which is on the average 3 to 5 %. Total error in the determination of Z in this case can reach 23 to 25 %.

Such errors become an obstacle to solving the tasks of material figure of merit improvement, as long as measurement accuracy can prove to be lower than improvement of material properties with a change of affecting factors.

More reliable results can be obtained with the use of the absolute method and the Harman method [2, 14]. The cycle of investigations performed at the Institute of Thermoelectricity has demonstrated that the errors in the measurement of figure of merit by the Harman method can be 5 to 6 % only in a number of cases, when a lot of additional parameters are known, such as: radiative properties of the sample and thermostat, thermal conductivity of conductors and thermocouples, etc.

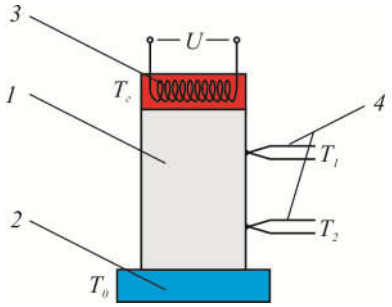

Fig. 8. Schematic of the absolute method of thermal conductivity measurement
1 – sample under study; 2 – thermostat; 3 – electrical heater; 4 – thermocouples.

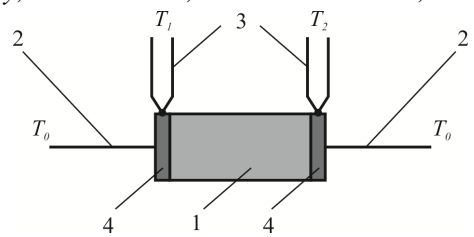

Fig. 9. Schematic of complex measurements by the Harman method
1 –sample; 2 –current conductors;
3 – thermocouples; 4 –contacts.

The most efficient is the absolute method which makes it possible to minimize instrumentally the majority of error sources. It is widely used for creation of references and offers important advantages, namely σ, α, κ, and *Z* are simultaneously measured on the same sample, which reduces the errors; small-size samples can be used for measurement; thermoelectric parameters are found from classical formulae without corrections.

The purpose of this work is research aimed at minimization of errors in the measurement by the absolute method and creation of high-precision measurement equipment for complex determination of thermoelectric material properties over a wide temperature range.

Physical, mathematical and computer models of the absolute method

A physical model of the method is given in Fig. 1. It comprises a sample which is in thermal and electrical contact with the thermostated base and a reference heat source on the upper surface of the sample. Under the ideal conditions the lateral and upper surfaces of the heat source are adiabatically isolated. Distortions in the determination of thermoelectric parameters are due to two main reasons.

The first reason results from instrumental errors in the determination of sample cross-section values, the distances between thermocouples and measuring probes, the values of current and potential difference between the probes, temperature difference, heat flow through the sample. With the use of up-to-date measurement equipment the total effect of these errors will be less than 0.2%.

The second component is method errors. They are due to a deviation from ideal physical model conditions, namely conditions of adiabaticity and uniformity of heat and current flows through the sample, as well as deviation from point-by-point measurements of measuring probes and thermocouples. The largest distortions take place in thermal conductivity measurement.

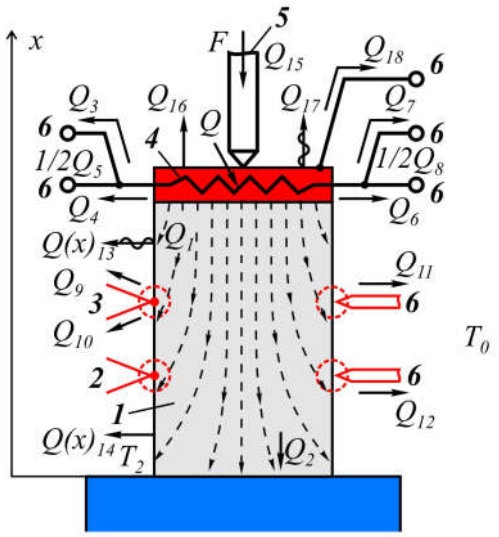

Fig 10. Real physical model of the absolute method.
1 –sample, 2, 3 – thermocouples,
4 – reference heater, 5 – pressure, 6 – electrodes

Heat Q which is released by the reference heater passes not only through the sample, but also through the electrodes connected to the sample. Moreover, there is heat rejection due to radiation and convection to the environment. The number of such heat losses depicted in Fig. 1 is 18. The situation is somewhat better when performing measurements in vacuum. In that case the values of distorting thermal

flows are somewhat reduced, and the number of heat losses is decreased to 16. Electric conductivity measurement also involves problems. The presence of the Peltier and Joule heat creates sample nonisothermality which can cause gross errors.

To determine the effect of these factors on measurement accuracy, it is necessary to solve the problem of finding the distributions of electrical potential and thermal flows in the presence of heat losses and the Joule and Peltier effect. Such problems are difficult to be solved analytically due to complexity of geometry, the presence of anisotropy and nonuniformity, the temperature dependences of sample material properties and structural members of measurement equipment. To calculate the temperature and electrical fields, as well as the effect of various factors on them, computer models of object-oriented simulation of real physical modes were used.

Such methods yield a solution of a system of second-order differential equations in partial derivatives written as follows

$$\begin{cases} -\nabla\left(\left(\kappa_i + \alpha_i{}^2\sigma_i T + \alpha_i\varphi\sigma_i\right)\nabla T\right) - \nabla\left(\left(\alpha_i\sigma_i T + \varphi\sigma_i\right)\nabla\varphi\right) = 0, \\ -\nabla\left(\sigma_i\nabla\varphi\right) - \nabla\left(\sigma_i\alpha_i\nabla T\right) = 0. \end{cases} \quad (i = 1..20) \qquad (1)$$

and derived from the laws of conservation of electrical charge and energy. In formula (1): α_i, σ_i, κ_i are the Seebeck coefficient, the electrical and thermal conductivities of physical model elements, T is temperature, φ is electrical potential.

Computer model was built with the use of COMSOL Multiphysics application program package [16], which allows by means of finite element method to find a solution of system (1) with the respective boundary conditions.

Methods for reduction of errors

The elaborated computer model was used to obtain the distributions of heat and current flows in the sample and structural components of the measurement system and to study possible measurement errors. They can be divided into two main groups. The first one is due to thermal radiation from the surface of sample and reference heater. According to investigations, these errors are the largest and can reach 75%. They were reduced with the use of additional heat source and radiation shield (Fig. 11).

The same temperature gradient is created on the shield as on the sample. However, due to re-radiation a radiation component along the sample is created.

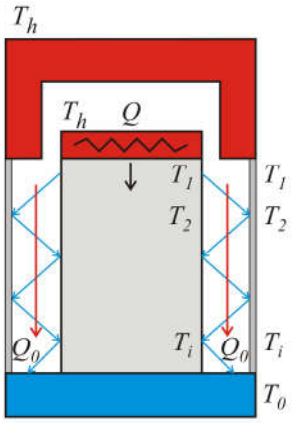

Fig. 11. Use of gradient radiation shield

For this reason radiation from the sample surface remains large and results in thermal conductivity measurement errors up to 15-20%. It was proposed to use radiation rings on the shield and a shiny reflector on the base. In so doing, heat losses and, accordingly, the errors are reduced to 1.5%.

The second group of errors is due to losses of heat along the electrodes of sample and reference heater. For their minimization it was proposed to use the so-called thermal switches. They are components made of heat-conducting insulators, such as beryllium oxide, whose thermal conductivity is close to that of copper (Fig. 12). Mounted in them are electrodes that are brought in thermal contact with ceramics. The latter, in turn, is in thermal contact with the radiation shield. In this case the difference in temperatures on the electrodes is considerable, heat flow through the electrodes is minimized and the error values are minimized accordingly. Computer simulation showed that total error due to these losses will be ~ 0.5%.

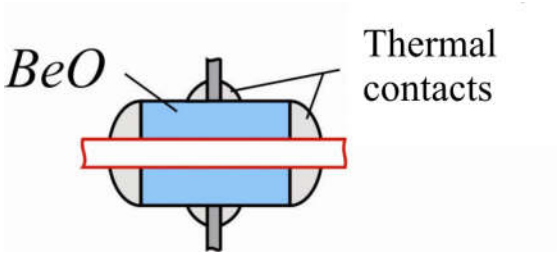

Fig. 12. Thermal switch

Another important factor causing the errors is the influence of current and thermal contacts of the sample. With the use of pressure contacts, the heater touches the sample at least at three points, which can distort the uniformity of heat and current flows. The latter will affect the distribution of temperatures and electrical potential in the sample.

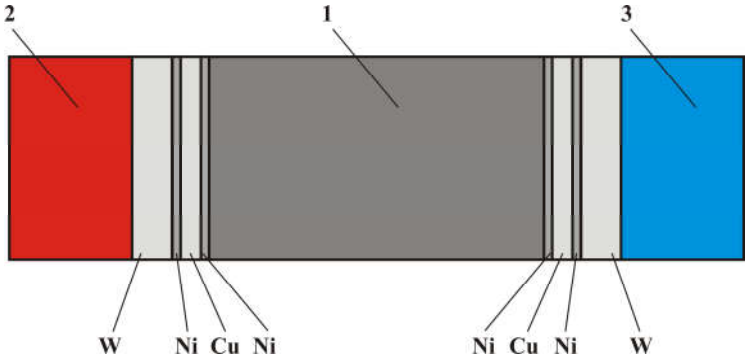

Fig. 13. Contact structures improving the quality of thermal and electrical contacts of sample to heat exchangers
1 – sample; 2 – reference heater; 3- thermostat.

Optimization calculations and computer simulation have shown that equalization of electric current and heat flow density requires metallization of sample ends. An optimal set of metal coatings was determined (Fig. 13.) Layer thicknesses: *Ni* – 10 μm, *Cu* – 100 μm, *Ni* – 10 μm, *W* – up to 200 μm.

Computer simulations were also made of electrical and thermal field distortions at places of sample contact to measurement probes. It was established that even at contact diameters 0.1 to 0.5 mm the probes average the temperature, yielding a reasonably precise temperature value, like at point contact. The error in this case does not exceed 0.05 %.

Thus, total error in the determination of figure of merit Z is 4.7%, which is 3 to 5 times better compared to other counterparts.

The issue of equipment rapidity improvement was studied. As long as to perform the experiment it is necessary to achieve steady-state conditions, time required to measure the temperature dependences of one sample properties is 15 hours, with the measurement of 12 temperature points.

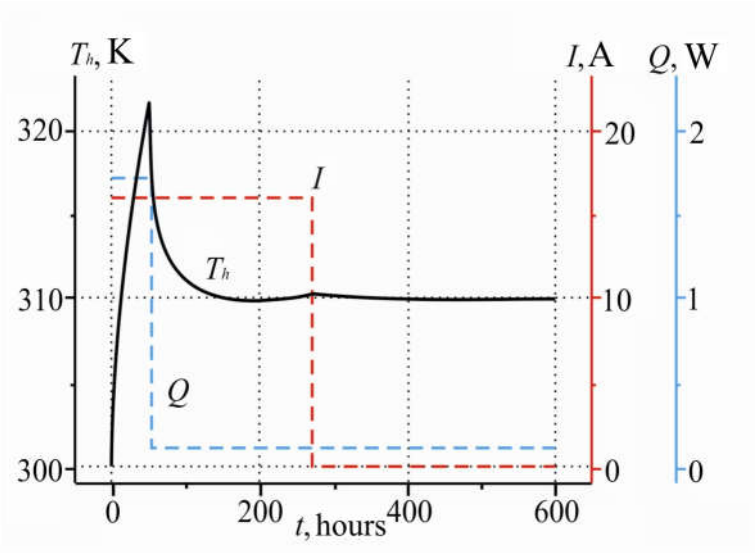

Fig. 14. Methods for increasing the rate of attainment of the steady-state.

Measurement rate can be increased by passing of alternating current through the sample (Fig. 14). This accelerates heating of sample central part due to the Joule heat release. This method allows achievement of steady-state temperature mode in the sample 3 times as fast. Measurement rate can be further improved by heating of the hot sample side with a reference heater. Due to combination of these two methods, measurement rapidity can be increased up to 8 to 10 times.

Description of measurement equipment

A design of experimental measurement unit is given in Fig. 15. It employs all methods for minimization of errors described above.

For convenience and minimization of the influence of human errors, the system is automated to the maximum. Its block-diagram is given in Fig. 16. It comprises power unit and measurement control unit based on high-precision multi-channel microcontroller analog-to-digital converter. On entering the measured temperature data, all measurement processes are performed unattended. Processed measurement results in the form of plots or tables are displayed in computer

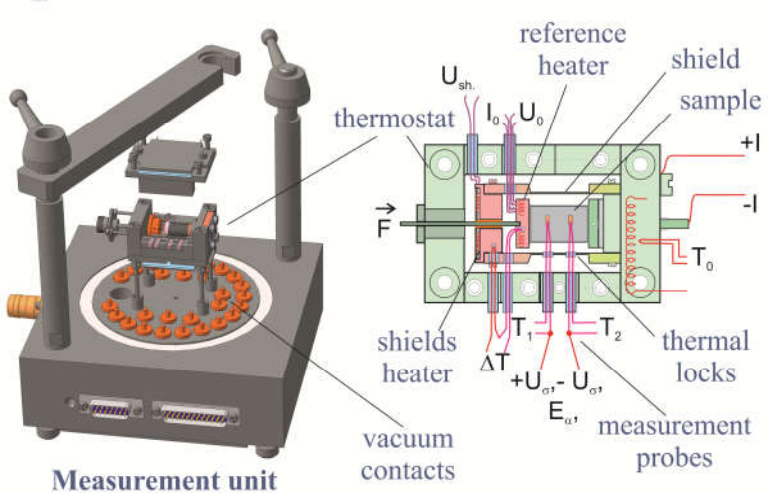

Fig. 15. Design of measurement unit

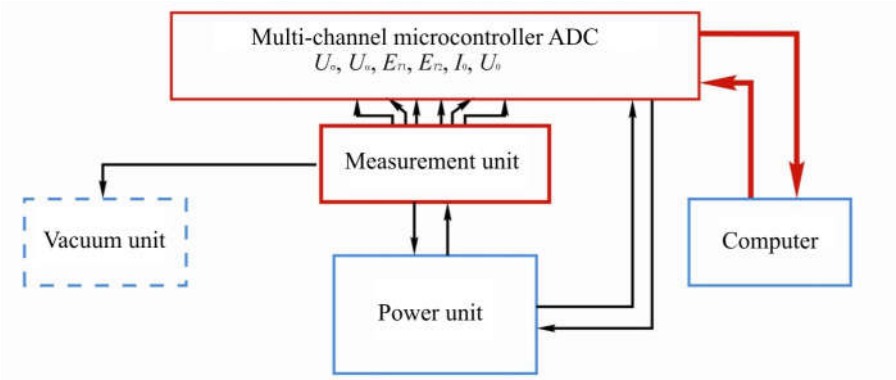

Fig. 16. System block-diagram

To study high-temperature materials, a modification of measurement unit was created that allows measurements to be made in the temperature range 30 to 900 ºC. Its key feature was using of insulation fills to eliminate radiation losses increasing at such temperatures. As well as the above contact structures with nickel, copper and tungsten layers.

External view of automated system for measurement of thermoelectric material properties in the temperature range 30 to 900 ºC is given in Fig. 17.

Such equipment was used to determine the temperature dependences of thermoelectric properties of various materials. In particular, its accuracy allowed realizing optimal parameter values of functionally graded materials for Bi – Te generator modules on which the efficiency values about 8% were obtained.

Fig. 17. External view of automated system for the determination of thermoelectric material properties in the temperature range 30 to 900 ºC

Conclusion

1. The influence of various factors on the accuracy of measurement of thermoelectric properties of materials by the absolute method has been studied. New methods for minimization of errors have been developed – gradient radiation shields with ring-shaped notches, thermostat reflector, thermal switches, metal contact structures for a reliable connection of sample end surfaces to current and thermal contacts. The achieved error values: thermal conductivity – 2.4 %, electric conductivity – 0.7 %, thermopower – 0.8 %, figure of merit – 4.7 %.
2. Error reduction methods were used to fabricate an automated measurement system for determination of thermoelectric material parameters in the temperature range 30 to 500 °C. A totality of measures taken allows reducing the figure of merit errors by a factor of 3 to 5.
3. Fort the investigation of high-temperature materials a modification of measurement unit was created that allows measurements to be made in the temperature range 30 to 900 ºC.

4. Methods for essential, up to 10-fold, increase of the rate of attainment of a steady-state in the measured samples have been developed.

References

1. Yepremyan A.O., Arutiunyan V.M., Vaganyan A.I. (2005). Figure of merit of novel thermoelectric materials. *Alternative Energetics and Ecology,* 5, 7-18.
2. Anatychuk L.I. (1978). Thermoelements and thermoelectric devices. *Kyiv: Naukova dumka [in Russian]*.
3. www.qdusa.com.
4. www.ipm.fraunhofer.de.
5. www.ulvac.com.
6. Anatychuk L.I., Pervozvansky S.V., Razinkov V.V. (1993). Precise measurement of cooling thermoelectric material parameters: methods, arrangements and procedures. *Proc. of the 12th Intern. Conf. Thermoelectrics (Japan, 1993)* (*pp.* 553-564).
7. Czichos H., Saito T., Smith L. (2011). *Springer Handbook of Metrology and Testing*. Springer.
8. Tritt T. (2006). Electrical and thermal transport measurement techniques for evaluation of the figure-of-merit of bulk thermoelectric materials. In: *Thermoelectric handbook: macro to nano. D.M. Rowe (Ed.). Boca-Raton: CRC Press.*
9. Okhotin A.S., Pushkarsky A.S., Borovikova R.P., Simonov V.A. (1974). *Metod izmereniia kharacteristik termoelektricheskikh materailov i preobrazovalekei [Method of measuring thermoelectric materials and converters characteristics]*. Moscow: Nauka [in Russian].
10. www.linseis.com.
11. www.dlr.de.
12. www.netzsch-thermal-analysis.com.
13. Freik D.M., Haluschak M.O., Ralchenko V.G., Tkachuk A.I. (2013). Methods of measuring thermal conductivity in massive solids and thin films (review). *Physics and Chemistry of Solid State,* 14(2), 17-344.
14. Lysko V.V. (2011). Modified Harman's method. *J.Thermoelectricity,* 84-92.

Submitted 15.05.2018

Анатичук Л.І. *ак. НАН України* [1,2], **Гаврилюк М.В.**[1],
Лисько В.В *канд. фіз.-мат. наук* [1,2].

[1]Інститут термоелектрики НАН і МОН України,
вул. Науки, 1, Чернівці, 58029, Україна;
[2]Чернівецький національний університет
ім. Юрія Федьковича, вул. Коцюбинського 2,
Чернівці, 58000, Україна, *e-mail: anatych@gmail.com*

ШЛЯХИ ПІДВИЩЕННЯ ЯКОСТІ ВИМІРІВ ТЕРМОЕЛЕКТРИЧНИХ ВЛАСТИВОСТЕЙ МАТЕРИАЛОВАБСОЛЮТНИМ МЕТОДОМ

Наведено результати аналізу значень похибок відомих методів вимірювання термоелектричних властивостей матеріалів. Встановлено, що ефективним методом вимірювання є абсолютний

метод, який дозволяє інструментально мінімізувати більшість джерел похибок. Наведено результати досліджень похибок вимірювання термоелектричних властивостей матеріалів абсолютним методом, отримані шляхом об'єктно-орієнтованого комп'ютерного моделювання. Встановлено вплив на точність вимірів радіаційного випромінювання, перенесення тепла вимірювальними електродами, спотворень електричного і теплового полів на контактах. Описано нові методи мінімізації похибок. Розглянуті також похибки, викликані відхиленнями розподілу температури в досліджуваному зразку від лінійного після досягнення стаціонарних станів. Досліджено швидкодію вимірів та розроблено методи її підвищення. Наведено опис двох модифікацій автоматизованого вимірювального устаткування, створених на основі розроблених методів, – для діапазонів температур 30 – 500 °С і 30 – 900 °С. Бібл.14, рис.17..
Ключові слова: абсолютний метод, вимір, електропровідність, термоЕРС, теплопровідність, похибки.

Анатычук Л.И., Гаврилюк Н.В., Лысько В.В.

[1]Институт термоэлектричества, Науки, 1, 58029, Черновцы, Украина
[2]Черновицкий национальный университет им. Юрия Федьковича,
ул. Коцюбинского 2, Черновцы, 58012, Украина
anatych@gmail.com

ПУТИ ПОВЫШЕНИЯ КАЧЕСТВА ИЗМЕРЕНИЙ ТЕРМОЭЛЕКТРИЧЕСКИХ СВОЙСТВ МАТЕРИАЛОВ АБСОЛЮТНЫМ МЕТОДОМ

Приведены результаты анализа значений погрешностей известных методов измерений термоэлектрических свойств материалов. Установлено, что эффективным методом измерений является абсолютный метод, позволяющий инструментально минимизировать большинство источников погрешностей Приведены результаты исследований погрешностей измерения термоэлектрических свойств материалов абсолютным методом, полученные объектно-ориентированным компьютерным моделированием.
Установлено влияние на точность измерений радиационного излучения, переноса тепла измерительными электродами, искажений электрического и теплового полей на контактах. Описаны новые методы минимизации погрешностей. Рассмотрены также погрешности, вызванные отклонениями от линейного распределения температуры в исследуемом образце при достижении стационарных состояний. Исследовано быстродействие измерений и разработаны методы его повышения.
Приведено описание двух модификаций автоматизированного измерительного оборудования, созданных на основе разработанных методов – для диапазонов температур 30 – 500 °С и 30 – 900 °С.. Библ. 14, Рис. 17.
Ключевые слова: термоэлектрический охладитель, среднеобъемная температура, динамика функционирования термоэлемента, показатели надежности, перепад температур.

References

1. Yepremyan A.O., Arutiunyan V.M., Vaganyan A.I. (2005). Figure of merit of novel thermoelectric materials. *Alternative Energetics and Ecology,* 5, 7-18.
2. Anatychuk L.I. (1978). Thermoelements and thermoelectric devices. *Kyiv: Naukova dumka [in*

Russian].
3. www.qdusa.com.
4. www.ipm.fraunhofer.de.
5. www.ulvac.com.
6. Anatychuk L.I., Pervozvansky S.V., Razinkov V.V. (1993). Precise measurement of cooling thermoelectric material parameters: methods, arrangements and procedures. *Proc. of the 12th Intern. Conf. Thermoelectrics (Japan, 1993)* (*pp.* 553-564).
7. Czichos H., Saito T., Smith L. (2011). *Springer Handbook of Metrology and Testing*. Springer.
8. Tritt T. (2006). Electrical and thermal transport measurement techniques for evaluation of the figure-of-merit of bulk thermoelectric materials. In: *Thermoelectric handbook: macro to nano. D.M. Rowe (Ed.). Boca-Raton: CRC Press.*
9. Okhotin A.S., Pushkarsky A.S., Borovikova R.P., Simonov V.A. (1974). *Metod izmereniia kharacteristik termoelektricheskikh materailov i preobrazovalekei [Method of measuring thermoelectric materials and converters characteristics]*. Moscow: Nauka [in Russian].
10. www.linseis.com.
11. www.dlr.de.
12. www.netzsch-thermal-analysis.com.
13. Freik D.M., Haluschak M.O., Ralchenko V.G., Tkachuk A.I. (2013). Methods of measuring thermal conductivity in massive solids and thin films (review). *Physics and Chemistry of Solid State,* 14(2), 17-344.
14. Lysko V.V. (2011). Modified Harman's method. *J.Thermoelectricity,* 84-92.

Submitted 15.05.2018

NEWS
OF INTERNATIONAL THERMOELECTRIC ACADEMY

VOLODYMYR OLEKSIYOVYCH SEMENYUK

(Dedicated to the 80-th anniversary)

On February 3 this year Volodymyr Oleksiyovych Semenyuk, a well-known scientist in thermoelectricity, academician of International Thermoelectric Academy, celebrated his 80th birthday.

In 1960 he graduated from Odessa State Academy of Refrigeration. For many years the scientific and pedagogical activity of Volodymyr Oleksiyovych has been related to this academic and research institution.

The research interests of V.O. Semenyuk were formed immediately under the influence of the founder of scientific school in the field of power engineering and refrigeration technology, professor V.S. Martynovsky, the scientists in thermoelectricity A.F. Ioffe, L.S. Stilbance, E.K. Iordanishvili and others.

Volodymyr Oleksiyovych made a major contribution to study of nonequilibrium thermodynamics and physics of thermoelectric effects. He was the first to solve a variety of variational problems as applied to thermoelectricity which made the basis for creation of modern computer methods for design of thermoelectric instruments and devices.

The scientist has solved a series of important engineering problems of thermoelectricity, in particular, the problems of heat exchange in thermoelectric devices, efficiency increase of multi-stage coolers, the problems of using the bulk thermoelectric cooling elements with programmed inhomogeneous legs. He studied and successfully solved contact problems in thermoelectric coolers, which allowed creating efficient microminiaturization technologies of thermoelectric devices. The theory and practice of thermoelectric instrument making was developed, the parametric series of thermoelectric micromodules were created which defy competition on global markets. In the development of some thermoelectric projects V.O. Semenyuk successfully cooperated with many scientific centers in the USA and Western Europe.

V.O. Semenyuk is the author of over 100 scientific works, certificates of authorship and patents, notably a monograph (in co-authorship with academician L.I. Anatychuk) “Optimal Control over the Properties of Thermoelectric Materials and Devices”. In 2006 and 2012 the results of his research in the theory and practice of thermoelectric instrument making were included as chapters into international handbooks “Thermoelectrics Handbook: Macro to Nano” and “Thermoelectrics and its Energy Harvesting”

Volodymyr Oleksiyovych gives special attention to training high-skilled scientific brainpower. He is an outstanding lector whose reports to scientific conferences and international forums arouse much interest and admiration among the attendees.

In recognition of the international level of his scientific achievements, V.O. Semenyuk was elected in 1995 full member of the International Thermoelectric Academy. V.O. Semenyuk is a member of the International and European Thermoelectric Societies, a member of American Institute of Aeronautics and Astronautics, a member of the Board of Directors of the European Thermoelectric Society.

International Thermoelectric Academy, Institute of Thermoelectricity of the National Academy of Sciences and Ministry of Education and Science, Youth and Sports of Ukraine, “Journal of Thermoelectricity” Publishers sincerely congratulate the esteemed Volodymyr Oleksiyovych on his glorious 80th jubilee, wishing him good health and happy longevity!

ARTICLE SUBMISSION GUIDELINES

For publication in a specialized journal, scientific works are accepted that have never been printed before. The article should be written on an actual topic, contain the results of an in-depth scientific study, the novelty and justification of scientific conclusions for the purpose of the article (the task in view).

The materials published in the journal are subject to internal and external review which is carried out by members of the editorial board and international editorial board of the journal or experts of the relevant field. Reviewing is done on the basis of confidentiality. In the event of a negative review or substantial remarks, the article may be rejected or returned to the author(s) for revision. In the case when the author(s) disagrees with the opinion of the reviewer, an additional independent review may be done by the editorial board. After the author makes changes in accordance with the comments of the reviewer, the article is signed to print.

The editorial board has the right to refuse to publish manuscripts containing previously published data, as well as materials that do not fit the profile of the journal or materials of research pursued in violation of ethical norms (for instance, conflicts between authors or between authors and organization, plagiarism, etc.). The editorial board of the journal reserves the right to edit and reduce the manuscripts without violating the author's content. Rejected manuscripts are not returned to the authors.

Submission of manuscript to the journal

The manuscript is submitted to the editorial office of the journal in paper form in duplicate and in electronic form on an electronic medium (disc, memory stick). The electronic version of the article shall fully correspond to the paper version. The manuscript must be signed by all co-authors or a responsible representative.

In some cases it is allowed to send an article by e-mail instead of an electronic medium (disc, memory stick).

English-speaking authors submit their manuscripts in English. Russian-speaking and Ukrainian-speaking authors submit their manuscripts in English and in Russian or Ukrainian, respectively. Page format is A4. The number of pages shall not exceed 15 (together with References and extended abstracts). By agreement with the editorial board, the number of pages can be increased.

To the manuscript is added:

1. Official recommendation letter, signed by the head of the institution where the work was carried out.

2. License agreement on the transfer of copyright (the form of the agreement can be obtained from the editorial office of the journal or downloaded from the journal website – Dohovir.pdf). The license agreement comes into force after the acceptance of the article for publication. Signing of the license agreement by the author(s) means that they are acquainted and agree with the terms of the agreement.

3. Information about each of the authors – full name, position, place of work, academic title, academic degree, contact information (phone number, e-mail address), ORCID code (if available). Information about the authors is submitted as follows:

authors from Ukraine - in three languages, namely Ukrainian, Russian and English;

authors from the CIS countries - in two languages, namely Russian and English;

authors from foreign countries – in English.

4. Medium with the text of the article, figures, tables, information about the authors in electronic form.

5. Colored photo of the author(s). Black-and-white photos are not accepted by the editorial staff. With the number of authors more than two, their photos are not shown.

Requirements for article design

The article should be structured according to the following sections:

- *Introduction*. Contains the problem statement, relevance of the chosen topic, analysis of recent research and publications, purpose and objectives.
- *Presentation of the main research material* and the results obtained.
- *Conclusions* summing up the work and the prospects for further research in this direction.
- *References*.

The first page of the article contains information:

1) in the upper left corner – UDC identifier (for authors from Ukraine and the CIS countries);

2) surname(s) and initials, academic degree and scientific title of the author(s);

3) the name of the institution where the author(s) work, the postal address, telephone number, e-mail address of the author(s);

4) article title;

5) abstract to the article – not more than 1 800 characters. The abstract should reflect the consistent logic of describing the results and describe the main objectives of the study, summarize the most significant results;

6) key words – not more than 8 words.

The text of the article is printed in Times New Roman, font size 11 pt, line spacing 1.2 on A4 size paper, justified alignment. There should be no hyphenation in the article.

Page setup: "mirror margins" – top margin – 2.5 cm, bottom margin – 2.0 cm, inside – 2.0 cm, outside – 3.0 cm, from the edge to page header and page footer – 1.27 cm.

Graphic materials, pictures shall be submitted in color or, as an exception, black and white, in .opj or .cdr formats, .jpg or .tif formats being also permissible. According to author's choice, the tables and partially the text can be also in color.

Figures are printed on separate pages. The text in the figures must be in the font size 10 pt. On the charts, the units of measure are separated by commas. Figures are numbered in the order of their arrangement in the text, parts of the figures are numbered with letters – a, b, .. On the back of the figure, the title of the article, the author (authors) and the figure number are written in pencil. Scanned images and graphs are not allowed to be inserted.

Tables are provided on separate pages and must be executed using the MSWord table editor. Using pseudo-graph characters to design tables is inadmissible.

Formulae shall be typed in Equation or MatType formula editors. Articles with formulae written by hand are not accepted for printing. It is necessary to give definitions of quantities that are first used in the text, and then use the appropriate term.

Captions to figures and tables are printed in the manuscript after the references.

Reference list shall appear at the end of the article. References are numbered consecutively in the order in which they are quoted in the text of the article. References to unpublished and unfinished works are inadmissible.

Attention! In connection with the inclusion of the journal in the international bibliographic abstract database, the reference list should consist of two blocks: CITED LITERATURE and REFERENCES (this requirement also applies to English articles):

CITED LITERATURE – sources in the original language, executed in accordance with the Ukrainian standard of bibliographic description DSTU 8302:2015. With the aid of VAK.in.ua (http://vak.in.ua) you can automatically, quickly and easily execute your "Cited literature" list in conformity with the requirements of State Certification Commission of Ukraine and prepare references to scientific sources in Ukraine in understandable and unified manner. This portal facilitates the processing of scientific sources when writing your publications, dissertations and other scientific papers.

REFERENCES – the same cited literature list transliterated in Roman alphabet (recommendations according to international bibliographic standard APA-2010, guidelines for drawing up a transliterated reference list "References" are on the site http//www.dse.org.ua, section for authors).

To speed up the publication of the article, please adhere to the following rules:

- in the upper left corner of the first page of the article – the UDC identifier;
- family name and initials of the author(s);
- academic degree, scientific title;

begin a new line, Times New Roman font, size 12 pt, line spacing 1.2, center alignment;

- name of organization, address (street, city, zip code, country), e-mail of the author(s);

begin a new line 1 cm below the name and initials of the author(s), Times New Roman font, size 11 pt, line spacing 1.2, center alignment;

- the title of the article is arranged 1 cm below the name of organization, in capital letters, semi-bold, font Times New Roman, size 12 pt, line spacing 1.2, center alignment. The title of the article shall be concrete and possibly concise;
- the abstract is arranged 1 cm below the title of the article, font Times New Roman, size 10 pt, in italics, line spacing 1.2, justified alignment in Ukrainian or Russian (for Ukrainian-speaking and Russian-speaking authors, respectively);
- key words are arranged below the abstract, font Times New Roman, size 10 pt, line spacing 1.2, justified alignment. The language of the key words corresponds to that of the abstract. Heading "Key words" - font Times New Roman, size 10 pt, semi-bold;
- the main text of the article is arranged 1 cm below the abstract, indent 1 cm, font Times New Roman, size 11 pt, line space spacing 1.2, justified alignment;
- formulae are typed in formula editor, fonts Symbol, Times New Roman. Font size is "normal" – 12 pt, "large index" – 7 pt, "small index" – 5 pt, "large symbol" – 18 pt, "small symbol" – 12 pt. The formula is arranged in the text, center aligned and shall not occupy more than 5/6 of the line width, formulae are numbered in parentheses on the right;
- dimensions of all quantities used in the article are represented in the International System of Units (SI) with the explication of the symbols employed;
- figures are arranged in the text. The figures and pictures shall be clear and contrast; the plot axes – parallel to sheet edges, thus eliminating possible displacement of angles in scaling; figures are submitted in color, black-and-white figures are not accepted by the editorial staff of the journal;
- tables are arranged in the text. The width of the table shall be 1 cm less than the line width. Above the table its ordinary number is indicated, right alignment. Continuous table numbering

throughout the text. The title of the table is arranged below its number, center alignment;

- references should appear at the end of the article. References within the text should be enclosed in square brackets behind the text. References should be numbered in order of first appearance in the text. Examples of various reference types are given below.

Examples of LITERATURE CITED

Journal articles

Anatychuk L.I., Mykhailovsky V.Ya., Maksymuk M.V., Andrusiak I.S. Experimental research on thermoelectric automobile starting pre-heater operated with diesel fuel. *J.Thermoelectricity*. 2016. №4. P.84–94.

Books

Anatychuk L.I. *Thermoelements and thermoelectric devices. Handbook.* Kyiv, Naukova dumka, 1979. 768 p.

Patents

Patent of Ukraine № 85293. Anatychuk L.I., Luste O.J., Nitsovych O.V. Thermoelement.

Conference proceedings

Lysko V.V. *State of the art and expected progress in metrology of thermoelectric materials*. Proceedings of the XVII International Forum on Thermoelectricity (May 14-18, 2017, Belfast). Chernivtsi, 2017. 64 p.

Authors' abstracts

Kobylianskyi R.R. *Thermoelectric devices for treatment of skin diseases*: extended abstract of candidate's thesis. Chernivtsi, 2011. 20 p.

Examples of REFERENCES

Journal articles

Gorskiy P.V. (2015). Ob usloviakh vysokoi dobrotnosti i metodikakh poiska perspektivnykh sverhreshetochnykh termoelektricheskikh materialov [On the conditions of high figure of merit and methods of search for promising superlattice thermoelectric materials]. *Termoelektrichestvo - J.Thermoelectricity,* 3, 5 – 14 [in Russian].

Books

Anatychuk L.I. (2003). *Thermoelectricity. Vol.2. Thermoelectric power converters*. Kyiv, Chernivtsi: Institute of Thermoelectricity.

Patents

Patent of Ukraine № 85293. Anatychuk L. I., Luste O.Ya., Nitsovych O.V. Thermoelements [In Ukrainian].

Conference proceedings

Rifert V.G. Intensification of heat exchange at condensation and evaporation of liquid in 5 flowing-down films. In: *Proc. of the 9th International Conference Heat Transfer.* May 20-25, 1990, Israel.

Authors'abstracts

Mashukov A.O. *Efficiency hospital state of rehabilitation of patients with color carcer.* PhD (Med.) Odesa, 2011 [In Ukrainian].